

**The modulating effect of soluble
amyloid- β dimers on amyloid- β aggregation
in vivo and *in vitro***

Inaugural dissertation

For the attainment of the title of doctor
in the Faculty of Mathematics and Natural Sciences
at the Heinrich Heine University Düsseldorf

presented by

Else Felicia van Gerresheim

from Almelo, the Netherlands

Düsseldorf, April 2022

From the Institute of Neuropathology
At the Heinrich Heine University Düsseldorf

Published by permission of the
Faculty of Mathematics and Natural Sciences at
Heinrich Heine University Düsseldorf

Supervisor: Prof. Dr. Carsten Korth
Co-supervisor: Prof. Dr. Dieter Willbold

Date of the oral examination: 07.07.2022

Concerning the submitted dissertation:

The modulating effect of soluble
amyloid- β dimers on amyloid- β aggregation
in vivo and *in vitro*

I declare under oath that I have compiled my dissertation independently and without any undue assistance from third parties under consideration of the 'Principles for the Safeguarding of Good Scientific Practice' at the Heinrich Heine University Düsseldorf

Furthermore, I declare that this dissertation has not been submitted to any other university or faculty before and that I have not made any other doctoral studies so far.

Düsseldorf, 28 April 2022

(Else F. van Gerresheim)

TABLE OF CONTENTS

1. Introduction	12
1.1 Neurodegenerative diseases	12
1.2 Alzheimer's disease	13
1.2.1 Genetics and risk factors	14
1.2.2 Heterogeneity of the disease	15
1.3 Amyloid-beta	15
1.3.1 Amyloid-beta multimer species	17
1.3.2 Prion-like spreading	19
1.4 Animal models of Alzheimer's disease	23
1.4.1 The tgDimer mouse	25
1.4.2 Behavioural tasks	26
1.4.3 In vivo bioluminescence imaging	29
1.5 Objectives of research	31
2. Studies I, II	31
2.1 Study I	32
Investigate how soluble A β -S8C dimers relate to the heterogeneity of amyloid plaque pathology: The interaction of insoluble Amyloid- β with soluble Amyloid- β dimers decreases Amyloid- β plaque numbers	
2.2 Study II	34
Investigate the influence of A β -S8C dimers on A β spreading and behaviour in the tgDimer mouse: Amyloid-beta dimers are anti prions inhibiting seeded nucleation in vivo	
3. Conclusion	36
4. Additional data	39
4.1 Burrowing as a measure of activity of daily living in AD	39
5. List of publications	46
6. Acknowledgments	47
7. Bibliography	49
8. Appendices: studies I, II	59

FIGURES

Figure 1: Protein aggregation in neurodegenerative diseases

Figure 2: Schematic diagram of human amyloid precursor protein (APP) processing

Figure 3: Extracellular aggregation of amyloid- β ($A\beta$) in a schematic overview – from monomers to fibrils

Figure 4: Seeding-nucleation model of amyloid aggregation

Figure 5: Schematic bird's eyes view of the Phenotyper cage

Figure 6: Seeding-nucleation model of amyloid aggregation and the addition of $A\beta$ -S8C dimers

Figure 7: Example of a burrow

Figure 8: TgDimer mice burrowed fewer food pellets at 13 months of age compared to WT mice

Figure 9: $A\beta$ inoculated tgAPP23 mice burrowed significantly fewer food pellets compared to $A\beta$ inoculated wild type mice at 6 months of age

Figure 10: Decrease in food pellets burrowed after 2h as mice ages

ABBREVIATIONS

A β	Amyloid-beta
A β -S8C	Amyloid-beta with S8C mutation
AD	Alzheimer's disease
ApoE	Apolipoprotein E
APP	Amyloid precursor protein
ALS	Amyotrophic lateral sclerosis
BACE1	β -secretase
BLI	Bioluminescence imaging
BSE	Bovine spongiform encephalopathy
CHO	Chinese ovarian hamster
CJD	Creutzfeldt-Jakob disease
CTF	C-terminal fragment
EOAD	Early-onset Alzheimer's disease
FUS	Fused in sarcoma protein
GFAP	Glial fibrillary acidic protein
GPI	Glycosylphosphatidylinositol
LOAD	Late-onset Alzheimer's disease
MAPT	Microtubule-associated protein tau
NFTs	Neurofibrillary tangles
PrP ^C	Prion protein
PSEN	Presenilin
pTau	hyperphosphorylated tau
RF	Rigid fibril
sAPP α	soluble APP- α
sAPP β	soluble APP- β
SDS	Sodium dodecyl sulfate

TDP-43	TAR DNA binding protein 43
ThT	Thioflavin T
TSE	Transmissible spongiform encephalopathies

ABSTRACT

Most neurodegenerative diseases, including Alzheimer's disease (AD), are characterized by the deregulation of the protein self-assembly process, resulting in amyloid formation. The most important causative factor in most neurodegenerative processes is the generation of specific aggregated proteins. In AD, phosphorylation and aggregation of Tau into neurofibrillary tangles (NFTs) are widely considered pathological hallmarks next to amyloid-beta ($A\beta$), which is the main component of the amyloid plaques. Multimerization of $A\beta$ is assumed a critical initial step eventually culminating in the massive deposition of extracellular amyloid plaques.

It is still unclear how $A\beta$ aggregates and spreads throughout the brain. The currently favoured explanation is the so-called amyloid cascade hypothesis, which postulates that AD is caused by abnormal accumulation of $A\beta$, leading to amyloid plaques eventually resulting in neuronal death. Another explanation is that $A\beta$ has prion-like properties. This would imply that misfolded $A\beta$ spreads via seeding, meaning that when a prion-like seed of $A\beta$ has originated, it could trigger the propagation of misfolded $A\beta$ throughout the brain. A common hypothesis is that $A\beta$ oligomers, especially $A\beta$ dimers, can readily accelerate $A\beta$ plaque formation, thus acting as a seed.

The tgDimer mouse is a transgenic mouse that expresses human *APP* with the Swedish mutation and an artificial mutation (S679C), replacing a serine at position 8 of $A\beta$ with a cysteine, resulting in the generation of exclusive, stable, and neurotoxic $A\beta$ -S8C dimers. These mice do not develop AD pathology during their lifetime; however, the $A\beta$ -S8C dimers are able to associate to $A\beta$ plaques.

This cumulative dissertation investigated how soluble $A\beta$ -S8C dimers relate to the heterogeneity of amyloid plaque pathology and whether $A\beta$ -S8C dimers influence $A\beta$ aggregation or modulate cognitive deficits. Furthermore, specific behavioural tasks were explored for the detection of early signs of cognitive deficits.

In the first study, the influence of $A\beta$ -S8C dimers on $A\beta$ aggregation and their relation to $A\beta$ plaque heterogeneity was investigated. Therefore, $A\beta$ plaque load in the brains of the tgDimer

mouse crossed with the tgCRND8 mouse, a transgenic mouse, expressing mutant human *APP* with the familial Swedish (K670 N/ M671L) and Indiana (V717F) mutation was quantified. Analysis of the A β plaque load showed a lower number, but not size, of A β plaques on brain sections of 3 month and 5-month-old mice of tgDimer/tgCRND8 mice compared with tgCRND8 mice. *In vitro* thioflavin T (ThT) assays show that the addition of A β -S8C dimers to wild type A β ₄₂ slowed down the aggregation.

In the second study, it was investigated whether A β -S8C dimers also modulated seeded nucleation *in vivo*. To this end, TgDimer mice were crossed with Gfap-luc mice, which express luciferase (luc) under the control of the Gfap promoter, which were then inoculated with brain extracts containing A β seeds. The tgDimer mouse was resistant to A β prions and did not develop astrogliosis or amyloid plaques in contrast to the positive control, the tgAPP23 mouse that did develop astrogliosis and AD pathology. Behavioural experiments showed no cognitive decline in inoculated tgDimer mice.

Our results suggest that A β -S8C dimers are inhibitors of A β aggregation, as we did not observe any A β plaques in tgDimer mice inoculated with A β seeds. We propose that A β -S8C dimers slow or inhibit A β seeding and have anti-prion properties.

ZUSAMMENFASSUNG

Die meisten neurodegenerativen Erkrankungen, darunter auch die Alzheimer-Demenz (AD), sind durch eine Dysregulierung der Protein-Selbstassemblierung gekennzeichnet, die zur Bildung von Amyloiden führt. Der primäre und vielleicht wichtigste ursächliche Faktor bei den meisten neurodegenerativen Prozessen ist die Bildung von spezifischen aggregierten Proteinen. Bei der Alzheimer-Krankheit gelten die Hyperphosphorylierung und Aggregation von Tau zu neurofibrillären Tangles (NFTs) neben der Entstehung von Amyloid-beta (A β) Plaques, dem Hauptbestandteil der Ablagerungen des aggregierten Proteins als neuropathologische Merkmale. Es wird angenommen, dass die Multimerisierung von A β ein kritischer erster Schritt ist, der schließlich zur massiven Ablagerung extrazellulärer Plaques führt.

Bislang ist noch unklar, was die Aggregation von A β initiiert und wie sie sich im Gehirn ausbreitet. Die am meiste diskutierte Erklärung ist die so genannte Amyloidkaskadenhypothese, die postuliert, dass die Alzheimer-Krankheit durch eine abnormale Anhäufung von A β verursacht wird, die Amyloid-Plaques bildet, und die anschliessend zu tau Fibrillen und zum Tod von Neuronen führt. Eine weitere Erklärung ist, dass A β Prion-ähnliche Eigenschaften hat. Dies würde bedeuten, dass sich fehlgefaltetes A β durch einen „seeding“ Prozess ausbreitet, d. h. wenn ein Prion-ähnliche Aggregat von A β entstanden ist, könnte er zyklisch über aufeinanderfolgenden Zerfall und Wachstum von A β Aggregaten die Ausbreitung von fehlgefaltetem A β im gesamten Gehirn auslösen. Eine verbreitete Hypothese ist, dass A β -Oligomere, insbesondere A β -Dimere, die Bildung von A β -Plaques leicht beschleunigen können und somit als Nukleus wirken.

Die tgDimer-Maus ist eine transgene Maus, die menschliches APP mit der schwedischen Mutation und einer künstlichen Mutation (S679C) exprimiert, die ein Serin an Position 8 von A β durch ein Cystein ersetzt, was zur Bildung von exklusiven, stabilen und neurotoxischen A β -S8C-Dimeren führt. Diese Mäuse entwickeln im Laufe ihres Lebens keine Alzheimer-Pathologie, aber die A β -S8C-Dimere sind in der Lage, an A β -Plaques zu binden.

In dieser kumulativen Dissertation, die sich mit A β -Dimeren und ihren Einfluss auf die A β -Aggregation und -Ausbreitung befasst, wurde untersucht, wie lösliche A β -S8C-Dimere mit der

Heterogenität der Amyloid-Plaque-Pathologie zusammenhängen und ob A β -S8C-Dimere die A β -Aggregation und -Ausbreitung beeinflussen oder kognitive Defizite modulieren. Mit Hilfe der tgDimer-Mäuse, die ausschließlich A β -S8C-Dimere exprimieren, wurde dies untersucht. Darüber hinaus wurde ein spezifischer Verhaltenstest entwickelt, um frühe Anzeichen kognitiver Defizite zu messen.

In der ersten Studie wurde der Einfluss von A β -S8C-Dimeren auf die A β -Aggregation und ihre Beziehung zur A β -Plaque-Heterogenität untersucht. Dazu wurde die A β -Plaque-Last in den Gehirnen von tgDimer-Mäusen, die mit der tgCRND8-Maus gekreuzt wurden, einer transgenen Maus, die mutiertes menschliches APP mit der familiären Swedish (K670 N/M671L) und Indiana (V717F) Mutation exprimiert, quantifiziert. Die A β -Plaque-Last wurde an Hirnschnitten von 3 Monate und 5 Monate alten Mäusen bestimmt und mit jenen der tgCRND8 Maus gleichen Alters verglichen. Die Analyse zeigte eine geringere Anzahl, aber nicht Grösse, von A β -Plaques in den Gehirnen von tgDimer/tgCRND8-Mäusen im Vergleich zu tgCRND8-Mäusen. Zellfreie *in vitro* Thioflavin T (ThT) Assays zeigten, dass die Zugabe von synthetischer A β -S8C-Dimere zu Wildtyp-A β 42 die Aggregation verlangsamt und die Keimbildung verringert.

In der zweiten Studie wurde untersucht, ob A β -Dimere auch die initiale Bildung von A β – Keimen, d.h. Prionen modulieren. Zu diesem Zweck wurden tgDimer-Mäuse mit Gfap-luc-Mäusen gekreuzt, die Luciferease (luc) unter Kontrolle des Gfap-Promotors exprimieren (um die Plaque-korrelierte Astroglieose *in vivo* zu messen), dann mit A β -Aggregationsvorstufen enthaltenden Gehirnexttrakten inokuliert wurden. Die tgDimer-Maus war resistent gegen A β -Prionen und entwickelte keine Astroglieose oder Amyloid-Plaques, im Gegensatz zu der Positivkontrolle, der tgAPP23-Maus, die Astroglieose und AD-Pathologie entwickelte. Verhaltensexperimente zeigten keine kognitive Verschlechterung bei inokulierten tgDimer-Mäusen.

Unsere Ergebnisse deuten darauf hin, dass A β -S8C-Dimere tatsächlich die A β -Aggregation hemmen, da wir bei tgDimer-Mäusen, die mit A β -Samen geimpft wurden, keine A β -Plaques beobachten konnten. Wir vermuten, dass A β -S8C-Dimere das A β -Seeding verlangsamen oder verhindern und somit Antiprion-Eigenschaften haben.

1. INTRODUCTION

1.1. NEURODEGENERATIVE DISEASES

Loss of neuronal function, selective neuronal loss, and neuroinflammation are typical characteristics of neurodegenerative diseases. The incidence of these diseases increases with age. In addition, the prognosis of neurodegenerative diseases today is very poor, being among the top ten causes of death, but also one of the leading causes of disability and dependency on other people. So far, treatments for these disorders are only able to relieve symptoms.

A common feature in neurodegenerative diseases is the misfolding, aggregation, and deposition of proteins, both intra- and extracellular (1, 2). In each neurodegenerative disease, the distribution and composition of protein aggregates in the brain are different, leading to the distinct clinical symptoms of each. Extracellular deposits of misfolded proteins are present in for example Alzheimer's disease (AD) or prion disease, with amyloid- β (A β) and prion protein (PrP^C) being the responsible proteins, respectively (3-5). Proteins that deposit intracellular include tau in several diseases including AD (6-9), α -synuclein, which is mainly detected in Parkinson's disease (10, 11), TAR DNA binding protein 43 (TDP-43) or fused in sarcoma protein (FUS) in Amyotrophic Lateral Sclerosis (ALS) (12-15) and mutated Huntingtin in Huntington's disease (16, 17) (Figure 1).

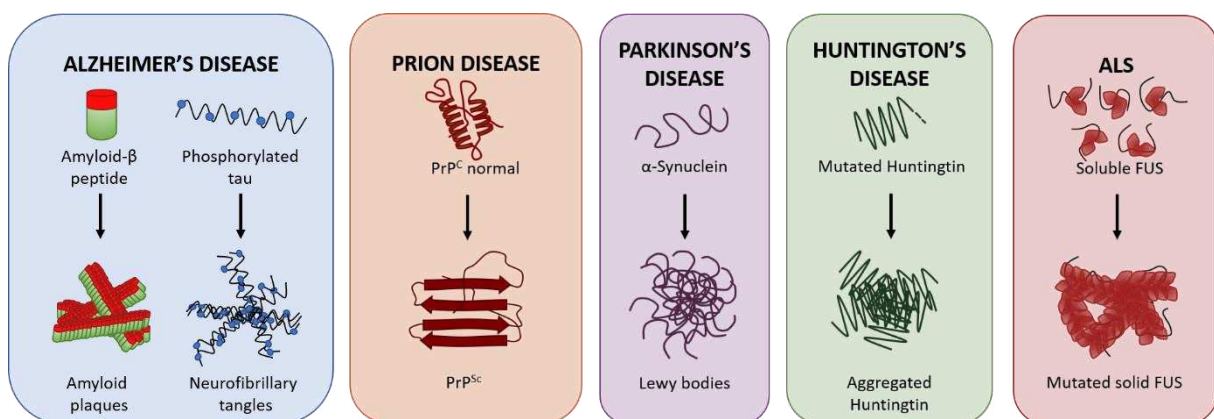


Figure 1. Protein aggregation in neurodegenerative diseases. In Alzheimer's disease, amyloid- β and phosphorylated tau form amyloid plaques and neurofibrillary tangles, respectively. α -synuclein accumulates together and forms Lewy bodies in Parkinson's disease. A conformational change results in PrP^{Sc} which aggregates and results in prion disease. Mutated huntingtin aggregates lead to Huntington's disease, and in ALS, several proteins, for example, FUS can be responsible for inclusion bodies. Adapted from 'Protein aggregation in late-onset neurodegenerative diseases'(18). ALS = Amyotrophic Lateral Sclerosis, FUS = fused in sarcoma protein

Treatments for these diseases are mainly relieving specific symptoms with limited success and do not modify their course. One of the main problems for treatment is that at the time point of diagnosis when patients exhibit first symptoms, loss of neurons in specific areas has occurred (19-22). Therefore, the treatment should start before the onset of clinical symptoms. Early biomarkers, especially those positive in the asymptomatic preclinical phase of the disease, could play an important role in the future for the diagnosis of neurodegenerative diseases in the preclinical stage. For AD, many treatments are under clinical trial investigation, with the treatments based on immunotherapy, where A β is targeted (23). Although these treatments showed great potential in *in vivo* animal models of AD, human trials have not been convincingly successful so far (24). The complex nature of AD possibly determines the failure of many therapies directed to one single target. The development of therapies focused on multiple targets might be the base of future strategies.

1.2. ALZHEIMER'S DISEASE

AD is one of the most common neurodegenerative diseases, with a worldwide estimated prevalence of 24 million people. The risk of AD onset increases exponentially with age, and the underlying pathophysiological triggers are thought to begin 20 years or more before the onset of clinical symptoms (25-28). One of the earliest symptoms is the difficulty in remembering recent events, and as the disease progresses, symptoms can include problems with language, disorientation, mood swings, loss of motivation, self-neglect, and behavioural issues. The end-stage involves losing bodily functions, ultimately leading to death. The majority of AD patients have sporadic AD and most of them start to show symptoms above the age of 65 years, called late-onset AD (LOAD). Early-onset familial Alzheimer's disease (EOAD) accounts for less than 5% of AD (29). Patients with familial AD carry inherited mutations that affect the expression of amyloid precursor protein (APP) or its processing to A β .

The disease was first discovered by Alois Alzheimer, a German psychiatrist and pathologist, who was first to describe extracellular aggregates and intracellular fibrils in a patient's brain who suffered from dementia in 1906 (30). This patient showed a severe change of personality at age 51, accompanied by disorientation to time and place, and confusion. This progressed

until she was apathetic and died, 5 years later. Examination of her brain revealed neurofibrillary tangles (NFTs) and senile plaques, as well as a massive loss of neurons (31).

In the 1980s, researchers discovered that A β and hyperphosphorylated tau (pTau) were the molecular basis of the senile plaques (amyloid plaques) and NFTs, respectively (5, 8, 32, 33). A β is a protein generated by the cleavage of APP. The second hallmark, NFTs, consist of intracellularly accumulated pTau. Tau is a microtubule-associated protein and in the human brain, six isoforms of tau are expressed, produced by alternative splicing from the gene *MAPT* (microtubule-associated protein tau) (6). Under normal conditions, tau is highly soluble and natively unfolded, interacts with tubulin, and promotes its assembly into microtubules (34). Tau shows abnormal hyperphosphorylation at many sites in AD, causing impairments in axonal transport and neuronal dysfunction. Self-assembly of pTau eventually results in the formation of NFTs (35, 36). Of note, mutations of tau are not associated to AD but to frontotemporal dementias (37).

Diagnosis of AD is usually based on clinical observations comprising medical history, and physical, neurological, and neuropsychological exams. A definite diagnosis can only be made *post-mortem* by the demonstration of amyloid plaques and NFTs in the brain.

1.2.1. GENETICS AND RISK FACTORS

Next to age (38), genetic factors contribute to the risk of AD. Three genes associated with EOAD identified by linkage studies with DNA markers are the genes encoding for *APP* (39, 40), as well as presenilin 1 (*PSEN1*) and *PSEN2* (41-44). Mutations in the *APP* gene might lead to altered metabolism of APP resulting in increased production of A β , or an increased production of the more aggregation-prone form of A β , A β ₄₂, accumulating into amyloid fibrils and eventually plaques. Mutations in both *PSEN1* and *PSEN2*, cause overproduction of the amyloidogenic A β ₄₂ (45).

The most important genetic risk factor for developing LOAD is the apolipoprotein E (ApoE) ϵ 4 allele. The *APOE* gene encodes ApoE, a 35 kDa glycoprotein highly expressed in the brain, which plays a crucial role in regulating cholesterol metabolism. There are three major isoforms of ApoE (ϵ 2, ϵ 3, and ϵ 4), which differ from each other because of two-point mutations

(rs429358 and rs7412) within exon 4 of the gene. Carriers of the $\epsilon 4$ allele have an increased risk of AD (46), whereas the $\epsilon 2$ allele confers a small protective effect (47, 48).

1.2.2. HETEROGENEITY OF ALZHEIMER'S DISEASE

AD is a highly complex disease, with considerable clinical and pathological variability. This is demonstrated in many of its aspects: age of onset, duration, disease progression, clinical course types and patterns of neurological and psychiatric symptoms, response to treatment, and neuropathological lesions, which indicates that there are different subtypes of AD (49, 50).

Some of the pathological variability can be explained by the presence of mutations in genes related to APP processing and A β production. For example, patients exhibiting EOAD mutations show variations in A β levels and distribution and morphology of A β plaques. Missense mutations in the *PSEN* gene can alter γ -secretase activity, resulting in a wide variation in type, number, and distribution of amyloid plaques, which leads to an array of subtly different biochemical, neuropathological, and clinical manifestations (51). Mutations of *APP* can also affect the aggregation properties of A β . For example, the Arctic *APP* mutation results in the formation of more protofibrils (52). The position where γ -secretase cleaves at the C-terminus of the APP protein can result in different isoforms of A β (53), of which each own different aggregation propensities and lead to structurally different fibrils and fiber morphology (54-56).

Thus, the heterogeneity could relate to A β being present in certain conformations, leading to different A β strains (57). Similarly, in prion diseases, such as Creutzfeldt-Jakob disease (CJD), the presence of specific strains of protein aggregates results in variable clinical and pathological phenotypes (58).

1.3. AMYLOID-BETA

A β , a 4 kDa protein product, is produced by several cell types in the brain, but mostly in neurons, by cleavage of APP. APP is a cellular ubiquitous type 1-transmembrane protein involved in cell adhesion (59-61). Alternative splicing leads to three major isoforms of APP, APP₆₉₅, APP₇₅₁, and APP₇₇₀. Human APP has two primary processing pathways: amyloidogenic

and non-amyloidogenic. In the non-amyloidogenic pathway, APP is cleaved by α -secretase, generating extracellular soluble APP- α (sAPP α) and the membrane-bound C-terminal fragment 83 (C83). C83 is further cleaved by γ -secretase, which results in the soluble fragment p3 and an APP intracellular domain (AICD). If APP is cleaved by β -secretase (BACE1) followed by γ -secretase (amyloidogenic pathway), the end products are an intracellularly APP domain, extracellularly soluble APP- β (sAPP β), and A β (Figure 2). Both pathways can result in a large variety of peptides starting either at position 1 or 11 caused by cleavage of BACE1 or at position 17 by α -secretase. γ -Secretase generates a variety of different A β s spanning from 34 to 50 amino acids in length (53). A β_{40} and A β_{42} are the most prominent species produced (62, 63) and even though secreted A β_{40} is more abundant, A β_{42} is the major component of A β plaques (64, 65).

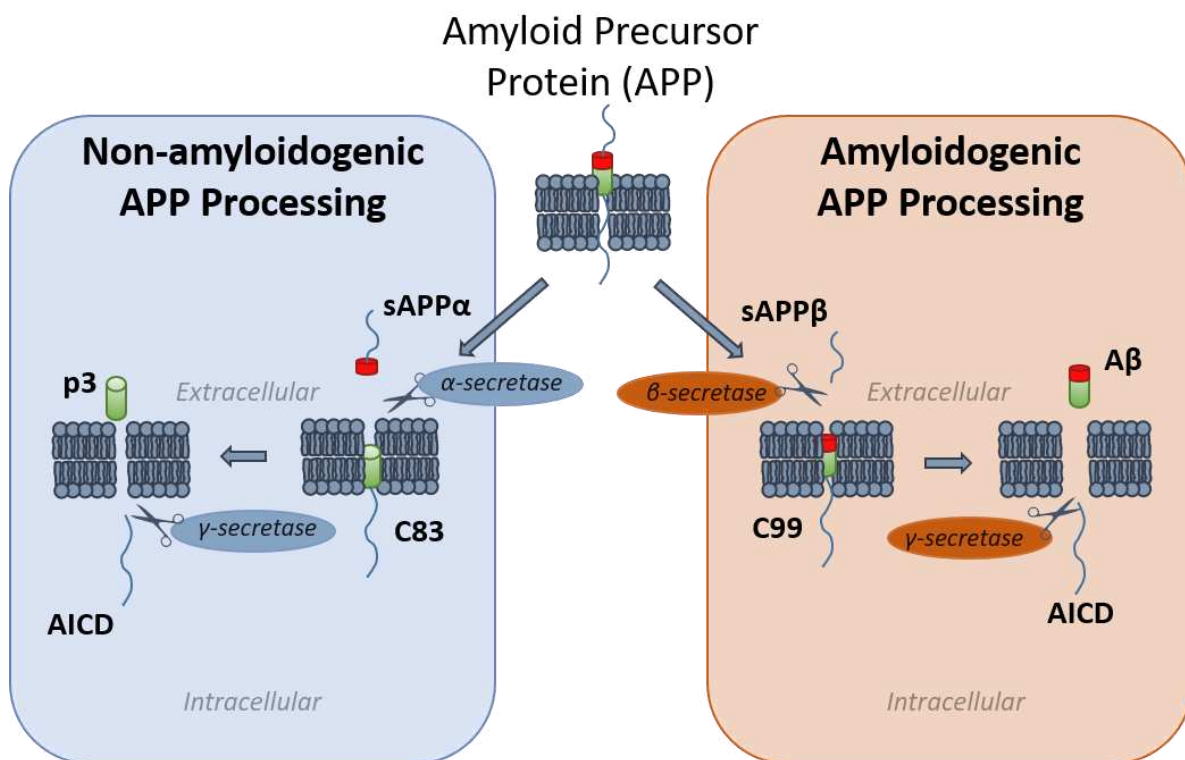


Figure 2. Schematic diagram of human amyloid precursor protein (APP) processing. Human APP can be processed through either the amyloidogenic or the non-amyloidogenic pathway. In the amyloidogenic pathway (right), the proteolytic cleavage of the APP by β -secretase produces a large soluble domain of APP (sAPP β) and a membrane-associated C-terminal fragment (C99). The C99 is subsequently cleaved by γ -secretase, releasing an amyloid β -peptide (A β) and an APP intracellular domain (AICD). In a non-amyloidogenic pathway (left), α -secretase-mediated cleavage of the APP generates a soluble domain of APP (sAPP α) and a membrane-associated C-terminal fragment (C83). The subsequent cleavage of the C83 by γ -secretase gives rise to a P3 peptide and an AICD. Adapted from: *New Insights Into Blood-Brain Barrier Maintenance: The Homeostatic Role of β Amyloid Precursor Protein in Cerebral Vasculature* (66)

Studies have identified various longer A β variants in cell lines, for example, A β_{43} , A β_{45} , A β_{46} , and A β_{48} (67) but also shorter C-terminus peptides, like A β_{34-42} , which only consist of 9 amino acids. A β_{43} has an additional threonine at the C-terminal through an alternative γ -secretase cleavage, and is like A β_{42} prone to aggregate *in vitro* (68), resulting in the faster formation of oligomers compared with A β_{40} (69).

N-terminally truncated forms of A β make up a substantial proportion of total A β in the human brain (70). However, the existence of N-terminal truncations cannot be explained by the action of the above-described enzymes (71). Secretory proteases such as an insulin-degrading enzyme, neprilysin, and aminopeptidase A are responsible for A β degradation (72), and truncations may arise from these enzymes. An example is the 2-x A β species, which is a result of a combined action of BACE1 followed by aminopeptidase A (73). Other N-terminal variants are also frequently found in the AD brain, for example, pyroGlu-3 A β , a modified A β peptide that starts with pyroglutamate at the third residue. PyroGlu-3 A β is exclusively found under pathological conditions in AD patients, is a highly stable, neurotoxic form of A β , and has a high propensity to aggregate (74).

1.3.1. AMYLOID-BETA MULTIMER SPECIES

After the identification of the A β peptide, researchers put forward the 'amyloid cascade hypothesis'. According to the amyloid cascade hypothesis, aggregation of A β is the initial causal event in AD pathology, followed by tau aggregation, neuron loss, and clinical symptoms (35-37). The A β peptide is secreted in its monomeric form as an intrinsically disordered protein. A β monomers aggregate with each other and form dimers, different forms of oligomers, protofibrils and then form fibrils, comprising cross- β structures (Figure 3). Mature fibrils of A β are deposited in the form of amyloid plaques.

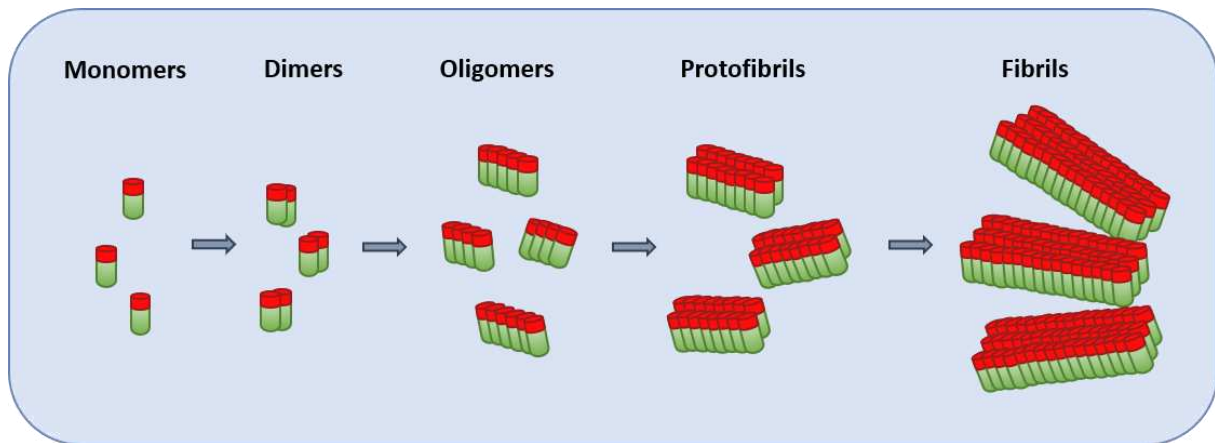


Figure 3. Extracellular aggregation of amyloid- β ($A\beta$) in a schematic overview – from monomers to fibrils. $A\beta$ monomers are produced via the amyloidogenic pathway. First, they will accumulate into dimers, and accumulate into small low molecular weight oligomers. Oligomer aggregation leads to the formation of protofibrils, which eventually can aggregate to mature fibrils, the main component of amyloid plaques.

Soluble $A\beta$ oligomers, defined as $A\beta$ species that are not pelleted from physiological fluids by high-speed centrifugation (75) exist throughout the brains, while $A\beta$ fibrils are larger and insoluble and as aggregation continues, the solubility decreases. Several studies suggested that smaller soluble oligomeric $A\beta$ species, which correlate better with disease severity, are the forms causing neurotoxicity (75-78), and are responsible for progressive neurodegeneration in AD (76, 78, 79). Because of the kinetic equilibrium where the monomeric, dimeric/oligomeric $A\beta$ concentration is in balance with fibrils, it has been difficult to study the effects of $A\beta$ oligomers on a neuropathological, biochemical, and behavioural level.

With the generation of synthetic $A\beta$ species, especially the $A\beta$ dimers, this has improved. An example of a synthetic $A\beta$ dimer is the dim $A\beta$ where two $A\beta_{40}$ units are connected via a flexible glycine–serine-rich linker. This dimer can readily form globular oligomers and curvilinear fibrils (80). Dimeric $A\beta$ variants can also be generated by introducing intra- or intermolecular disulfide bridges (81-85). For example, $A\beta_{C1833}$, a disulfide-stabilized analogue of $A\beta_{42}$, forms stable homogeneous dimers in lipid environments but does not aggregate to form insoluble fibrils and is readily expressed in *Escherichia coli* and purified by reverse-phase HPLC (86). Moreover, three other dimers were developed, each with another mutation within the $A\beta$ sequence: at position 8 (S8C), 26 (S26C), and 35 (M35C) (87). These mutations allowed dimer formation already in the early stages of the $A\beta$ -processing pathways. The S8C mutation

resulted in an exclusive homogeneous and neurotoxic A β dimer (A β -S8C) and the M35C mutant assembles into large oligomers (A β M35C). Expression of the APP A β -S8C mutant in Chinese Ovarian Hamster (CHO) cells, results in the production of a naturally secreted A β dimers but no sodium dodecyl sulfate (SDS)-resistant oligomers of higher order. CHO cells expressing the APP (A β S26C) mutant produced no oligomeric A β , whereas the APP (A β M35C) produced dimers, SDS-resistant tetramers, and higher-order oligomers (87).

Introduction of the mutant APP (S8C) into the human APP (Swedish mutation) transgene expressed in a mouse line resulted in the tgDimer mouse, which produces only highly soluble A β dimers, and showed impaired learning, memory deficits, and inhibition of long-term potentiation (88). Detailed information about the tgDimer mouse will be provided in section 1.4.1.

1.3.2. PRION-LIKE SPREADING

It is established that A β plaques may arise *de novo* from spontaneous seeds (nuclei) or may spread by the disintegration of existing fibrils into smaller ones providing seeds and thus accelerating A β -related neuropathology. This replication of proteins mimics classical prion replication (89) and could be an explanation for the aggregation and spreading of A β . So far, the underlying mechanism of how initial A β triggers nuclei that subsequently spread throughout the brain is still unclear.

The transmissibility of prions was first established in studies of transmissible spongiform encephalopathies (TSE) or prion diseases. TSE are caused by prions, the infectious conformation of the prion protein (PrP), which affect the nervous systems and give rise to a range of rare incurable transmissible diseases in a variety of mammals. Bovine spongiform encephalopathy (BSE), scrapie of sheep, and CJD of humans are the most prominent prion diseases. Mammals affected show spongiform degeneration with vacuoles (4).

In these diseases, the infectious prion replicates by converting the normal alpha-helical cellular prion protein PrP^C into the β -sheet rich and aggregation-prone PrP^{Sc}, a proteinase K-resistant abnormal isoform of PrP^C (89). The prion protein gene *PRNP* encodes for PrP^C, which is a glycosylphosphatidylinositol (GPI)-anchored membrane protein that is mostly expressed by neurons (90). Events like spontaneous misfolding, genetic mutation of the human *PRNP*

gene or exposure to an external prion can lead to the conversion of PrP^C into PrP^{Sc} (3). Studies have suggested that PrP^{Sc} aggregation is preceded by a conformation change from a structure composed mostly of α -helical elements to a β -sheet rich conformation, which is thought to be the disease-associated form (91). The β -sheet rich form can interact and convert the normal α -helix rich form to the β -sheet rich form in a template-directed manner, called permissive templating or seeding (92, 93). In addition, the β -sheet rich form is also able to aggregate into amyloid-like fibrils (94). PrP^C conformation to PrP^{Sc} can be replicated *in vitro*, by adding seeds of aggregated PrP^{Sc} to PrP^C (95).

Prion aggregation follows a seeding-nucleation process, starting with the formation of ‘nuclei’ or seeds, the so-called nucleation/lag phase, which involves partially misfolding of the protein leading to small oligomers. This is followed by the much faster elongation/polymerization phase, in which the aggregation increases in an exponential manner, and is sped up by preformed seeds. Adding preformed seeds increases the aggregation, leading to a shorter lag phase (Figure 4) (96, 97). Possible intervention mechanisms in the prion aggregation process are blocking misfolded protein, facilitating folding of native proteins, blocking the disintegration of fibrils or blocking propagation (98).

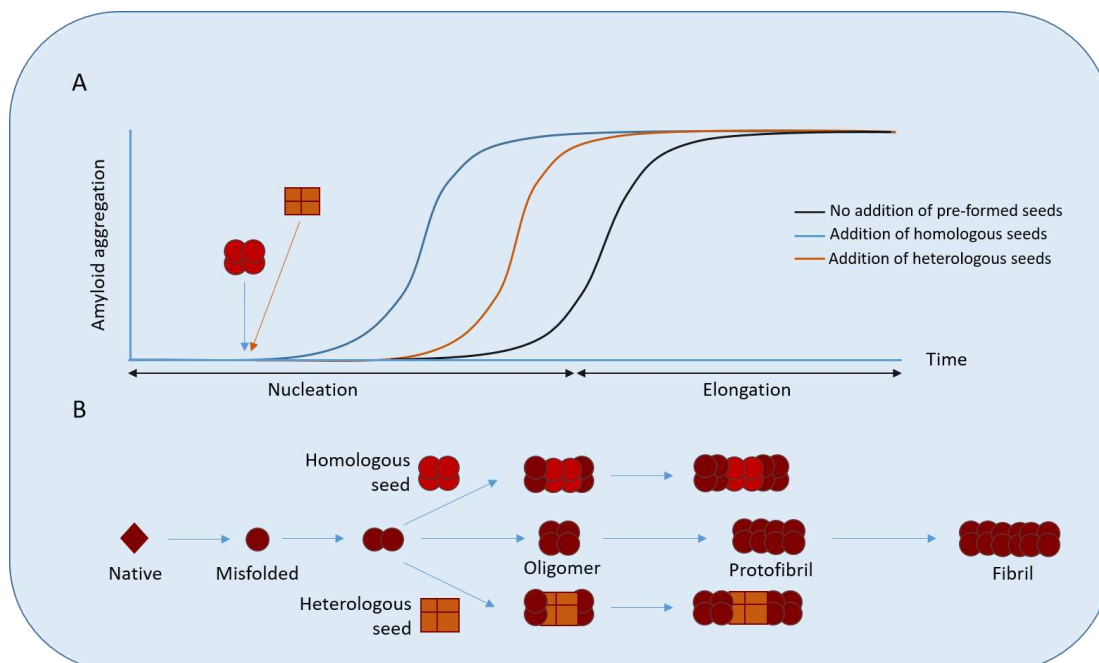


Figure 4. Seeding-nucleation model of amyloid aggregation. (A) Amyloid aggregation follows the seeding-nucleation polymerization model, which is divided into two phases. The first phase is the nucleation/lag phase, and the second phase is the elongation/polymerization phase. The addition of pre-formed seeds reduced the lag phase. (B) Seeding can occur by adding a seed (nuclei), that occurred spontaneously or by the disintegration of existing fibrils. They can have different conformations, either similar to the nuclei (homologous seed), or a different conformer (heterologous seed). Adapted from: Cross-Seeding of Misfolded Proteins: Implications for Etiology and Pathogenesis of Protein Misfolding Diseases (96)

Prions are found with many distinct biochemical properties, called prion strains. Prion strains, which differ in the conformation and/or the assembled states of the prion protein and can result from the same amino acid sequence, cause diseases with specific characteristics when inoculated into new hosts. These differences can be for example duration of incubation time, PrP^{Sc} distribution pattern, and severity of lesions in the brain (99-102).

After the discovery of prions, researchers speculated that the brains of patients with other neurodegenerative diseases might also harbour causative agents with prion-like properties (103, 104). The seeding-nucleation process is similar to the process that for example also occurs to the A β peptide that aggregates into amyloid fibrils (105), where the initially misfolding of the monomeric peptide is followed by the formation of small oligomers and eventually nucleate the formation of larger amyloid fibrils.

In AD, the progressive spread of A β through the brain is an indication of a prion-like mechanism of propagation (106). Already in 1993, researchers discovered that A β load is increased in the brains of non-human primates after intracerebral inoculation with AD brain homogenates (107), however, the incubation period was long and the causative agent remained uncertain. In later years, researchers showed that A β aggregation is expedited in transgenic mice expressing human APP by the presence of preformed A β aggregates obtained from brain extracts from human AD patients or aged AD mice models (108-111). Furthermore, administration of extracts containing A β intraperitoneal induced A β aggregation in the brain blood vessels (109). No plaques were found in non-transgenic mice inoculated with A β containing extracts. These findings indicate that A β seeding requires both a donor extract containing A β and a host that is capable of generating A β plaques. Depleting the brain extracts of A β using antibodies inhibited the seeding effect, pointing toward that the presence of A β is essential for seeding.

To determine whether A β deposits can also be generated *de novo* in relatively resistant animals, A β seeding experiments were undertaken in APP-transgenic mice (112) and rats (113) that do not generate A β plaques within their normal life spans. In both instances, A β deposition was induced in the brain after a suitable incubation period, suggesting that in an experimental setting, misfolded A β aggregates can behave similarly to infectious prions. Next to that, A β seeds, which are minute amounts of misfolded A β , and prions share several other similarities. For example, A β has been shown to transfer from neuron to neuron (114) and can

form a strain-like variant *in vitro* (115). Furthermore, A β seeds vary in size and sensitivity to proteinase K (116), and can, as mentioned before, spread systematically in a prion-like manner within the brain (117).

Furthermore, the clinical and pathological heterogeneity of AD could be explained by the existence of A β strains, which are increasingly well established (118-124). Differences in A β plaque morphology are likely a result of A β posttranslational modification, variation of A β length or mutations in for example the *APP* gene. Inoculation of a transgenic APP mouse with two different brain extracts containing A β resulted in the induction of different morphology of A β deposits (108). The injection of A β rich brain extract in different brain regions led to induced A β plaques with differences in the amount and type of amyloid (125).

In the study by Watts et al., the authors found evidence for distinct strains of A β prions in brain homogenates prepared from patients with heritable AD. Certain properties of the A β prion strains, such as the relative amounts of cerebrovascular A β ₃₈ deposition, were maintained after multiple passages in transgenic mice. The existence of distinct A β strains and their ability to be serially propagated in mice corresponds with prions strain properties (123). In addition, different preparations of A β ₄₀ and A β ₄₂ resulted in differences in the physical and biological properties of amyloid fibrils. Inoculation of mice with these preparations of synthetic A β ₄₀ or A β ₄₂ showed the development of a different number of plaques, plaque size and severity of astrogliosis (124), and they suggested that all A β isoforms may adopt distinct conformations, each of which undergoes self-propagation. This molecular mixture of A β prion strains may be partially responsible for the variations in clinical and pathological presentations observed in patients with AD.

The prion-like mechanism could also apply to other pathogenic proteins as mentioned before. Similarly to A β , tau spreads to the brain in a topological manner, which was first reported by Braak in 2003 (126). Emerging experimental evidence studies showed that tau seeds, derived from, for example, brain homogenates of tauopathy patients, tau transgenic mice, conditioned media from tau-aggregate producing transfected cells, or recombinant tau were able to induce aggregation of soluble tau (127-130). Interestingly, tau seeds are, similarly to A β and prions, of many sizes, of which the small, soluble assemblies are the most effective seeds (131).

1.4. ANIMAL MODELS OF ALZHEIMER'S DISEASE

Animal models of AD are critical to gaining insights into the relationship between the biochemical and pathological changes in the brain and the impact on memory and behaviour. Rodents, like mice and rats, do not naturally develop either A β or tau pathology. Aged dogs and non-human primates naturally demonstrate accumulation of A β plaques but not neurofibrillary tangles, while transgenic A β -based mouse models fail to exhibit abnormal tau fibrils (132-137). Furthermore, animal models of tau pathology fail to demonstrate A β pathology. To model AD in rodents, both genetic and non-genetic approaches are being used, alone or in combination.

The most frequently used species to model AD is the mouse (*Mus musculus*), because of their high gene homologies to the human genome, the ease of genetic manipulation and breeding and the relatively low cost of husbandry. The most commonly used AD-related animal models are transgenic mice that overexpress human genes associated with EOAD, such as *APP*, *PSEN1* and *PSEN2*. Because of sequence differences between mice and human *APP*, within the A β sequence, mice do not form amyloid plaques (138). Therefore, the expression of human *APP* is needed for amyloid plaque formation. Transgenic mice expressing wild type human *APP* showed increased A β production, however, failed to consistently show extensive AD-associated neuropathology. Contrarily, mice expressing human *APP* containing mutations associated with EOAD showed consistent A β -related AD pathology and associated cognitive impairment (139).

Of the more than 20 pathogenic mutations that have been identified in *APP*, several have been expressed in transgenic mice. For example, the V717I 'London' mutation, which was the first mutation linked to EOAD, increases the A β_{42} /A β_{40} ratio by increasing A β_{42} levels with little effect on A β_{40} levels (40), similar to the V717F 'Indiana' mutation (140). The K670D/M671L 'Swedish or APP_{swe}' mutation results in an overall increase of A β_{42} and A β_{40} levels (141). The E693G 'Arctic' mutation is also modelled in transgenic mice, this mutation results in A β_{40} that readily forms protofibrils at a faster rate compared with wild type A β_{40} (52).

The well-known AD mouse model, the tgAPP23 mouse-line, expresses human APP₇₅₁ with the familial Swedish mutation under the control of the neuronal murine Thy1.2 promoter. A β plaques are first observed at 6 months of age, and after 24 months, 25% of the neocortex and

hippocampus are occupied with A β plaques, with female mice displaying plaque development earlier than males. Neuronal loss is observed in the hippocampus region (142). At 3 months of age, these mice already show deficits in spatial memory, measured with the Morris water maze, becoming more severe with age (143, 144).

Another widely used mouse model bearing mutations in the human mutant *APP* gene is the tgCRND8 transgenic mice, which also express human APP with the Swedish mutation and in addition the Indiana mutation. In these mice, the levels of 'human' A β ₄₀ and A β ₄₂ increases, with A β ₄₂ being more present (145). Already at 9-10 weeks of age, diffuse and compact plaques are detected, followed by activated astrocytes around the plaques at 13-14 weeks of age (146). Cognitive deficits are observed in the reference memory version of the Morris water maze, at 3 months of age (145).

A major limitation of transgenic mouse models is the lack of the widespread neurodegeneration and brain atrophy seen in AD. Another major limitation is the lack of development of neurofibrillary tangles. The development of mouse models with both plaques and tangles followed. These models rely on the concurrent expression of mutated forms of *APP*, *MAPT* and *PSEN1* or *PSEN2* for plaque and tangle formation in the same model. The downside here is that the development of both hallmarks is only observed at the old age of these models.

By artificial manipulation such as surgical procedures, administration of some drug or injection of brain lysates, also non-genetic models can display AD features. For example, brain trauma seemed to elicit an increase in amyloidogenic enzymes such as BACE1, resulting in amyloidosis (147). Another method used is intracranial stereotaxic injection-based models, to understand what triggers AD pathology or demonstrate the inducible nucleation of protein aggregates or enhance AD pathology. For example, intraperitoneal injection of A β aggregates has been shown to induce cerebral brain amyloidosis (109). The injection of oligomeric A β into the dorsal hippocampus leads to long-lasting memory impairment, corresponding to the early stages of AD (148). Furthermore, intracerebral infusion of A β containing brain extracts into B6/P301L tau transgenic mice resulted in induced tau pathology in the hippocampus but also other brain regions well beyond the injection sites. Infusion of A β containing brain extracts into a double transgenic mouse, B6/P301L crossed with tgAPP23 mice, revealed next to tau pathology, also a high A β plaque load (149).

1.4.1. THE TGDIMER MOUSE

In this thesis, the tgDimer mouse (88) was used for the studies described below. This mouse was developed using the same expression vector that led to the generation of the tgAPP23 model and is based on the same mouse strain (C57BL/6). In addition to the Swedish mutation, the mutation for A β -S8C (APP-S679C) was introduced into the expression vector. This construct was microinjected into C57BL/6N embryos, which resulted in the tgDimer mouse. This mouse shows a 7-fold overexpression of APP and generates high levels of A β -S8C dimers, but not A β monomers or higher structured oligomers within the brains. The A β ₄₀ and A β ₄₂ levels in the brain remained constant during their lifetime, similar to young tgAPP23 mice that had not yet developed A β plaques. No insoluble A β or A β plaques were detected in aged tgDimer mice after biochemical fractionation of brain extracts. There was no change in phosphorylation of endogenous tau in biochemical analysis of brain homogenates, or immunohistochemical staining (88).

The cognition of the tgDimer mice was tested in the Morris water maze, a task used to assess hippocampal dysfunction-related deficits in spatial learning and memory. A learning deficit was observed in escape time from the water maze, at both 7 and 12 months of age. Adult tgDimer mice needed significantly more time to find the platform compared with C57BL/6N mice on several days during testing. Interestingly, the aged tgDimer mice showed no savings from the learning level achieved at 7 months of age and did not exhibit a learning curve over the 9 days of testing, implying ageing-related progression in the severity of cognitive decline (88).

Evaluating this mouse model suggests that A β dimers in the absence of plaques may play a causal role in the learning and memory deficits described in plaque-bearing AD models. More in-depth behavioural analysis of this model showed impaired non-selective attention, motor learning as well as anxiety- and despair-related behaviours. TgDimer mice also had lower serotonin turnover rates in the hippocampus, ventral striatum and amygdale relative to wild type controls. Aged tgDimer mice had less hippocampal acetylcholine than adult tgDimer mice. This data suggests that A β dimers contribute to neurotransmitter dysfunction and behavioural impairments, which are hallmarks of the early stages of AD (150).

1.4.2. BEHAVIOURAL TASKS

Rodent behavioural tests play an important role in the evaluation of sensory-motor function, anxiety-like and depressive-like behaviour, and various forms of cognitive function in animal models. Cognition refers to the learning and memory processes. Tasks on cognitive behaviour analyse the capability of an animal to form representations of the outer world that lead to altered behavioural performances on subsequent confrontation with distinct stimuli and situations (151).

Typically, to test cognition in mice but also rats, deprivations or stimulations have to be employed to motivate the animals to participate in a learning task and to display memory-related behaviour. Over the last years, certain cognitive tests have become leading paradigms to study memory processes that rely on distinct brain structures. For example, to study hippocampal function, which coordinates many independent sensory features, learning tasks that require identification of the spatial and temporal relationships between distinct stimuli of different modality, texture or shape, are applied. Reversal learning is also a process that is sensitive to changes in hippocampus function, although hippocampus formation is only critical for memory recall over 3 to 4 weeks (152).

One of the most used tasks is the Morris water maze, which is used to study and compare learning and memory in rodents and is based on a rodent's aversion to water. It consists of a water-filled pool with a hidden escape platform just beneath the surface of the water and spatial cues on the wall surrounding the pool. In several trials, the animal has to learn where to find the platform to escape the water. Spatial memory is separately assessed in a probe trial without the platform (153).

Another widely used task to study spatial learning and short-term memory is the Y-maze. In this maze, the rodents are allowed to explore all three arms of the maze and are driven by the innate curiosity of rodents to explore previously unvisited areas (154). Other mazes, like the Radial arm maze or T-maze, are used to assess reference memory and working memory (155).

The elevated plus-maze is one of the most popular tasks used to evaluate anxiety-like behaviour in rodents (156, 157). It is a maze with four arms; two open and two enclosed, in a

plus shape. Anxiety is assessed by using the ratio of time spent on the open arms to the time spent on the closed arms (158).

In the last years, automated testing has gained increased attention to study animal behaviour because of its many advantages. Automated testing reduces the influence of the experimenter on the animals, reduces the workload, and is believed to increase reproducibility. Animals can be tracked for extended test durations and can be tested during their active phase. Limitations are the amount of data produced, as well as the limited number of animals that can be analysed in a single unit. Animal tracking in video-based tracking systems is mostly limited to one animal at a time, however, by the application of different fluorescent dyes to the animals' fur, tracking of individual animals within a group can be achieved (159). Fully automated testing can be carried out in the animals' home cage (160, 161) with test equipment added to the home cage, for example in combination with the IntelliCage (161) as well as the PhenoTyper (160).

The PhenoTyper cage is an instrumented observation cage developed by the company Noldus, (the Netherlands). In this cage, behaviour can be tracked by video and hardware actions can be triggered by the location of the mouse (162). The CognitionWall is an add-on to the PhenoTyper cage and is the basis for operant cognitive tasks performed in the PhenoTyper cage. The CognitionWall is a wall with three entrances, which is placed in front of the pellet dispenser, and enables discrimination learning and reversal learning without human intervention and the need for food deprivation (Figure 5) (163). This cognitive test can be used to assess cognitive impairments in mouse models at an earlier age, and in much less time than conventional cognitive tests. This paradigm is more sensitive than the standard used Morris Water Maze and showed that APP/PS1 mice have impaired learning at 6-7 months of age compared with wild type mice (163).

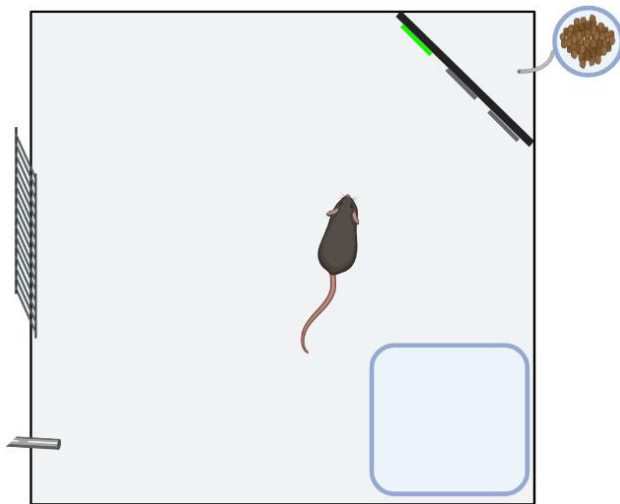


Figure 5. Schematic bird's eyes view of the Phenotyper cage. The CognitionWall is placed in the upper right corner. The green (left) entrance is the rewarded entrance. After entering the Cognitionwall via the rewarded entrance, the pellet dispenser will release a sucrose pellet. On the left side of the cage, the food tray and the water bottle are located. In the right bottom corner, there is a shelter in which the mice usually sleep. Created with BioRender.com

Rodents show species-specific behaviours, meaning behaviours mostly related to their social and natural environment (151). Examples of species-specific behaviours are grooming, nest building, play and burrowing. These behaviours rely on intact neuronal function, for example, for nest building the limbic system and medial frontal cortex are needed, and for grooming the cortex, striatum and cerebellum (164). The burrowing task is based on the species-typical behaviour of mice to spontaneously displace pellets from tubes within their home cage. With experience, the mice show some tendency to increase their burrowing, although not significantly (165). It is said to be a sensitive assay for models of prion disease (166, 167) but also in AD transgenic mice (168).

Burrowing can be seen as the equivalent of so-called "activities of daily living (ADL", an important clinical aspect when handling AD patients. A decrease in burrowing is explained as a readout for the animals' general condition and wellbeing and to be able to detect early signs of neurological disorders. In patients with AD, their functional status, reflected by measures of ADLs, deteriorates as AD progresses (169, 170).

1.4.3. *IN VIVO* BIOLUMINESCENCE IMAGING (BLI)

In the brains of AD patients, an increase in reactive astrocytic gliosis is observed as a response to A β plaque deposition. Reactive astrocytes are associated with A β plaques in various transgenic mouse models of AD (145, 171-173). A commonly used marker for reactive astrocytes is the glial fibrillary acidic protein (GFAP). By using a transgenic mouse, the tg(Gfap-luc) mice, which expresses the firefly luciferase (luc) under the control of the murine Gfap promoter, researchers can follow reactive astrocytic gliosis *in vivo*. The tgGfap-luc mouse is one of the mouse models that can be used for bioluminescence imaging (BLI) and carries a 12 kb fragment of the Gfap promoter (174).

Expression driven by the Gfap promoter is primarily observed in the brain, however basal expression was also observed in the ears, paws and tails of non-treated mice. Up-regulation of Gfap mRNA and hence, luciferase protein, can be visualized in living mice after injection with the luciferase substrate D-luciferin. The emission wavelength of the firefly luciferase can be imaged as deep as several centimetres within the tissue, which allows at least organ-level resolution. With this method, the progress of disease-inducing astrogliosis can be followed without killing the experimental animal.

With BLI and the Gfap-luc mouse, researchers could already diagnose prion disease in mice at ~55 days post-inoculation, while neurological dysfunction could only be observed at ~117 days post-inoculation (175). They then wondered whether they could also use the Gfap-luc mouse in combination with transgenic AD mouse models. First, they found a correlation between Gfap and A β levels in the brains of tgCRND8 and tgAPP23 mice, suggesting that Gfap levels can be used to assess A β deposition in the brains of these mice. They then crossed the AD mouse models with the tgGfap-luc mouse and observed an increase in BLI signal in the bigenic tgCRND8/Gfap-luc mice compared with age-matched tgGfap-luc controls. Similarly, tgAPP23/Gfap-luc mice also showed a higher BLI signal compared with age-matched tgGfap-luc mice. Inoculation with A β seeds reduced the time until the onset of increased BLI signals to 9.5 months compared with 14.5 months in non-inoculated tgAPP23 mice (176).

The crossing of the Gfap-luc mouse with mouse models for AD, the tgCRND8 and tgAPP23 mice showed an age-dependent increase in brain bioluminescence signals, which reflected the development of neuropathological changes in the brains and by inoculating these mice with

brain homogenates containing A β , they could accelerate the development of neuropathological changes (176, 177).

1.5. OBJECTIVES OF THE RESEARCH

As described in the sections before, the interaction of different A β species on AD plaque heterogeneity is not well understood. To investigate how A β plaque heterogeneity may relate to interactions of different A β conformers, the influence of A β dimers on A β plaque formation was investigated. An *in vitro* study showed the effect of synthetic A β_{42} -S8C dimers on the aggregation of wild type A β_{42} . The following research questions were addressed in this study:

- 1) How do soluble A β -S8C dimers relate to the heterogeneity of amyloid plaque pathology *in vivo*?
- 2) Do A β -S8C dimers modulate induced seeded nucleation *in vivo*?
- 3) Is the emergence of A β -plaques related to behavioural deficits measured by both a learning and memory task as well as species-specific behaviours?

2. STUDIES I, II

2.1. INVESTIGATE HOW SOLUBLE ABETA-S8C DIMERS RELATE TO THE HETEROGENEITY OF AMYLOID PLAQUE PATHOLOGY

The interaction of insoluble Amyloid- β with soluble Amyloid- β dimers decreases Amyloid- β plaque numbers

Else F. van Gerresheim¹ | Arne Herring² | Lothar Gremer^{3,4,5} | Andreas Müller-Schiffmann¹ | Kathy Keyvani² | Carsten Korth¹

¹Department of Neuropathology, Heinrich Heine University Düsseldorf, Düsseldorf, Germany

²Institute of Neuropathology, University of Duisburg-Essen, Essen, Germany ³Institute of Physical Biology, Heinrich Heine University Düsseldorf, Düsseldorf, Germany

⁴Institute of Biological Information Processing (IBI-7) and JuStruct, Jülich Center for Structural Biology, Research Centre Jülich, Jülich, Germany

⁵Research Center for Molecular Mechanisms of Aging and Age-Related Diseases, Moscow Institute of Physics and Technology (State University), Dolgoprudny, Russia

Neuropathology and Applied Neurobiology

10.1111/nan.12685

Impact Factor 8.1

Author's contribution (70%)

- Conceiving and planning the study
- qPCRs for gene dose determination
- Fractionation studies
- Measurement of A β ₄₀ and A β ₄₂ levels using ELISA
- Preparation of A β ₄₂ and A β ₄₂-S8C dimers (together with Dr Lothar Gremer)

- Performing ThT assays
- Western blots
- Statistical analysis
- Co-writing of the manuscript

The study presented here aimed to discuss how soluble A β -S8C dimers relate to the heterogeneity of amyloid plaque pathology by crossing the tgDimer mouse to the tgCRND8 mouse, which develops amyloid plaques already at 3 months of age.

The number and size of amyloid plaques can vary between patients with AD and often do not correlate with cognitive deficits. Previous studies implicated soluble A β oligomers as the primary neurotoxic species, which are also better correlates of cognitive decline. Molecular interactions between soluble A β oligomers and insoluble A β have been difficult to study due to the equilibrium that exists between the A β species. Here, we investigated how A β plaque heterogeneity may relate to interactions of different A β conformers. To this end, the tgDimer mouse, expressing soluble A β -S8C dimers was crossed with the tgCRND8 mouse and the number of A β plaques, and levels of A β were quantified.

In 3 and 5 months old tgCRND8/tgDimer mice, reduced numbers of diffuse and core plaques were observed in the neocortex and hippocampus compared with tgCRND8 mice. Adding A β ₄₂-S8C dimers to the aggregation-prone wild type A β ₄₂ *in vitro*, increased the time of seeding onset supporting the idea that A β dimers inhibit fibril formation but not growth.

This study showed that A β -S8C dimers decrease amyloid plaque seeding *in vivo* and *in vitro*, and contribute to the clinical amyloid plaque heterogeneity observed in AD patients.

Keywords: Amyloid-beta, Alzheimer's disease, dimer, fibril formation

2.2. INVESTIGATE WHETHER A β -S8C DIMERS MODULATE SEEDING NUCLEATION *IN VIVO*

Soluble amyloid- β dimers are resistant to amyloid- β prions suggesting anti-prion properties

Else F. van Gerresheim¹, Andreas Müller-Schiffmann¹, Sandra Schäble², Bastijn Koopmans³, Maarten Loos³, Carsten Korth^{1*}

¹Department Neuropathology, Heinrich Heine University Düsseldorf, Düsseldorf, Germany

²Comparative Psychology, Institute of Experimental Psychology, Heinrich Heine University Düsseldorf, Düsseldorf, Germany

³Sylycs (Synaptologics BV), Antonie van Leeuwenhoeklaan 9, Bilthoven, The Netherlands

Neuropathology and Applied Neurobiology, submitted

Impact factor 8.1

Author's contribution (90%)

- Installing behavioural set-up
- Complete execution of experiments and data analysis of the study
- Co-writing the manuscript

In the second study, the effect of A β -S8C dimers on A β prion-like seeding was studied. A β seeds were injected into the brains of tgDimer mice, as well as negative and positive control mice, to investigate whether A β -S8C dimers could modulate the A β aggregation.

A β , the major component of amyloid plaques in AD, has been shown to follow prion-like replication from A β seeds. Since amyloid plaques are the consequence of decade-long aggregation of A β oligomer precursors, a common assumption was that this process can be accelerated by providing precursors or A β seeds.

To investigate whether A β dimers also influence seeded nucleation or prion-like spreading, the tgDimer mouse was crossed with the Gfap-luc mouse and stereotactically inoculated A β

seeds into the brain. The tgDimer mouse was resistant to A β prions and did not develop astrogliosis or amyloid plaques in contrast to the positive control, the tgAPP23 mouse, that did develop astrogliosis and AD pathology as previously described. Behavioural experiments showed no cognitive decline in tgDimer mice. This data suggests that A β -S8C dimers slow down or prevent A β aggregation and have anti-prion properties.

Keywords: Alzheimer's disease, A β -S8C dimer, aggregation, anti-prion

3. CONCLUSIONS

The A β -S8C dimer's inhibitory role on A β seeding is discussed in this thesis. As described in Study 1, the presence of A β -S8C dimers resulted in a lower number of A β plaques in tgCRND8/tgDimer mice compared with tgCRND8 mice but not in size. Corroborating cell-free *in vitro* seeding experiments demonstrated that A β -S8C dimers slowed wild type A β ₄₂ aggregation. These findings are notable because they not only show that A β dimers, the oligomeric A β species likely most abundant in the brains of AD patients, inhibit A β seeding but also that A β plaque seeding and growth follow different dynamics. Nuclei (seed) formation requires a series of events that costs energy and is thermodynamically unfavourable, whereas the addition of monomers to a growing protofibril is thermodynamically favourable (178). The addition of a preformed seed can accelerate fibrillization. These seeds can be formed by the interactions of either the same (homologous) or different amino acid sequences (heterologous) (96, 178, 179). Previous research reported that A β dimers are not able to form nuclei by themselves (87), however, do associate with existing wild type A β plaques (88). A β -S8C dimers thus intercept nucleation, thereby inhibiting growth, in the initial stages of seeding, when the nuclei are unstable (178).

Recently, a study was published that supports our *in vivo* and *in vitro* data. In that study, a single-chain dimeric variant of A β ₄₀, with two A β ₄₀ units, named dimA β , connected via a flexible glycine–serine-rich linker, readily formed globular oligomers and curvilinear fibrils (80). The addition of dimA β to A β monomers progressively slowed rigid fibril (RF) formation in a similar cell-free *in vitro* assay as used in our study, which was evident in the increasing RF lag periods. By analogy, A β -S8C dimers may interfere with fibril formation, by inhibiting nucleation (Figure 6).

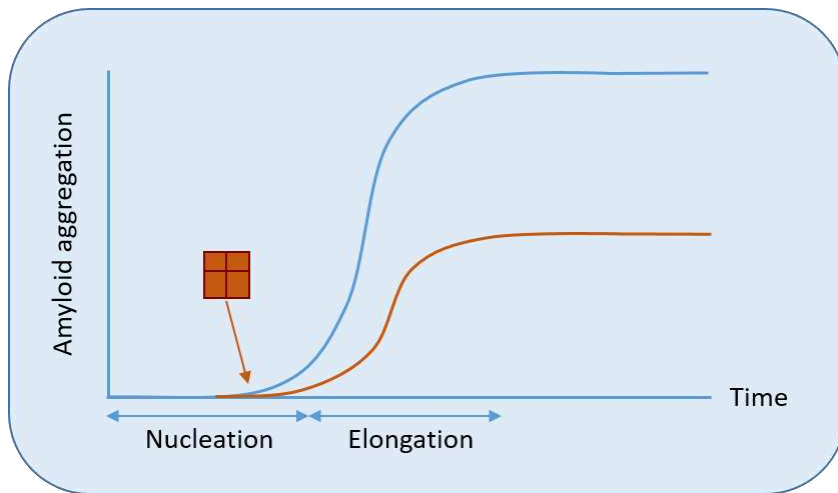


Figure 6. Seeding-nucleation model of amyloid aggregation and the addition of A β -S8C dimers. Addition of A β -S8C dimers to inhibit nucleation and thereby slow down amyloid aggregation (orange line). The solid line indicates aggregate formation.

In Study 2, we explored the potential of the A β -S8C dimer to propagate seeds of brain-inoculated insoluble A β to induce full A β pathology in the otherwise A β plaque-free tgDimer mice. After inoculation of tgDimer mice with A β seeds, we observed that this transgenic mouse model was resistant to developing astrogliosis and AD pathology. Behavioural analysis of the inoculated tgDimer mice using the CognitionWall showed no cognitive decline. Histological analysis revealed the absence of A β plaques in the brains of inoculated tgDimer mice. In contrast, the tgAPP23 mice, inoculated with the same A β seeds in parallel as a positive control, did show astrogliosis and amyloid plaques after inoculation with A β seeds. Our findings presented here indicate that A β -S8C dimers are resistant to A β prion propagation by seeded nucleation *in vivo*.

Since the term 'prions' was coined by Prusiner in 1982 (89), the term has been used to mention 'infectious proteins', regardless of the species. Because of the presence of endogenous yeast prions (180-182), yeast has been an excellent model system to study prion replication and seeding between heterologous amyloid proteins (183). Yeast prions are also known to exist as biological variants, exhibiting variable phenotypes, and aggregation and seeding abilities (184-186). The process of prion replication in yeast showed that cellular systems could act at various levels to block prion infection, for example, to block prion formation, correct most prions formed, or prevent the distribution of prions to the next generation. These cellular systems, or proteins that, at normal levels in cells could cure prions, showed that this cellular system is an intricate system regulated by both homologous and heterologous factors, with the inhibiting ones termed 'anti-prions' (98).

Based on above data, the A β -S8C dimer could have anti-prion like properties, since it slows down the A β ₄₂ aggregation *in vivo* and *in vitro*. A β -S8C dimers also seem to be resistant to A β seeding, as no A β pathology was observed in the brains of tgDimer mice after seeding. Because of the same nature of the A β -S8C dimers compared to wild type A β , the A β -S8C dimer could be termed a homologous 'antiprion' that inhibits A β prion propagation *in vivo* and *in vitro*.

The data presented here broaden our knowledge on the A β -S8C dimer and the tgDimer mouse. With the introduction of a cysteine at place 8 instead of serine, the A β -S8C dimer was developed. After introducing this mutation to inducible CHO cells, purified dimers could be obtained (87). Whole cell patch clamp analysis showed that purified A β -S8C dimers are highly synaptotoxic. Introducing the mutation in a mouse model resulted in the development of the tgDimer mouse. Studies showed that the tgDimer mouse does not exhibit AD pathology during its lifetime, even though the tgDimer mouse overexpresses mutant human *APP*. No insoluble A β or A β plaques were detected in aged tgDimer mice after biochemical fractionation of brain extracts. There was no change in phosphorylation of endogenous Tau in biochemical analysis of brain homogenates, or in immunohistochemical staining. TgDimer mice showed hippocampal dysfunction-related deficits in spatial learning and memory in the Morris Water Maze (88). More in-depth behavioural analysis of this model showed impaired non-selective attention, motor learning as well as anxiety- and despair-related behaviours (150).

The tgDimer mouse solely expressing A β -S8C dimers, shows no AD pathology during their lifetime, however does show behavioural deficits characteristic for the early stages of AD, likely caused by the neurotoxic soluble A β dimers. However, probably because of the exclusive presence of A β -S8C dimers, the tgDimer mouse is resistant to A β seeding and aggregation. Thus, while A β -S8C dimers inhibit seeding and aggregates, they are nevertheless highly synaptotoxic and cause learning and memory deficits in the Morris Water Maze assay.

The presented results should now lead to a more critical evaluation of A β -plaques as hallmarks of AD since these are subject to modulation by homologous oligomeric species. In how far A β -dimers are valuable targets for developing tailored drugs remains to be established.

4. ADDITIONAL DATA

4.1. BURROWING AS A MEASURE OF ACTIVITY OF DAILY LIVING IN AD

Behavioural experiments in neurodegenerative diseases provided invaluable information on the progression of the disease. Many of these behavioural experiments mentioned before, take up an incredible amount of time, money, workforce and animals. Another disadvantage is that animals need to be externally stimulated or food-deprived.

The development of a species-specific behavioural task would add to the field of behavioural experiments. Burrowing is a species-specific task, resembling 'activities of daily living' (ADLs) in AD patients. ADLs is a term to describe fundamental skills required to care for oneself, for example, eating, bathing, getting dressed, and mobility. As AD progresses, AD patients lose their ability to perform ADLs. It would be of great advantage if cognitive decline and AD progression in AD mouse models could be tested by this simple and low-cost burrowing task. To this end, the tgDimer mice, which shows early cognitive deficits in the absence of A β plaques and compared their burrowing behaviour with wild type mice at 7 months of age in the Morris Water, were tested with the burrowing task and compared with control groups.

Introduction

Burrowing is a species-specific behavioural task, developed by Robert Deacon as a laboratory test in Oxford (187). It emerged from the need to develop a mouse hoarding paradigm. In the hoarding paradigm, a distant food source has to be coupled to the home cage by a connecting passage (188, 189). To do this, a hole had to be made in the home cage to connect it to a passage and food source. Researchers then considered putting the food source inside the cage. Initially, a container filled with food pellets was placed in the home cage. The next morning, the container was emptied, with the pellets deposited in front of the container entrance instead of placed away when a mouse is hoarding food pellets. After observations, the researchers discovered that the mice were performing digging (burrowing) movements, to empty the container.

Studying scrapie (PrP^{Sc}) infection, they found impairment in burrowing in mice infected with scrapie. During immunohistochemical analysis, they found a loss of synaptic density in the hippocampus. This was the first time that cognitive impairment was found already at 12 weeks after infection, normally clinical signs can earliest be observed at 22 weeks after infection (167). These findings resulted in the testing of other species-typical behaviour tests, hoarding and nesting, which also seemed to be impacted by lesions of the hippocampus (190). The advantages of burrowing are simplicity and low costs. In terms of animal welfare, it seems to be less stressful and does not need food or water rationing or other motivational cues.

AD progression is often measured in the loss of the ability to perform 'activities of daily living' (ADLs). These activities include getting dressed, washing, and in general taking care of themselves (191, 192). Species-specific behaviour, such as burrowing, could resemble ADLs in humans and can be an easy way to monitor disease progression in animals (193).

We used the tgDimer mice, which show early cognitive deficits in absence of A β plaques (88) and compared their burrowing behaviour with wild type (WT) littermates. Furthermore, we tested the paradigm on tgDimer, tgAPP23 and WT mice inoculated with A β seeds, and tgDimer mice inoculated with wild type brain homogenates.

Methods and material

Mice. TgDimer mice express human APP₇₅₁ with the Swedish mutation and the dimer mutation within the A β domain (S679C) that generates A β -S8C dimers (88). For the first part, homozygous mice and their WT littermates were used. For the second part, tgDimer mice were crossed with the tgGfap-luc mice, expressing the firefly gene under the Gfap promoter (174). TgAPP23 mice express human APP₇₅₁ with the Swedish mutation under the Thy1.2 promoter (171), which were also crossed with the tgGfap-luc mice on an FVB/N background. Wild type/Gfap-luc mice were used as a control group. Mice were inoculated with brain homogenate containing A β or not (WT). Animal experiments were performed in accordance with the German Animal Protection Law and were authorized by local authorities (LANUV NRW, Germany). Mice were housed under standard laboratory conditions with lights on from 7 a.m. to 7 p.m. and with water and food provided *ad libitum*. Both males and females were used in this study.

Burrowing. The burrow was constructed by cutting a 68 mm diameter drainpipe into 20 cm long pipes. One side was closed with an end cap. Screws (5 cm long) were used to raise the other end of the tube 3 cm off the floor. Two holes were drilled 1 cm from the open end of the burrowing tube at an angle of 90° and the screws were inserted and tightened (165).



Figure 7. Example of a burrow. A 68 mm diameter tube with a length of 20 cm long. One side is closed with an end cap. Screws (5 cm long) are used to raise the other end of the tube 3 cm off the floor.

Burrow diameter is important, as it has been observed that mice in the wild 'burrow cleaned' mainly from burrows similar in size (194). The tube is filled with 200 g food pellets, which the mice are familiar with. The closed end of the tube is placed against the wall of the cage. During the burrowing period, food is removed from the food tray of the cage, since it may distract the mice. Water is available during the task. After 2 hours, the weight of food pellets displaced from the tube was measured. The next morning, the weight of the displaced food pellets was measured again. Generally, the 2 hours measurement is more sensitive, as overnight almost all food will be displaced (165).

Results

For the first group, mice burrowed for the first time at 6 months of age. TgDimer mice (n=6) burrowed less than WT mice (n=8) although not significantly less after 2 hours. At 13 months of age, tgDimer mice (n=10) burrowed significantly less than their WT littermates (n=10) (Figure 8, $p=0.0011$). In both groups, the same number of naive mice was added per genotype that had not burrowed before at the 13 months measurement. At 18 months, tgDimer mice

(n=8) burrowed less compared with WT mice (n=8) measured after 2 hours, although not significantly less (Figure 8). In this batch of mice, no age effect was observed.

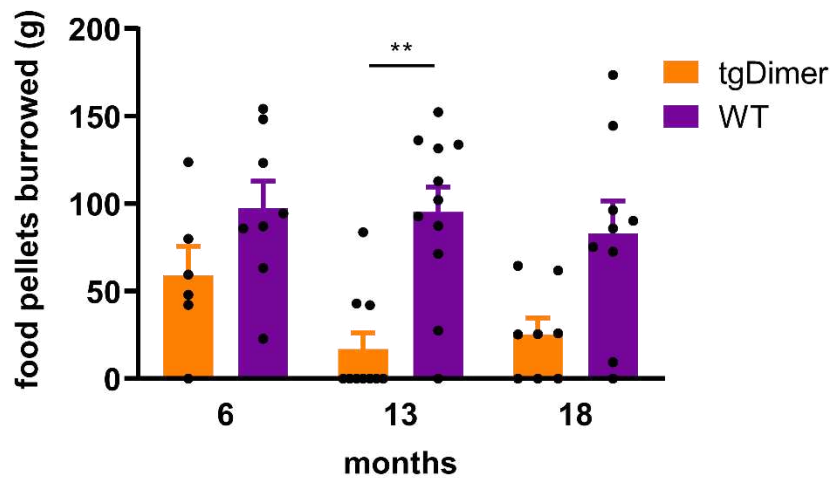


Figure 8. *TgDimer* mice burrowed fewer food pellets at 13 months of age compared to WT mice. The weight of displaced food pellets was measured after 2 hours and at the ages of 6, 13 and 18 months in the same mice. At 6 months of age, *tgDimer* and wild type (WT) mice burrowed the same number of pellets. At 13 months of age, *tgDimer* mice burrow significantly fewer food pellets compared with WT mice after 2h. The same effect, although not significant, is also observed at 18 months, when *tgDimer* mice burrow fewer food pellets compared with WT mice.

In the second batch of mice that underwent burrowing, *tgDimer* mice inoculated with brain homogenate containing A β seeds or not were compared with wild type mice and *tgAPP23* mice both inoculated with brain homogenates containing A β seeds. Before inoculation, at 8-12 weeks of age, there was no difference between the genotypes in how many food pellets they burrowed. Only at 6 months, *tgAPP23* mice inoculated with A β seeds burrowed significantly less compared with wild type, A β inoculated mice (p=0.0256). At 13 and 18 months of age, no differences were observed between the genotypes (Figure 9).

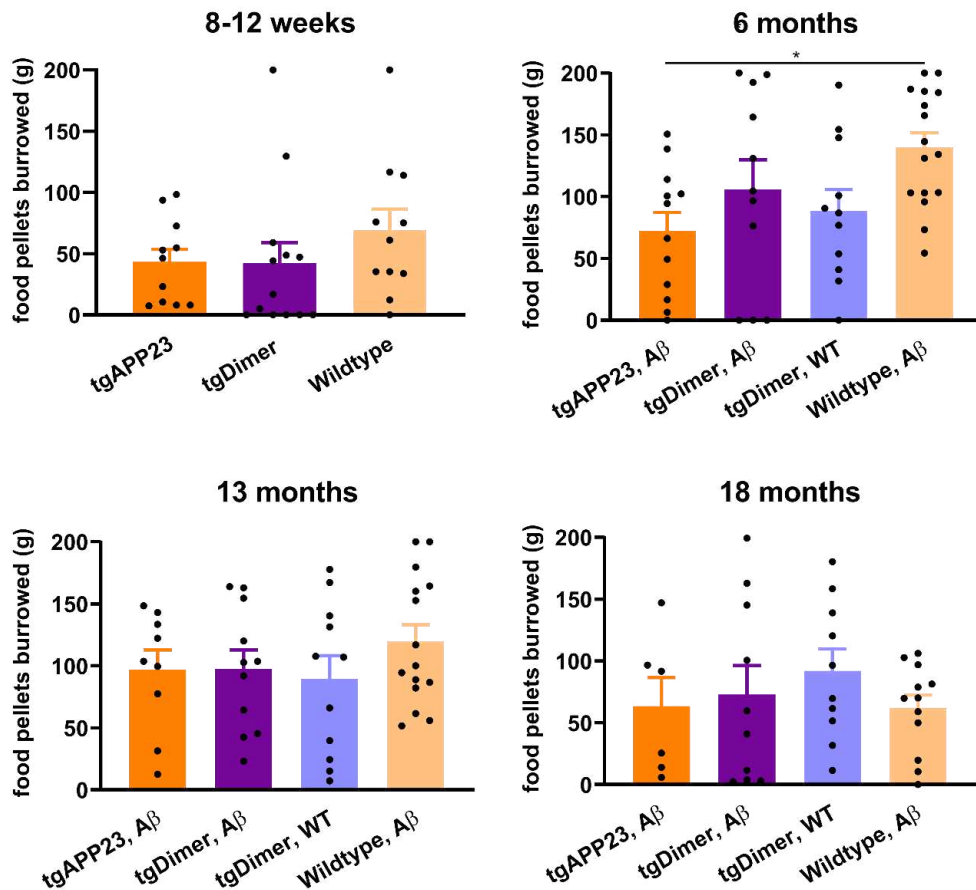


Figure 9. A β inoculated tgAPP23 mice burrowed significantly fewer food pellets compared to A β inoculated wild type mice at 6 months of age. The weight of displaced food pellets was measured after 2 hours and at the ages of 8-12 weeks and 6, 13 and 18 months in the same mice. At 6 months of age, tgAPP23 mice burrowed significantly less than wild type mice ($p=0.0256$). No differences in the amount of food pellets burrowed were observed at a later age.

In this batch of mice, an age effect was observed for almost all genotypes, except for tgDimer, WT inoculated mice. Comparing 8-12 weeks to 6 months revealed a significant increase in the amount of food pellets burrowed ($p=0.0027$) for A β inoculated wild type mice, likely related to a learning effect. At a later age, an ageing-related effect was observed in the wild type, A β inoculated mice, where aged mice (18 months of age) burrowed significantly less compared with the amount they burrowed at 6 months and 13 months of age ($p=0.0006$ and $p=0.0182$ respectively, Figure 10).

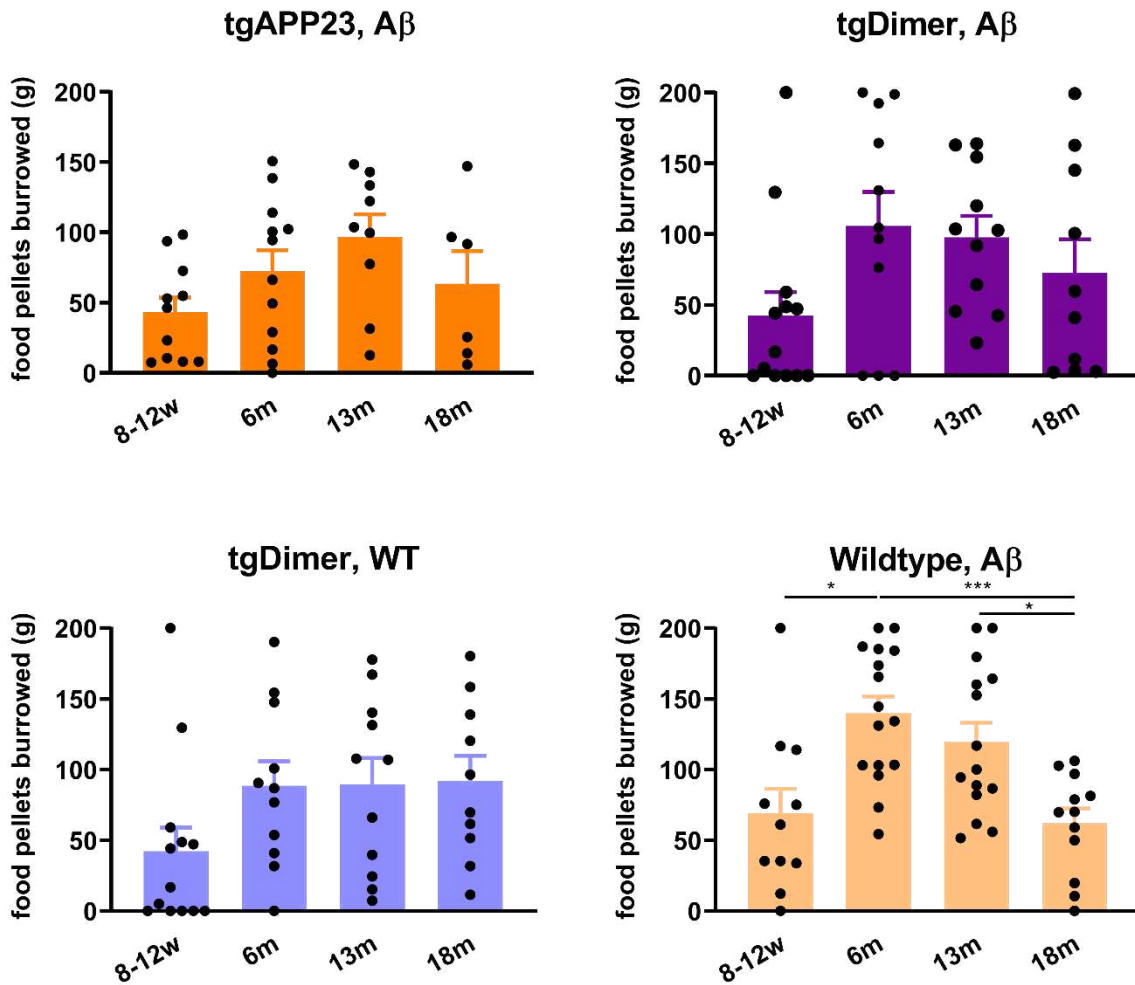


Figure 10. Decrease in food pellets burrowed after 2h as mice age. A decrease in food pellets burrowed is observed in all groups, except for the tgDimer, WT inoculated mice. However, the amount in food pellets burrowed was only significantly decreased in the wild type, A β inoculated mice (6 vs 18 months $p=0.0006$; 13 vs 18 months $p=0.0182$).

Discussion

As AD progresses in patients, there is a decline in day-to-day functioning, also known as the ability to perform activities of daily living (ADL). Measuring ADLs provides insights into the progression of the disease. To study the progression of disease in animal models of disease, Deacon and colleagues discovered that species-specific behaviour could be used. In this study, I tried to establish the burrowing protocol in the tgDimer mice that express only A β -S8C dimers and show early signs of AD (88, 150).

In the first group, where tgDimer mice were compared with WT littermates, we observed a significant reduction in the amount of pellets burrowed for tgDimer mice compared with WT mice.

In the second group, mice burrowed the same amount of food pellets at 3 months of age, before inoculation. At 6 months of age, tgAPP23 mice burrowed less compared with wild-type mice, however, this difference was not observed at later ages. Interestingly, we observed a significant decrease in burrowing with age, which was visible in all groups but was only found significantly different in wild-type mice. TgDimer, inoculated with WT brain homogenate do not show a decline in burrowing with age.

The burrowing test proved to work in a study where the researchers infected two groups of mice with scrapie. Initially, both groups burrowed equally amounts of pellets. Later, burrowing declined in both groups. However, after depletion of the prion protein in one group, this group recovered its burrowing activity, while the untreated group continued to deteriorate (195).

By implementing a practice run in addition to a baseline test, mice can improve and standardize burrowing ability, especially if mice are housed in groups. In addition, by putting a full burrow into the home cage with group-housed mice, burrowing behaviour will further develop. Deacon et al. divided the animals into groups based on their baseline performance which would reduce variability (165). However, this was not possible for the present study-set up, since several genotypes were tested which resulted in a lot of variation within groups. Furthermore, some mice will not burrow even though they were exposed to burrowing before and habituated to the burrow.

A decrease in burrowing was explained as a readout for the animals' general condition and wellbeing and to be able to detect early signs of neurological disorders. We chose the burrowing test since it's rodent specific behaviour, which was suggested to be related to mouse well-being, and its relation to activities of daily living in humans. Summarizing the performed burrowing experiments: because of the high variability within groups, it is difficult to give a definite conclusion on whether this paradigm can be used to study disease progression in the tested models of AD.

5. LIST OF PUBLICATIONS

van Gerresheim EF, Müller-Schiffmann A, Schäble S, Koopmans B, Loos M, Korth C. Soluble amyloid- β dimers are resistant to amyloid- β prions suggesting anti-prion properties. Manuscript submitted

van Gerresheim EF, Herring A, Gremer L, Müller-Schiffmann A, Keyvani K, Korth C. The interaction of insoluble Amyloid- β with soluble Amyloid- β dimers decreases Amyloid- β plaque numbers. *Neuropathol Appl Neurobiol.* 2021 Aug;47(5):603-610. doi: 10.1111/nan.12685. Epub 2021 Jan 7. PMID: 33338256.

6. ACKNOWLEDGMENTS

I want to express my gratitude to all the people who made this dissertation possible and supported me during the last years.

To start, I would like to thank Prof. Dr. Carsten Korth who gave me the opportunity to pursue my PhD in his lab. His expertise and guidance throughout the years led to this thesis which I'm very happy with. I was able to work on multiple interesting projects and gained experience in a broad range of techniques and methods.

I want to thank Prof. Dr. Dieter Willbold who consented to be my mentor. In addition, I want to thank the collaboration partners that made it possible to publish my results. My work could not have been done without the help of Dr. Lothar Gremer, who helped me with the biophysical part of the thesis and Dr. Sandra Schäble for teaching me how to do the stereotactic surgery and for the discussions and support. I would like to thank Maarten Loos and Bastijn Koopmans from Sylics for their help with the implementation of the CognitionWall experiments.

I want to thank the DFG (Deutsche Forschungsgemeinschaft) for their financial support and for making it possible to visit interesting scientific meetings as well as iBrain for their financial support to attend scientific meetings.

Next, my colleagues. Many thanks to all of you for the various forms of support during my doctorate thesis, for helping me with new techniques, for discussing results and for the good atmosphere in the office. Especially I want to thank my direct colleagues: Dr. Andreas Müller-Schiffmann, Dr. Svenja Trossbach and Ingrid Prikulis and for all scientific and not-so-scientific discussions, lunches and coffee breaks. Many thanks for helping me out during challenging times!

I want to thank my family for supporting me, thanks to you I got where I am now. And not to forget, I owe my gratitude to Maarten. Who from the start supported me and had faith in me

even when I lost it for a moment. I am forever grateful for your presence in my life, now and hopefully for many more years.

Finally, my dear friends, thank you for all the precious moments we have shared. The dinners, the wine tastings, and the visits to Düsseldorf; thank you for being there for me.

I want to thank all the people mentioned here, who in different ways supported me during my PhD. Thank you!

7. BIBLIOGRAPHY

1. Kovacs GG, Botond G, Budka H. Protein coding of neurodegenerative dementias: the neuropathological basis of biomarker diagnostics. *Acta neuropathologica*. 2010;119(4):389-408.
2. Soto C, Estrada LD. Protein misfolding and neurodegeneration. *Archives of neurology*. 2008;65(2):184-9.
3. Prusiner SB. Molecular biology of prion diseases. *Science*. 1991;252(5012):1515-22.
4. Prusiner SB. Prions. *Proc Natl Acad Sci U S A*. 1998;95(23):13363-83.
5. Glenner GG, Wong CW. Alzheimer's disease: initial report of the purification and characterization of a novel cerebrovascular amyloid protein. *Biochem Biophys Res Commun*. 1984;120(3):885-90.
6. Goedert M, Spillantini MG, Jakes R, Rutherford D, Crowther RA. Multiple isoforms of human microtubule-associated protein tau: sequences and localization in neurofibrillary tangles of Alzheimer's disease. *Neuron*. 1989;3(4):519-26.
7. Mroczko B, Groblewska M, Litman-Zawadzka A. The Role of Protein Misfolding and Tau Oligomers (TauOs) in Alzheimer's Disease (AD). *Int J Mol Sci*. 2019;20(19).
8. Ihara Y, Nukina N, Miura R, Ogawara M. Phosphorylated tau protein is integrated into paired helical filaments in Alzheimer's disease. *J Biochem*. 1986;99(6):1807-10.
9. Kosik KS, Joachim CL, Selkoe DJ. Microtubule-associated protein tau (tau) is a major antigenic component of paired helical filaments in Alzheimer disease. *Proc Natl Acad Sci U S A*. 1986;83(11):4044-8.
10. Polymeropoulos MH, Lavedan C, Leroy E, Ide SE, Dehejia A, Dutra A, et al. Mutation in the alpha-synuclein gene identified in families with Parkinson's disease. *Science*. 1997;276(5321):2045-7.
11. Spillantini MG, Crowther RA, Jakes R, Hasegawa M, Goedert M. alpha-Synuclein in filamentous inclusions of Lewy bodies from Parkinson's disease and dementia with lewy bodies. *Proc Natl Acad Sci U S A*. 1998;95(11):6469-73.
12. Sun Z, Diaz Z, Fang X, Hart MP, Chesi A, Shorter J, et al. Molecular determinants and genetic modifiers of aggregation and toxicity for the ALS disease protein FUS/TLS. *PLoS Biol*. 2011;9(4):e1000614.
13. Prasad A, Bharathi V, Sivalingam V, Girdhar A, Patel BK. Molecular Mechanisms of TDP-43 Misfolding and Pathology in Amyotrophic Lateral Sclerosis. *Front Mol Neurosci*. 2019;12:25.
14. Berning BA, Walker AK. The Pathobiology of TDP-43 C-Terminal Fragments in ALS and FTLD. *Frontiers in neuroscience*. 2019;13:335.
15. Neumann M, Sampathu DM, Kwong LK, Truax AC, Micsenyi MC, Chou TT, et al. Ubiquitinated TDP-43 in frontotemporal lobar degeneration and amyotrophic lateral sclerosis. *Science*. 2006;314(5796):130-3.
16. Wellington CL, Ellerby LM, Gutekunst CA, Rogers D, Warby S, Graham RK, et al. Caspase cleavage of mutant huntingtin precedes neurodegeneration in Huntington's disease. *J Neurosci*. 2002;22(18):7862-72.
17. Ide K, Nukina N, Masuda N, Goto J, Kanazawa I. Abnormal gene product identified in Huntington's disease lymphocytes and brain. *Biochem Biophys Res Commun*. 1995;209(3):1119-25.
18. Bäck S. CDNF in an experimental model of Parkinson's disease: studies on gene therapy and protein infusion. 2014.
19. Gomez-Isla T, Price JL, McKeel DW, Jr., Morris JC, Growdon JH, Hyman BT. Profound loss of layer II entorhinal cortex neurons occurs in very mild Alzheimer's disease. *J Neurosci*. 1996;16(14):4491-500.

20. Fearnley JM, Lees AJ. Ageing and Parkinson's disease: substantia nigra regional selectivity. *Brain*. 1991;114 (Pt 5):2283-301.
21. Damier P, Hirsch EC, Agid Y, Graybiel AM. The substantia nigra of the human brain. II. Patterns of loss of dopamine-containing neurons in Parkinson's disease. *Brain*. 1999;122 (Pt 8):1437-48.
22. Arendt T, Bruckner MK, Morawski M, Jager C, Gertz HJ. Early neurone loss in Alzheimer's disease: cortical or subcortical? *Acta Neuropathol Commun*. 2015;3:10.
23. Ferrero J, Williams L, Stella H, Leitermann K, Mikulskis A, O'Gorman J, et al. First-in-human, double-blind, placebo-controlled, single-dose escalation study of aducanumab (BIIB037) in mild-to-moderate Alzheimer's disease. *Alzheimers Dement (N Y)*. 2016;2(3):169-76.
24. van Dyck CH. Anti-Amyloid-beta Monoclonal Antibodies for Alzheimer's Disease: Pitfalls and Promise. *Biol Psychiatry*. 2018;83(4):311-9.
25. Braak H, Thal DR, Ghebremedhin E, Del Tredici K. Stages of the pathologic process in Alzheimer disease: age categories from 1 to 100 years. *J Neuropathol Exp Neurol*. 2011;70(11):960-9.
26. Gordon BA, Blazey TM, Su Y, Hari-Raj A, Dincer A, Flores S, et al. Spatial patterns of neuroimaging biomarker change in individuals from families with autosomal dominant Alzheimer's disease: a longitudinal study. *Lancet Neurol*. 2018;17(3):241-50.
27. Bateman RJ, Xiong C, Benzinger TL, Fagan AM, Goate A, Fox NC, et al. Clinical and biomarker changes in dominantly inherited Alzheimer's disease. *N Engl J Med*. 2012;367(9):795-804.
28. Villemagne VL, Burnham S, Bourgeat P, Brown B, Ellis KA, Salvado O, et al. Amyloid beta deposition, neurodegeneration, and cognitive decline in sporadic Alzheimer's disease: a prospective cohort study. *Lancet Neurol*. 2013;12(4):357-67.
29. Tanzi RE. The genetics of Alzheimer disease. *Cold Spring Harb Perspect Med*. 2012;2(10).
30. Alzheimer A. About a Peculiar Disease of the Cerebral Cortex. *Allgemeine Zeitschrift fur Psychiatrie und Psychisch-Gerichtlich Medicin*. 1907;64:146-8.
31. Alzheimer A, Stelzmann RA, Schnitzlein HN, Murtagh FR. An English translation of Alzheimer's 1907 paper, "Uber eine eigenartige Erkankung der Hirnrinde". *Clin Anat*. 1995;8(6):429-31.
32. Grundke-Iqbal I, Iqbal K, Tung YC, Quinlan M, Wisniewski HM, Binder LI. Abnormal phosphorylation of the microtubule-associated protein tau (tau) in Alzheimer cytoskeletal pathology. *Proc Natl Acad Sci U S A*. 1986;83(13):4913-7.
33. Masters CL, Simms G, Weinman NA, Multhaup G, McDonald BL, Beyreuther K. Amyloid plaque core protein in Alzheimer disease and Down syndrome. *Proc Natl Acad Sci U S A*. 1985;82(12):4245-9.
34. Weingarten MD, Lockwood AH, Hwo SY, Kirschner MW. A protein factor essential for microtubule assembly. *Proc Natl Acad Sci U S A*. 1975;72(5):1858-62.
35. Trojanowski JQ, Lee VM. Phosphorylation of paired helical filament tau in Alzheimer's disease neurofibrillary lesions: focusing on phosphatases. *FASEB J*. 1995;9(15):1570-6.
36. Mandelkow EM, Biernat J, Drewes G, Gustke N, Trinczek B, Mandelkow E. Tau domains, phosphorylation, and interactions with microtubules. *Neurobiology of aging*. 1995;16(3):355-62; discussion 62-3.
37. Poorkaj P, Bird TD, Wijsman E, Nemens E, Garruto RM, Anderson L, et al. Tau is a candidate gene for chromosome 17 frontotemporal dementia. *Ann Neurol*. 1998;43(6):815-25.
38. Herrup K. Reimagining Alzheimer's disease--an age-based hypothesis. *J Neurosci*. 2010;30(50):16755-62.
39. Chartier-Harlin MC, Crawford F, Houlden H, Warren A, Hughes D, Fidani L, et al. Early-onset Alzheimer's disease caused by mutations at codon 717 of the beta-amyloid precursor protein gene. *Nature*. 1991;353(6347):844-6.
40. Goate A, Chartier-Harlin MC, Mullan M, Brown J, Crawford F, Fidani L, et al. Segregation of a missense mutation in the amyloid precursor protein gene with familial Alzheimer's disease. *Nature*. 1991;349(6311):704-6.

41. Sherrington R, Rogaev EI, Liang Y, Rogaeva EA, Levesque G, Ikeda M, et al. Cloning of a gene bearing missense mutations in early-onset familial Alzheimer's disease. *Nature*. 1995;375(6534):754-60.
42. Sherrington R, Froelich S, Sorbi S, Campion D, Chi H, Rogaeva EA, et al. Alzheimer's disease associated with mutations in presenilin 2 is rare and variably penetrant. *Hum Mol Genet*. 1996;5(7):985-8.
43. Rogaev EI, Sherrington R, Rogaeva EA, Levesque G, Ikeda M, Liang Y, et al. Familial Alzheimer's disease in kindreds with missense mutations in a gene on chromosome 1 related to the Alzheimer's disease type 3 gene. *Nature*. 1995;376(6543):775-8.
44. Levy-Lahad E, Wijsman EM, Nemens E, Anderson L, Goddard KA, Weber JL, et al. A familial Alzheimer's disease locus on chromosome 1. *Science*. 1995;269(5226):970-3.
45. Sun L, Zhou R, Yang G, Shi Y. Analysis of 138 pathogenic mutations in presenilin-1 on the in vitro production of Abeta42 and Abeta40 peptides by gamma-secretase. *Proc Natl Acad Sci U S A*. 2017;114(4):E476-E85.
46. Farrer LA, Cupples LA, Haines JL, Hyman B, Kukull WA, Mayeux R, et al. Effects of age, sex, and ethnicity on the association between apolipoprotein E genotype and Alzheimer disease. A meta-analysis. APOE and Alzheimer Disease Meta Analysis Consortium. *JAMA*. 1997;278(16):1349-56.
47. Perry EK, McKeith I, Thompson P, Marshall E, Kerwin J, Jabeen S, et al. Topography, extent, and clinical relevance of neurochemical deficits in dementia of Lewy body type, Parkinson's disease, and Alzheimer's disease. *Ann N Y Acad Sci*. 1991;640:197-202.
48. McKeith I. Dementia with Lewy bodies. *Dialogues in clinical neuroscience*. 2004;6(3):333-41.
49. Lam B, Masellis M, Freedman M, Stuss DT, Black SE. Clinical, imaging, and pathological heterogeneity of the Alzheimer's disease syndrome. *Alzheimers Res Ther*. 2013;5(1):1.
50. Van der Flier WM. Clinical heterogeneity in familial Alzheimer's disease. *Lancet Neurol*. 2016;15(13):1296-8.
51. Maarouf CL, Dausgs ID, Spina S, Vidal R, Kokjohn TA, Patton RL, et al. Histopathological and molecular heterogeneity among individuals with dementia associated with Presenilin mutations. *Mol Neurodegener*. 2008;3:20.
52. Nilsberth C, Westlind-Danielsson A, Eckman CB, Condron MM, Axelman K, Forsell C, et al. The 'Arctic' APP mutation (E693G) causes Alzheimer's disease by enhanced Abeta protofibril formation. *Nature neuroscience*. 2001;4(9):887-93.
53. Kummer MP, Heneka MT. Truncated and modified amyloid-beta species. *Alzheimers Res Ther*. 2014;6(3):28.
54. Petkova AT, Leapman RD, Guo Z, Yau WM, Mattson MP, Tycko R. Self-propagating, molecular-level polymorphism in Alzheimer's beta-amyloid fibrils. *Science*. 2005;307(5707):262-5.
55. Seilheimer B, Bohrmann B, Bondolfi L, Muller F, Stuber D, Dobeli H. The toxicity of the Alzheimer's beta-amyloid peptide correlates with a distinct fiber morphology. *J Struct Biol*. 1997;119(1):59-71.
56. Yoshiike Y, Chui DH, Akagi T, Tanaka N, Takashima A. Specific compositions of amyloid-beta peptides as the determinant of toxic beta-aggregation. *J Biol Chem*. 2003;278(26):23648-55.
57. Lau HHC, Ingelsson M, Watts JC. The existence of Abeta strains and their potential for driving phenotypic heterogeneity in Alzheimer's disease. *Acta neuropathologica*. 2021;142(1):17-39.
58. Soto C, Pritzkow S. Protein misfolding, aggregation, and conformational strains in neurodegenerative diseases. *Nature neuroscience*. 2018;21(10):1332-40.
59. Storey E, Beyreuther K, Masters CL. Alzheimer's disease amyloid precursor protein on the surface of cortical neurons in primary culture co-localizes with adhesion patch components. *Brain Res*. 1996;735(2):217-31.
60. Kitazume S, Tachida Y, Kato M, Yamaguchi Y, Honda T, Hashimoto Y, et al. Brain endothelial cells produce amyloid {beta} from amyloid precursor protein 770 and preferentially secrete the O-glycosylated form. *J Biol Chem*. 2010;285(51):40097-103.

61. Toledano A, Alvarez MI, Rivas L, Lacruz C, Martinez-Rodriguez R. Amyloid precursor proteins in the cerebellar cortex of Alzheimer's disease patients devoid of cerebellar beta-amyloid deposits: immunocytochemical study of five cases. *J Neural Transm (Vienna)*. 1999;106(11-12):1151-69.
62. Chow VW, Mattson MP, Wong PC, Gleichmann M. An overview of APP processing enzymes and products. *Neuromolecular Med*. 2010;12(1):1-12.
63. Seubert P, Vigo-Pelfrey C, Esch F, Lee M, Dovey H, Davis D, et al. Isolation and quantification of soluble Alzheimer's beta-peptide from biological fluids. *Nature*. 1992;359(6393):325-7.
64. Miller DL, Papayannopoulos IA, Styles J, Bobin SA, Lin YY, Biemann K, et al. Peptide compositions of the cerebrovascular and senile plaque core amyloid deposits of Alzheimer's disease. *Arch Biochem Biophys*. 1993;301(1):41-52.
65. Iwatsubo T, Odaka A, Suzuki N, Mizusawa H, Nukina N, Ihara Y. Visualization of A beta 42(43) and A beta 40 in senile plaques with end-specific A beta monoclonals: evidence that an initially deposited species is A beta 42(43). *Neuron*. 1994;13(1):45-53.
66. Ristori E, Donnini S, Ziche M. New Insights Into Blood-Brain Barrier Maintenance: The Homeostatic Role of beta-Amyloid Precursor Protein in Cerebral Vasculature. *Front Physiol*. 2020;11:1056.
67. Miravalle L, Calero M, Takao M, Roher AE, Ghetti B, Vidal R. Amino-terminally truncated Abeta peptide species are the main component of cotton wool plaques. *Biochemistry*. 2005;44(32):10810-21.
68. Jarrett JT, Berger EP, Lansbury PT, Jr. The carboxy terminus of the beta amyloid protein is critical for the seeding of amyloid formation: implications for the pathogenesis of Alzheimer's disease. *Biochemistry*. 1993;32(18):4693-7.
69. Bitan G, Kirkitadze MD, Lomakin A, Vollers SS, Benedek GB, Teplow DB. Amyloid beta -protein (Abeta) assembly: Abeta 40 and Abeta 42 oligomerize through distinct pathways. *Proc Natl Acad Sci U S A*. 2003;100(1):330-5.
70. Lewis H, Behr D, Cookson N, Oakley A, Piggott M, Morris CM, et al. Quantification of Alzheimer pathology in ageing and dementia: age-related accumulation of amyloid-beta(42) peptide in vascular dementia. *Neuropathology and applied neurobiology*. 2006;32(2):103-18.
71. Ancolio K, Dumanchin C, Barelli H, Warter JM, Brice A, Campion D, et al. Unusual phenotypic alteration of beta amyloid precursor protein (betaAPP) maturation by a new Val-715 --> Met betaAPP-770 mutation responsible for probable early-onset Alzheimer's disease. *Proc Natl Acad Sci U S A*. 1999;96(7):4119-24.
72. Wang DS, Dickson DW, Malter JS. beta-Amyloid degradation and Alzheimer's disease. *J Biomed Biotechnol*. 2006;2006(3):58406.
73. Wiltfang J, Esselmann H, Cupers P, Neumann M, Kretzschmar H, Beyermann M, et al. Elevation of beta-amyloid peptide 2-42 in sporadic and familial Alzheimer's disease and its generation in PS1 knockout cells. *J Biol Chem*. 2001;276(46):42645-57.
74. Harigaya Y, Saido TC, Eckman CB, Prada CM, Shoji M, Younkin SG. Amyloid beta protein starting pyroglutamate at position 3 is a major component of the amyloid deposits in the Alzheimer's disease brain. *Biochem Biophys Res Commun*. 2000;276(2):422-7.
75. Haass C, Selkoe DJ. Soluble protein oligomers in neurodegeneration: lessons from the Alzheimer's amyloid beta-peptide. *Nature reviews Molecular cell biology*. 2007;8(2):101-12.
76. McLean CA, Cherny RA, Fraser FW, Fuller SJ, Smith MJ, Beyreuther K, et al. Soluble pool of Abeta amyloid as a determinant of severity of neurodegeneration in Alzheimer's disease. *Ann Neurol*. 1999;46(6):860-6.
77. Kim HJ, Chae SC, Lee DK, Chromy B, Lee SC, Park YC, et al. Selective neuronal degeneration induced by soluble oligomeric amyloid beta protein. *FASEB J*. 2003;17(1):118-20.
78. Shankar GM, Li S, Mehta TH, Garcia-Munoz A, Shepardson NE, Smith I, et al. Amyloid-beta protein dimers isolated directly from Alzheimer's brains impair synaptic plasticity and memory. *Nat Med*. 2008;14(8):837-42.
79. Glabe CG. Structural classification of toxic amyloid oligomers. *J Biol Chem*. 2008;283(44):29639-43.

80. Hasecke F, Miti T, Perez C, Barton J, Scholzel D, Gremer L, et al. Origin of metastable oligomers and their effects on amyloid fibril self-assembly. *Chem Sci*. 2018;9(27):5937-48.
81. Yamaguchi T, Yagi H, Goto Y, Matsuzaki K, Hoshino M. A disulfide-linked amyloid-beta peptide dimer forms a protofibril-like oligomer through a distinct pathway from amyloid fibril formation. *Biochemistry*. 2010;49(33):7100-7.
82. Sandberg A, Luheshi LM, Sollvander S, Pereira de Barros T, Macao B, Knowles TP, et al. Stabilization of neurotoxic Alzheimer amyloid-beta oligomers by protein engineering. *Proc Natl Acad Sci U S A*. 2010;107(35):15595-600.
83. Schmechel A, Zentgraf H, Scheuermann S, Fritz G, Pipkorn R, Reed J, et al. Alzheimer beta-amyloid homodimers facilitate A beta fibrillization and the generation of conformational antibodies. *J Biol Chem*. 2003;278(37):35317-24.
84. O'Nuallain B, Freir DB, Nicoll AJ, Risse E, Ferguson N, Herron CE, et al. Amyloid beta-protein dimers rapidly form stable synaptotoxic protofibrils. *J Neurosci*. 2010;30(43):14411-9.
85. Hu NW, Smith IM, Walsh DM, Rowan MJ. Soluble amyloid-beta peptides potently disrupt hippocampal synaptic plasticity in the absence of cerebrovascular dysfunction in vivo. *Brain*. 2008;131(Pt 9):2414-24.
86. Zhang S, Yoo S, Snyder DT, Katz BB, Henrickson A, Demeler B, et al. A Disulfide-Stabilized Abeta that Forms Dimers but Does Not Form Fibrils. *Biochemistry*. 2022;61(4):252-64.
87. Muller-Schiffmann A, Andreyeva A, Horn AH, Gottmann K, Korth C, Sticht H. Molecular engineering of a secreted, highly homogeneous, and neurotoxic abeta dimer. *ACS Chem Neurosci*. 2011;2(5):242-8.
88. Muller-Schiffmann A, Herring A, Abdel-Hafiz L, Chepkova AN, Schable S, Wedel D, et al. Amyloid-beta dimers in the absence of plaque pathology impair learning and synaptic plasticity. *Brain*. 2016;139(Pt 2):509-25.
89. Prusiner SB. Novel proteinaceous infectious particles cause scrapie. *Science*. 1982;216(4542):136-44.
90. Manson J, West JD, Thomson V, McBride P, Kaufman MH, Hope J. The prion protein gene: a role in mouse embryogenesis? *Development*. 1992;115(1):117-22.
91. Pan KM, Baldwin M, Nguyen J, Gasset M, Serban A, Groth D, et al. Conversion of alpha-helices into beta-sheets features in the formation of the scrapie prion proteins. *Proc Natl Acad Sci U S A*. 1993;90(23):10962-6.
92. Hardy J. Expression of normal sequence pathogenic proteins for neurodegenerative disease contributes to disease risk: 'permissive templating' as a general mechanism underlying neurodegeneration. *Biochem Soc Trans*. 2005;33(Pt 4):578-81.
93. Walker LC, Levine H, 3rd, Mattson MP, Jucker M. Inducible proteopathies. *Trends Neurosci*. 2006;29(8):438-43.
94. McKinley MP, Meyer RK, Kenaga L, Rahbar F, Cotter R, Serban A, et al. Scrapie prion rod formation in vitro requires both detergent extraction and limited proteolysis. *J Virol*. 1991;65(3):1340-51.
95. Castilla J, Saa P, Hetz C, Soto C. In vitro generation of infectious scrapie prions. *Cell*. 2005;121(2):195-206.
96. Morales R, Moreno-Gonzalez I, Soto C. Cross-seeding of misfolded proteins: implications for etiology and pathogenesis of protein misfolding diseases. *PLoS Pathog*. 2013;9(9):e1003537.
97. Gilch S, Krammer C, Schatzl HM. Targeting prion proteins in neurodegenerative disease. *Expert Opin Biol Ther*. 2008;8(7):923-40.
98. Wickner RB, Edskes H, Son M, Wu S, Niznikiewicz M. Innate immunity to prions: anti-prion systems turn a tsunami of prions into a slow drip. *Current Genetics*. 2021.
99. Aguzzi A, Heikenwalder M, Polymenidou M. Insights into prion strains and neurotoxicity. *Nature reviews Molecular cell biology*. 2007;8(7):552-61.
100. Collinge J, Clarke AR. A general model of prion strains and their pathogenicity. *Science*. 2007;318(5852):930-6.

101. Safar J, Wille H, Itri V, Groth D, Serban H, Torchia M, et al. Eight prion strains have PrP(Sc) molecules with different conformations. *Nat Med.* 1998;4(10):1157-65.
102. Jones EM, Surewicz WK. Fibril conformation as the basis of species- and strain-dependent seeding specificity of mammalian prion amyloids. *Cell.* 2005;121(1):63-72.
103. Prusiner SB. Some speculations about prions, amyloid, and Alzheimer's disease. *N Engl J Med.* 1984;310(10):661-3.
104. Gajdusek DC. Spontaneous generation of infectious nucleating amyloids in the transmissible and nontransmissible cerebral amyloidoses. *Mol Neurobiol.* 1994;8(1):1-13.
105. Arosio P, Knowles TP, Linse S. On the lag phase in amyloid fibril formation. *Phys Chem Chem Phys.* 2015;17(12):7606-18.
106. Jucker M, Walker LC. Self-propagation of pathogenic protein aggregates in neurodegenerative diseases. *Nature.* 2013;501(7465):45-51.
107. Baker HF, Ridley RM, Duchen LW, Crow TJ, Bruton CJ. Experimental induction of beta-amyloid plaques and cerebral angiopathy in primates. *Ann N Y Acad Sci.* 1993;695:228-31.
108. Meyer-Luehmann M, Coomaraswamy J, Bolmont T, Kaeser S, Schaefer C, Kilger E, et al. Exogenous induction of cerebral beta-amyloidogenesis is governed by agent and host. *Science.* 2006;313(5794):1781-4.
109. Eisele YS, Obermuller U, Heilbronner G, Baumann F, Kaeser SA, Wolburg H, et al. Peripherally applied Abeta-containing inoculates induce cerebral beta-amyloidosis. *Science.* 2010;330(6006):980-2.
110. Kane MD, Lipinski WJ, Callahan MJ, Bian F, Durham RA, Schwarz RD, et al. Evidence for seeding of beta-amyloid by intracerebral infusion of Alzheimer brain extracts in beta-amyloid precursor protein-transgenic mice. *J Neurosci.* 2000;20(10):3606-11.
111. Walker LC, Callahan MJ, Bian F, Durham RA, Roher AE, Lipinski WJ. Exogenous induction of cerebral beta-amyloidosis in betaAPP-transgenic mice. *Peptides.* 2002;23(7):1241-7.
112. Morales R, Duran-Aniotz C, Castilla J, Estrada LD, Soto C. De novo induction of amyloid-beta deposition in vivo. *Mol Psychiatry.* 2012;17(12):1347-53.
113. Rosen RF, Fritz JJ, Dooyema J, Cintron AF, Hamaguchi T, Lah JJ, et al. Exogenous seeding of cerebral beta-amyloid deposition in betaAPP-transgenic rats. *J Neurochem.* 2012;120(5):660-6.
114. Domert J, Rao SB, Agholme L, Brorsson AC, Marcusson J, Hallbeck M, et al. Spreading of amyloid-beta peptides via neuritic cell-to-cell transfer is dependent on insufficient cellular clearance. *Neurobiol Dis.* 2014;65:82-92.
115. Mehta AK, Rosen RF, Childers WS, Gehman JD, Walker LC, Lynn DG. Context dependence of protein misfolding and structural strains in neurodegenerative diseases. *Biopolymers.* 2013;100(6):722-30.
116. Langer F, Eisele YS, Fritschi SK, Staufenbiel M, Walker LC, Jucker M. Soluble Abeta seeds are potent inducers of cerebral beta-amyloid deposition. *J Neurosci.* 2011;31(41):14488-95.
117. Ye L, Hamaguchi T, Fritschi SK, Eisele YS, Obermuller U, Jucker M, et al. Progression of Seed-Induced Abeta Deposition within the Limbic Connectome. *Brain pathology.* 2015;25(6):743-52.
118. Eisenberg D, Jucker M. The amyloid state of proteins in human diseases. *Cell.* 2012;148(6):1188-203.
119. Lu JX, Qiang W, Yau WM, Schwieters CD, Meredith SC, Tycko R. Molecular structure of beta-amyloid fibrils in Alzheimer's disease brain tissue. *Cell.* 2013;154(6):1257-68.
120. Hatami A, Albay R, 3rd, Monjazeb S, Milton S, Glabe C. Monoclonal antibodies against Abeta42 fibrils distinguish multiple aggregation state polymorphisms in vitro and in Alzheimer disease brain. *J Biol Chem.* 2014;289(46):32131-43.
121. Spirig T, Ovchinnikova O, Vagt T, Glockshuber R. Direct evidence for self-propagation of different amyloid-beta fibril conformations. *Neuro-degenerative diseases.* 2014;14(3):151-9.
122. Cohen ML, Kim C, Haldiman T, ElHag M, Mehndiratta P, Pichet T, et al. Rapidly progressive Alzheimer's disease features distinct structures of amyloid-beta. *Brain.* 2015;138(Pt 4):1009-22.

123. Watts JC, Condello C, Stohr J, Oehler A, Lee J, DeArmond SJ, et al. Serial propagation of distinct strains of Abeta prions from Alzheimer's disease patients. *Proc Natl Acad Sci U S A*. 2014;111(28):10323-8.
124. Stohr J, Condello C, Watts JC, Bloch L, Oehler A, Nick M, et al. Distinct synthetic Abeta prion strains producing different amyloid deposits in bigenic mice. *Proc Natl Acad Sci U S A*. 2014;111(28):10329-34.
125. Eisele YS, Bolmont T, Heikenwalder M, Langer F, Jacobson LH, Yan ZX, et al. Induction of cerebral beta-amyloidosis: intracerebral versus systemic Abeta inoculation. *Proc Natl Acad Sci U S A*. 2009;106(31):12926-31.
126. Braak H, Del Tredici K, Rub U, de Vos RA, Jansen Steur EN, Braak E. Staging of brain pathology related to sporadic Parkinson's disease. *Neurobiology of aging*. 2003;24(2):197-211.
127. Furman JL, Vaquer-Alicea J, White CL, 3rd, Cairns NJ, Nelson PT, Diamond MI. Widespread tau seeding activity at early Braak stages. *Acta neuropathologica*. 2017;133(1):91-100.
128. Sanders DW, Kaufman SK, DeVos SL, Sharma AM, Mirbaha H, Li A, et al. Distinct tau prion strains propagate in cells and mice and define different tauopathies. *Neuron*. 2014;82(6):1271-88.
129. Clavaguera F, Akatsu H, Fraser G, Crowther RA, Frank S, Hench J, et al. Brain homogenates from human tauopathies induce tau inclusions in mouse brain. *Proc Natl Acad Sci U S A*. 2013;110(23):9535-40.
130. Falcon B, Cavallini A, Angers R, Glover S, Murray TK, Barnham L, et al. Conformation determines the seeding potencies of native and recombinant Tau aggregates. *J Biol Chem*. 2015;290(2):1049-65.
131. Lasagna-Reeves CA, Castillo-Carranza DL, Sengupta U, Guerrero-Munoz MJ, Kiritoshi T, Neugebauer V, et al. Alzheimer brain-derived tau oligomers propagate pathology from endogenous tau. *Sci Rep*. 2012;2:700.
132. Gearing M, Tigges J, Mori H, Mirra SS. A beta40 is a major form of beta-amyloid in nonhuman primates. *Neurobiology of aging*. 1996;17(6):903-8.
133. Gearing M, Tigges J, Mori H, Mirra SS. beta-Amyloid (A beta) deposition in the brains of aged orangutans. *Neurobiology of aging*. 1997;18(2):139-46.
134. Walker LC, Kitt CA, Struble RG, Wagster MV, Price DL, Cork LC. The neural basis of memory decline in aged monkeys. *Neurobiology of aging*. 1988;9(5-6):657-66.
135. Struble RG, Price DL, Jr., Cork LC, Price DL. Senile plaques in cortex of aged normal monkeys. *Brain Res*. 1985;361(1-2):267-75.
136. Cummings BJ, Head E, Ruehl W, Milgram NW, Cotman CW. The canine as an animal model of human aging and dementia. *Neurobiology of aging*. 1996;17(2):259-68.
137. Head E, Callahan H, Muggenburg BA, Cotman CW, Milgram NW. Visual-discrimination learning ability and beta-amyloid accumulation in the dog. *Neurobiology of aging*. 1998;19(5):415-25.
138. Xu G, Ran Y, Fromholt SE, Fu C, Yachnis AT, Golde TE, et al. Murine Abeta over-production produces diffuse and compact Alzheimer-type amyloid deposits. *Acta Neuropathol Commun*. 2015;3:72.
139. Drummond E, Wisniewski T. Alzheimer's disease: experimental models and reality. *Acta neuropathologica*. 2017;133(2):155-75.
140. Murrell J, Farlow M, Ghetti B, Benson MD. A mutation in the amyloid precursor protein associated with hereditary Alzheimer's disease. *Science*. 1991;254(5028):97-9.
141. Mullan M, Crawford F, Axelman K, Houlden H, Lilius L, Winblad B, et al. A pathogenic mutation for probable Alzheimer's disease in the APP gene at the N-terminus of beta-amyloid. *Nat Genet*. 1992;1(5):345-7.
142. Calhoun ME, Wiederhold KH, Abramowski D, Phinney AL, Probst A, Sturchler-Pierrat C, et al. Neuron loss in APP transgenic mice. *Nature*. 1998;395(6704):755-6.
143. Van Dam D, D'Hooge R, Staufenbiel M, Van Ginneken C, Van Meir F, De Deyn PP. Age-dependent cognitive decline in the APP23 model precedes amyloid deposition. *The European journal of neuroscience*. 2003;17(2):388-96.

144. Kelly PH, Bondolfi L, Hunziker D, Schlecht HP, Carver K, Maguire E, et al. Progressive age-related impairment of cognitive behavior in APP23 transgenic mice. *Neurobiology of aging*. 2003;24(2):365-78.
145. Chishti MA, Yang DS, Janus C, Phinney AL, Horne P, Pearson J, et al. Early-onset amyloid deposition and cognitive deficits in transgenic mice expressing a double mutant form of amyloid precursor protein 695. *J Biol Chem*. 2001;276(24):21562-70.
146. Dudal S, Krzywkowski P, Paquette J, Morissette C, Lacombe D, Tremblay P, et al. Inflammation occurs early during the Aβ deposition process in TgCRND8 mice. *Neurobiology of aging*. 2004;25(7):861-71.
147. Yu F, Zhang Y, Chuang DM. Lithium reduces BACE1 overexpression, beta amyloid accumulation, and spatial learning deficits in mice with traumatic brain injury. *J Neurotrauma*. 2012;29(13):2342-51.
148. Faucher P, Mons N, Micheau J, Louis C, Beracochea DJ. Hippocampal Injections of Oligomeric Amyloid beta-peptide (1-42) Induce Selective Working Memory Deficits and Long-lasting Alterations of ERK Signaling Pathway. *Frontiers in aging neuroscience*. 2015;7:245.
149. Bolmont T, Clavaguera F, Meyer-Luehmann M, Herzog MC, Radde R, Staufenbiel M, et al. Induction of tau pathology by intracerebral infusion of amyloid-beta -containing brain extract and by amyloid-beta deposition in APP x Tau transgenic mice. *The American journal of pathology*. 2007;171(6):2012-20.
150. Abdel-Hafiz L, Muller-Schiffmann A, Korth C, Fazari B, Chao OY, Nikolaus S, et al. Aβ dimers induce behavioral and neurochemical deficits of relevance to early Alzheimer's disease. *Neurobiology of aging*. 2018;69:1-9.
151. Sousa N, Almeida OF, Wotjak CT. A hitchhiker's guide to behavioral analysis in laboratory rodents. *Genes Brain Behav*. 2006;5 Suppl 2:5-24.
152. Wiltgen BJ, Brown RA, Talton LE, Silva AJ. New circuits for old memories: the role of the neocortex in consolidation. *Neuron*. 2004;44(1):101-8.
153. Morris R. Developments of a water-maze procedure for studying spatial learning in the rat. *Journal of neuroscience methods*. 1984;11(1):47-60.
154. Kraeuter AK, Guest PC, Sarnyai Z. The Y-Maze for Assessment of Spatial Working and Reference Memory in Mice. *Methods Mol Biol*. 2019;1916:105-11.
155. Samuelson DSORJ. Remembrance of places passed: Spatial memory in rats. *Journal of Experimental Psychology*. 1976;2:97-116.
156. Hogg S. A review of the validity and variability of the elevated plus-maze as an animal model of anxiety. *Pharmacol Biochem Behav*. 1996;54(1):21-30.
157. Rodgers RJ, Dalvi A. Anxiety, defence and the elevated plus-maze. *Neurosci Biobehav Rev*. 1997;21(6):801-10.
158. Handley SL, Mithani S. Effects of alpha-adrenoceptor agonists and antagonists in a maze-exploration model of 'fear'-motivated behaviour. *Naunyn Schmiedeberg's Arch Pharmacol*. 1984;327(1):1-5.
159. Shemesh Y, Sztainberg Y, Forkosh O, Shlapobersky T, Chen A, Schneidman E. High-order social interactions in groups of mice. *eLife*. 2013;2:e00759.
160. de Visser L, van den Bos R, Kuurman WW, Kas MJ, Spruijt BM. Novel approach to the behavioural characterization of inbred mice: automated home cage observations. *Genes Brain Behav*. 2006;5(6):458-66.
161. Krackow S, Vannoni E, Codita A, Mohammed AH, Cirulli F, Branchi I, et al. Consistent behavioral phenotype differences between inbred mouse strains in the IntelliCage. *Genes Brain Behav*. 2010;9(7):722-31.
162. Maroteaux G, Loos M, van der Sluis S, Koopmans B, Aarts E, van Gassen K, et al. High-throughput phenotyping of avoidance learning in mice discriminates different genotypes and identifies a novel gene. *Genes Brain Behav*. 2012;11(7):772-84.

163. Rummelink E, Smit AB, Verhage M, Loos M. Measuring discrimination- and reversal learning in mouse models within 4 days and without prior food deprivation. *Learn Mem.* 2016;23(11):660-7.
164. Berridge KC. Progressive degradation of serial grooming chains by descending decerebration. *Behav Brain Res.* 1989;33(3):241-53.
165. Deacon RM. Burrowing in rodents: a sensitive method for detecting behavioral dysfunction. *Nature protocols.* 2006;1(1):118-21.
166. Cunningham C, Deacon RM, Chan K, Boche D, Rawlins JN, Perry VH. Neuropathologically distinct prion strains give rise to similar temporal profiles of behavioral deficits. *Neurobiol Dis.* 2005;18(2):258-69.
167. Cunningham C, Deacon R, Wells H, Boche D, Waters S, Diniz CP, et al. Synaptic changes characterize early behavioural signs in the ME7 model of murine prion disease. *The European journal of neuroscience.* 2003;17(10):2147-55.
168. Deacon RM, Cholerton LL, Talbot K, Nair-Roberts RG, Sanderson DJ, Romberg C, et al. Age-dependent and -independent behavioral deficits in Tg2576 mice. *Behav Brain Res.* 2008;189(1):126-38.
169. Marshall GA, Olson LE, Frey MT, Maye J, Becker JA, Rentz DM, et al. Instrumental activities of daily living impairment is associated with increased amyloid burden. *Dement Geriatr Cogn Disord.* 2011;31(6):443-50.
170. McKhann GM, Knopman DS, Chertkow H, Hyman BT, Jack CR, Jr., Kawas CH, et al. The diagnosis of dementia due to Alzheimer's disease: recommendations from the National Institute on Aging-Alzheimer's Association workgroups on diagnostic guidelines for Alzheimer's disease. *Alzheimers Dement.* 2011;7(3):263-9.
171. Sturchler-Pierrat C, Abramowski D, Duke M, Wiederhold KH, Mistl C, Rothacher S, et al. Two amyloid precursor protein transgenic mouse models with Alzheimer disease-like pathology. *Proc Natl Acad Sci U S A.* 1997;94(24):13287-92.
172. Oddo S, Caccamo A, Shepherd JD, Murphy MP, Golde TE, Kaye R, et al. Triple-transgenic model of Alzheimer's disease with plaques and tangles: intracellular A β and synaptic dysfunction. *Neuron.* 2003;39(3):409-21.
173. Irizarry MC, McNamara M, Fedorchak K, Hsiao K, Hyman BT. APP^{Sw} transgenic mice develop age-related A β deposits and neuropil abnormalities, but no neuronal loss in CA1. *J Neuropathol Exp Neurol.* 1997;56(9):965-73.
174. Zhu L, Ramboz S, Hewitt D, Boring L, Grass DS, Purchio AF. Non-invasive imaging of GFAP expression after neuronal damage in mice. *Neurosci Lett.* 2004;367(2):210-2.
175. Tamguney G, Francis KP, Giles K, Lemus A, DeArmond SJ, Prusiner SB. Measuring prions by bioluminescence imaging. *Proc Natl Acad Sci U S A.* 2009;106(35):15002-6.
176. Watts JC, Giles K, Grillo SK, Lemus A, DeArmond SJ, Prusiner SB. Bioluminescence imaging of A β deposition in bigenic mouse models of Alzheimer's disease. *Proc Natl Acad Sci U S A.* 2011;108(6):2528-33.
177. Stohr J, Watts JC, Mensinger ZL, Oehler A, Grillo SK, DeArmond SJ, et al. Purified and synthetic Alzheimer's amyloid β (A β) prions. *Proc Natl Acad Sci U S A.* 2012;109(27):11025-30.
178. Jarrett JT, Lansbury PT, Jr. Seeding "one-dimensional crystallization" of amyloid: a pathogenic mechanism in Alzheimer's disease and scrapie? *Cell.* 1993;73(6):1055-8.
179. Morales R, Green KM, Soto C. Cross currents in protein misfolding disorders: interactions and therapy. *CNS Neurol Disord Drug Targets.* 2009;8(5):363-71.
180. Wickner RB, Masison DC, Edsles HK. [PSI] and [URE3] as yeast prions. *Yeast.* 1995;11(16):1671-85.
181. Wickner RB. [URE3] as an altered URE2 protein: evidence for a prion analog in *Saccharomyces cerevisiae*. *Science.* 1994;264(5158):566-9.
182. Patel BK, Gavin-Smyth J, Liebman SW. The yeast global transcriptional co-repressor protein Cyc8 can propagate as a prion. *Nature cell biology.* 2009;11(3):344-9.

183. Verma M, Girdhar A, Patel B, Ganguly NK, Kukreti R, Taneja V. Q-Rich Yeast Prion [PSI(+)] Accelerates Aggregation of Transthyretin, a Non-Q-Rich Human Protein. *Front Mol Neurosci*. 2018;11:75.
184. Derkatch IL, Chernoff YO, Kushnirov VV, Inge-Vechtomov SG, Liebman SW. Genesis and variability of [PSI] prion factors in *Saccharomyces cerevisiae*. *Genetics*. 1996;144(4):1375-86.
185. Schlumpberger M, Prusiner SB, Herskowitz I. Induction of distinct [URE3] yeast prion strains. *Mol Cell Biol*. 2001;21(20):7035-46.
186. Uptain SM, Sawicki GJ, Caughey B, Lindquist S. Strains of [PSI(+)] are distinguished by their efficiencies of prion-mediated conformational conversion. *EMBO J*. 2001;20(22):6236-45.
187. Deacon RM, Raley JM, Perry VH, Rawlins JN. Burrowing into prion disease. *Neuroreport*. 2001;12(9):2053-7.
188. Wallace RJ, Tigner JC. Effect of cortical and hippocampal lesions on hoarding behavior in the albino rat. *Physiology & behavior*. 1972;8(5):937-42.
189. Wishart T, Brohman L, Mogenson G. Effects of lesions of the hippocampus and septum on hoarding behaviour. *Anim Behav*. 1969;17(4):781-4.
190. Deacon RM, Penny C, Rawlins JN. Effects of medial prefrontal cortex cytotoxic lesions in mice. *Behav Brain Res*. 2003;139(1-2):139-55.
191. Katz S. Assessing self-maintenance: activities of daily living, mobility, and instrumental activities of daily living. *J Am Geriatr Soc*. 1983;31(12):721-7.
192. Bienkiewicz MM, Brandi ML, Goldenberg G, Hughes CM, Hermsdorfer J. The tool in the brain: apraxia in ADL. Behavioral and neurological correlates of apraxia in daily living. *Front Psychol*. 2014;5:353.
193. Deacon RM, Rawlins JN. Hippocampal lesions, species-typical behaviours and anxiety in mice. *Behav Brain Res*. 2005;156(2):241-9.
194. SCHMID-HOLMES S, DRICKAMER LC, ROBINSON AS, GILLIE LL. Burrows and Burrow-Cleaning Behavior of House Mice (*Mus musculus domesticus*). *The American Midland Naturalist*. 2001;146(1):53-62, 10.
195. Mallucci GR, White MD, Farmer M, Dickinson A, Khatun H, Powell AD, et al. Targeting cellular prion protein reverses early cognitive deficits and neurophysiological dysfunction in prion-infected mice. *Neuron*. 2007;53(3):325-35.

8. APPENDICES

Study I

The interaction of insoluble Amyloid- β with soluble Amyloid- β dimers decreases Amyloid- β plaque numbers.

van Gerresheim EF, Herring A, Gremer L, Müller-Schiffmann A, Keyvani K, Korth C.

Neuropathology and Applied Neurobiology 2021 Aug;47(5):603-610

doi: 10.1111/nan.12685

PMID: 33338256



ORIGINAL ARTICLE

The interaction of insoluble Amyloid- β with soluble Amyloid- β dimers decreases Amyloid- β plaque numbers

Else F. van Gerresheim¹ | Arne Herring² | Lothar Gremer^{3,4,5} |
Andreas Müller-Schiffmann¹ | Kathy Keyvani² | Carsten Korth¹ ¹Department of Neuropathology, Heinrich Heine University Düsseldorf, Düsseldorf, Germany²Institute of Neuropathology, University of Duisburg-Essen, Essen, Germany³Institute of Physical Biology, Heinrich Heine University Düsseldorf, Düsseldorf, Germany⁴Institute of Biological Information Processing (IBI-7) and JuStruct, Jülich Center for Structural Biology, Research Centre Jülich, Jülich, Germany⁵Research Center for Molecular Mechanisms of Aging and Age-Related Diseases, Moscow Institute of Physics and Technology (State University), Dolgoprudny, Russia**Correspondence**Carsten Korth, Department of Neuropathology, Heinrich Heine University Düsseldorf, Moorenstrasse 5, 40225 Düsseldorf, Germany.
Email: ckorth@hhu.de**Funding information**

Deutsche Forschungsgemeinschaft, Grant/Award Number: KO 1679/10-1; BMBF, Grant/Award Number: 01GQ1422; Russian Science Foundation, Grant/Award Number: 20-64-46027

Abstract

Objectives: The heterogeneity of Amyloid-beta ($A\beta$) plaque load in patients with Alzheimer's disease (AD) has puzzled neuropathology. Since brain $A\beta$ plaque load does not correlate with cognitive decline, neurotoxic soluble $A\beta$ oligomers have been championed as disease-causing agents in early AD. So far, investigating molecular interactions between soluble oligomeric $A\beta$ and insoluble $A\beta$ *in vivo* has been difficult because of the abundance of $A\beta$ oligomer species and the kinetic equilibrium in which they coexist. Here, we investigated whether $A\beta$ plaque heterogeneity relates to interactions of different $A\beta$ conformers.

Materials and Methods: We took advantage of transgenic mice that generate exclusively $A\beta$ dimers (tgDimer mice) but do not develop $A\beta$ plaques or neuroinflammation during their lifetime, crossed them to the transgenic CRND8 mice that develop plaques after 90 days and measured $A\beta$ plaque load using immunohistochemical and biochemical assays. Furthermore, we performed *in vitro* thioflavin T (ThT) aggregation assays titrating synthetic $A\beta_{42}$ -S8C dimers into fibril-forming synthetic $A\beta_{42}$.

Results: We observed a lower number of $A\beta$ plaques in the brain of double transgenic mice compared to tgCRND8 mice alone while the average plaque size remained unaltered. Corroborating these *in vivo* findings, synthetic $A\beta$ -S8C dimers inhibited fibril formation of wild-type $A\beta$ also *in vitro*, seen by an increased half-time in the ThT assay.

Conclusions: Our study indicates that $A\beta$ dimers directly interfere with $A\beta$ fibril formation *in vivo* and *in vitro*. The variable interaction of $A\beta$ dimers with insoluble $A\beta$ seeds could thus contribute to the heterogeneity of $A\beta$ plaque load in AD patients.

KEYWORDS

Amyloid-beta, Alzheimer's disease, dimer, fibril formation

Abbreviations: AD, Alzheimer's disease; APP, Amyloid precursor protein; $A\beta$, Amyloid beta; EDTA, Ethylenediaminetetraacetic Acid; ELISA, Enzyme-Linked Immunosorbent Assay; gDNA, Genomic DNA; haPrP, Syrian hamster prion gene; HFIF, Hexafluoroisopropanol; qPCR, Quantitative real-time Polymerase Chain Reaction; RF, Rigid Fibril; RP-HPLC, Reverse-Phase High-Performance Liquid Chromatography; SDS, Sodium Dodecyl Sulphate; TBS, Tris-Buffered Saline; TBST, Tris-Buffered Saline/0.025% Tween 20; ThT, Thioflavin T.

This is an open access article under the terms of the Creative Commons Attribution-NonCommercial-NoDerivs License, which permits use and distribution in any medium, provided the original work is properly cited, the use is non-commercial and no modifications or adaptations are made.

© 2020 The Authors. *Neuropathology and Applied Neurobiology* published by John Wiley & Sons Ltd on behalf of British Neurological Society.

INTRODUCTION

Amyloid-beta ($A\beta$) plaque load in patients with Alzheimer's disease (AD) is heterogeneous and often does not correlate with cognitive deficits (1-4). This has remained a conundrum, as $A\beta$ plaques have been a defining feature of AD since its inception. To this end, $A\beta$ oligomers and tau fibrillization are better correlates of failing cognition (5). Accordingly, the amyloid cascade hypothesis of AD, claiming that $A\beta$ multimerization is causal in the neuropathology of AD, has consequently shifted to $A\beta$ oligomers as causative agents in early AD (5).

However, the term $A\beta$ "oligomer", at this stage, is poorly defined and comprises anything from dimers to 24-mers (6), each with potentially different and possibly even opposing effects. For example, $A\beta$ oligomers have been proposed to be predecessors of $A\beta$ plaques (7), to be sequestered by $A\beta$ plaques as a protective mechanism (8), but also to be shed from plaques, which act as a reservoir (9). The ongoing problem with studying the effects of different species of insoluble/multimeric and soluble/oligomeric species of $A\beta$ in brains, cellular systems or cell-free systems is the existence of a kinetic equilibrium between different species, that is, the inability to investigate exclusive $A\beta$ species at defined concentrations without permanently ongoing dynamic changes in their multimerization or conformation. For these reasons, stabilized dimeric $A\beta$ variants have been generated, either by introducing intermolecular disulfide bridges (10,11) or by linking two $A\beta$ peptides head to tail via a flexible glycine-serine-rich linker (12).

We previously generated a disulfide-stabilized $A\beta$ dimer via replacing a serine at position 8 of the $A\beta$ domain with a cysteine. This mutant allowed preparations of synthetic $A\beta$ -S8C dimers as well as the generation of naturally secreted $A\beta$ -S8C dimers after processing of a corresponding active amyloid precursor protein (APP) mutant in cell culture and in an *in vivo* mouse model termed tgDimer mouse (13,14). We took advantage of these tgDimer mice that express human APP₇₅₁ K670 N / M671L (Swedish) / S679C under control of the Thy1 promoter and in which exclusively $A\beta$ -S8C dimers are generated but no other $A\beta$ species including monomers (14). TgDimer mice are remarkable since they express no insoluble $A\beta$, hence, do not develop $A\beta$ plaques, astrogliosis or neuroinflammation during their lifetime. Yet they show learning and memory deficits as well as anxiety and despair-related behaviours with aberrant serotonin and acetylcholine levels and thus reflect features of early AD (14,15).

To investigate how $A\beta$ plaque heterogeneity may relate to interactions of different $A\beta$ conformers, we analysed the aggregation propensity of $A\beta$ -S8C dimers in the presence of wild-type $A\beta$ seeds by crossing the tgDimer mouse with the transgenic CRND8 (tgCRND8) mouse, a mouse line expressing human APP₆₉₅ K670 N / M671L (Swedish) / V717F (Indiana) under control of the Syrian hamster (ha) PrP promoter (16). We investigated plaque formation in 3- and 5-month-old tgCRND8/tgDimer mouse brains and compared them to tgCRND8 brains of same age. In order to simulate these $A\beta$ interactions *in vitro*, we used the thioflavin T (ThT) assay, where we

added varying amounts of stabilized synthetic $A\beta_{42}$ -S8C dimers to wild-type $A\beta_{42}$.

Our data suggest that the presence of $A\beta$ -S8C inhibits $A\beta$ plaque seeding, although plaque size remained the same when compared to tgCRND8 mice suggesting an inhibitory effect of $A\beta$ -S8C dimers on amyloid fibril formation. By adding $A\beta_{42}$ -S8C to the aggregation-prone wild-type $A\beta_{42}$ *in vitro*, we observed an increased time of seeding onset supporting the idea that $A\beta$ dimers inhibit fibril formation but not growth.

MATERIALS AND METHODS

Animals

TgCRND8 mice express human APP₆₉₅ with the familial Swedish (K670 N/ M671L) and Indiana (V717F) mutations under control of the Syrian hamster prion gene (haPrP) promoter, and have been extensively characterized before (16). TgDimer mice express human APP₇₅₁ with the Swedish mutation and the dimer mutation within the $A\beta$ domain (S679C) that generates $A\beta$ -S8C dimers. The mice used here (tgCRND8/tgDimer) were hemizygous for APP carrying the Swedish and Indiana mutation (from CRND8) and hemizygous for APP carrying the Swedish and $A\beta$ -S8C mutation (from tgDimer). Animal experiments were performed in accordance with the German Animal Protection Law and were authorized by local authorities (LANUV NRW, Germany). Mice were housed under standard laboratory conditions with lights on from 7 a.m. to 7 p.m. and with water and food provided *ad libitum*.

Antibodies

Iba1 antibody (EPR16588) was bought from Abcam. GFAP-specific antibody (Z0334) and the $A\beta$ antibodies 6F/3D, M0872, were purchased from DAKO. IC16 and CT15 antibodies were described elsewhere (17,18) and used in combination with secondary goat anti-mouse or goat anti-rabbit POD-linked antibodies (ThermoFisher 1:25,000). In addition, anti-Actin (A2066) and anti-Tubulin (T9026) antibodies were purchased from Sigma. Additionally, goat anti-mouse IRDye 680RD and goat anti-rabbit 800CW (from LI-COR) were used as secondary antibodies.

Brain tissue preparation

At postnatal day 90 (P90) and 150 (P150), tgCRND8, tgCRND8/tgDimer and tgDimer mice were euthanized and their brains removed. One hemisphere was fixed overnight in 4% buffered formaldehyde, followed by paraffin embedding. Afterwards, the hemisphere was cut into 10- μ m-thick coronal sections. The other hemisphere was snap-frozen in liquid N_2 before genomic DNA (gDNA) was extracted from homogenized tissue of this hemisphere

to quantify gene expression by quantitative real-time polymerase chain reaction (qPCR).

Immunohistochemistry

A β plaques were visualized by immunohistochemistry using the 6F/3D antibody at a dilution of 1:100 and stereologically quantified in 8 coronal brain sections (with 100 μ m interspace between sections) per animal at 200 \times magnification. A β plaque number (n/ mm²) was determined in an unbiased manner by an area fraction fractionator (counting frame 300 \times 300 μ m, grid size 425 \times 425 μ m for both probes). The average plaque size (μ m²) was calculated by dividing the total A β plaque-positive area by the total plaque number. Absolute values were related to the investigated area. A Nikon 80i microscope, a colour digital camera (3/4" chip, 36-bit colour, DV-20, MicroBrightField) and MicroBrightField software Stereo Investigator 11 were used.

Quantitative real-time RT-PCR

gDNA was isolated using a lysis buffer containing EDTA and 1% SDS from the 10% brain homogenate samples. Expression levels of the APP transgene in CRND8 were determined using the following primers: haPrP-5'-3' TGGCTAGTCAGGGCTTTGTT (forward primer) and haPrP-5'-3' TGGGAGGCTGTTCTTAGGG (reverse primer) both targeting the promoter region of haPrP.

The APP (A β -S8C) transgene was quantified with: pTSCAPPswe3600-5'-3' CTGCCTCTCTGCCTCTCTGC (forward primer) and APPseq3R-5'-3' CACAGAACATGGCAATCTGG (reverse primer) to target the Thy1 promoter region. Raw Ct values were used to calculate relative expression levels of target genes, after normalization to the internal control gene β -actin.

Four-step ultracentrifugation fractionation

The amount of insoluble A β in tgCRND8 and in tgCRND8/tgDimer mouse brains was determined by performing a four-step ultracentrifugation as described previously (19). Briefly, 100 μ L of 10% homogenates Tris-buffered saline (TBS) were centrifuged at 100,000 \times g for 1 h at 4°C. The supernatants (soluble free A β) were harvested and the pellets were resuspended in 100 μ L TBS/1% Triton TX-100 by sonication. After centrifugation at 100,000 \times g at 4°C for 1 h, the supernatants (membrane bound A β) were taken and the precipitates dissolved in 100 μ L TBS/2% SDS by sonication. After centrifugation at 100,000 \times g at room temperature, the supernatants (protein bound A β) were harvested and the precipitates were finally dissolved in 100 μ L of 70% formic acid (plaque-associated insoluble A β) before being centrifuged again for 1 h at 100,000 \times g at room temperature. The first three supernatants were diluted 20-fold in TBS and the formic acid

fraction was neutralized by adding 20 volumes of 1 M unbuffered Tris solution.

A β ELISA

Insoluble A β ₄₀ and A β ₄₂ were extracted from brain homogenates after four-step fractionation with 70% formic acid and quantified using the A β ₄₀ or A β ₄₂ kit from Invitrogen (Invitrogen; KHB3481 and KHB3441) according to the manufacturer's protocol. A β concentrations were calculated relative to the monomer concentration of the standard and are indicated as pmol/g protein. A β levels were normalized using the protein concentration measured with the DC™ (detergent compatible) protein assay (Bio-Rad).

Western Blot

For visualization of Iba1 and GFAP, 30 and 20 g of 10% whole-brain homogenates respectively in 100 mM Tris HCl pH 7.5, 140 mM NaCl and 3 mM KCl (TBS) containing Complete protease inhibitor cocktail (Roche) were separated on a NuPAGE 4–12% Bis-Tris Gel (Life technologies), using NuPAGE Sample buffer with addition of 2% (v/v) of β -mercaptoethanol and transferred to a 0.2 μ m nitrocellulose membrane. The membranes were blocked with PBS/5% skimmed milk and incubated with either primary antibodies against Iba1 (1:2,000) or GFAP (1:2,500) and actin (1:5,000) or tubulin (1:5,000) diluted in TBS/0.025% Tween20 (TBST). After 3x washing with TBST and incubation with appropriate secondary antibodies, signals were quantified by densitometric analysis using the Odyssey infrared imaging system (LI-COR).

For A β species visualization, 10% brain homogenates and the fractions derived from four-step fractionation were incubated with IC16-coupled NHS agarose beads (13). After washing with PBS, bound APP/A β was eluted with NuPAGE sample buffer/2% β -mercaptoethanol, and afterwards separated on a 4–12% Bis-Tris Gel. The membrane was boiled for 10 min in PBS after separation, before blocking with PBS/5% skimmed milk. The membrane was incubated with the antibody 4G8 against A β (1:500) diluted in TBST respectively. After washing three times with TBST and incubation with secondary horseradish peroxidase conjugated (POD) antibody, signals were detected with SuperSignal™ West Pico PLUS Chemiluminescent Substrate (ThermoFisher). The same blot was washed and incubated with CT15 (1:3,500) in TBST for APP fragment detection, and signals were visualized using the LI-COR system.

A β ₄₂ and A β ₄₂-S8C dimer preparation

A β ₄₂ was purchased from Bachem, A β ₄₂-S8C was synthesized by JPT Peptide Technologies. Both were treated with hexafluoroisopropanol (HFIP) and lyophilized before use. Subsequently, A β ₄₂-S8C was dissolved in 50 mM HEPES NaOH pH 7.6 and incubated for at least 4 h

to complete dimerization. Thereafter, the dimerized fraction was purified by reverse-phase high-performance liquid chromatography (RP-HPLC) on a Zorbax 300 SB-C8 column (4.6 mm x 250 mm) connected to an Agilent 1260 system and lyophilized again. Another HFIP treatment ensured the presence of pure non-aggregated $A\beta_{42}$ -S8C dimers. Immediately before use, the $A\beta$ proteins were dissolved in 50 mM HEPES NaOH pH 7.6 buffer to a stock concentration of 20 μ M.

Thioflavin T (ThT) assay

Five μ M $A\beta_{42}$ were mixed with varying amounts of $A\beta_{42}$ -S8C dimers (between 0.25 and 2.5 μ M) in 50 mM HEPES NaOH pH 7.6 containing 10 μ M ThT (Abcam) up to a volume of 55 μ L into wells of a half area black/clear flat bottom polystyrene 96-wells plate (Corning). On the same plate, varying amounts of $A\beta_{42}$ -S8C dimers in 50 mM HEPES NaOH pH 7.6 were mixed with 10 μ M ThT. The ThT fluorescence of $A\beta_{42}$ -S8C dimers was later subtracted from the ThT fluorescence obtained from 5 μ M $A\beta_{42}$ mixed with $A\beta_{42}$ -S8C dimers. The outermost wells of the plate were filled with buffer and ThT

only, in order to reduce artefactual measurements on marginal rows and columns. ThT fluorescence was measured using a FluoStar plate reader (BMG Labtech) at 30°C with orbital shaking at 700 rpm for at least 24 h. ThT fluorescence was excited at 448 nm and emission collected at 482 nm.

Statistical analysis

Data are depicted as means \pm SEM. Normal distribution of the data sets was tested by Pearson's normality test. Mann-Whitney Test was applied for the analyses of two groups, unless stated otherwise. Differences were considered significant at $p < 0.05$. All tests were performed utilizing GraphPad Prism 8.4.2.

RESULTS

APP transgene expression levels of tgDimer, tgCRND8 and tgCRND8/tgDimer mice were measured by qPCR. The expression

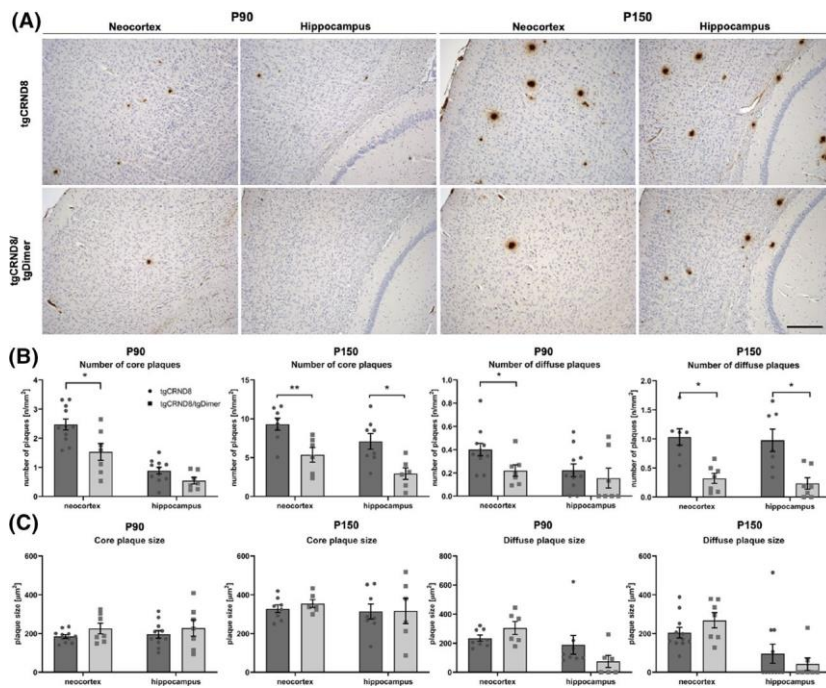


FIGURE 1 Morphological and biochemical differences between tgCRND8 (P90, $n = 11$; P150, $n = 8$) and tgCRND8/tgDimer (P90, $n = 7$; P150, $n = 6$) mice. Core plaques were defined as compact dense plaques, whereas diffuse plaques were defined as an amorphous structure, without a clear border. Mann-Whitney tests were used to test for statistical significance. (A) Representative immunohistochemical images of the neocortex and hippocampus for A β are presented for tgCRND8 and tgCRND8/tgDimer mice at P90 and P150. At P90, few plaques are detected in both genotypes, whereas at P150 more A β deposits are detected in the tgCRND8 mouse compared to the tgCRND8/tgDimer mouse. Antibody 6F/3D. Scale bar = 200 μ m. (B) There is a significantly higher number of core plaques in the neocortex of the tgCRND8 mice (2.5 ± 0.2) compared to the tgCRND8/tgDimer mice (1.5 ± 0.3 ; $p = 0.0268$) at P90. The number of core plaques in the neocortex and hippocampus is significantly higher in tgCRND8 mice (9.3 ± 0.8 and 7.1 ± 1.0) versus tgCRND8/tgDimer mice at P150 (5.4 ± 0.9 and 2.9 ± 0.8 ; $p = 0.0127$, $p = 0.0200$) at P150. The number of diffuse plaques is significantly higher in the neocortex at P90 in tgCRND8 mice (0.4 ± 0.05) compared to tgCRND8/tgDimer mice (0.2 ± 0.05 ; $p = 0.0346$). At P150, the number of diffuse plaques is significantly higher in both brain regions of the tgCRND8 mice (1.1 ± 0.1 , 0.9 ± 0.2) compared to the tgCRND8/tgDimer mice (0.4 ± 0.1 , 0.3 ± 0.1 ; $p = 0.0013$ and $p = 0.0073$, respectively). (C) The size of the core and diffuse plaques (in μ m²) in the neocortex and hippocampus are not different between the groups.

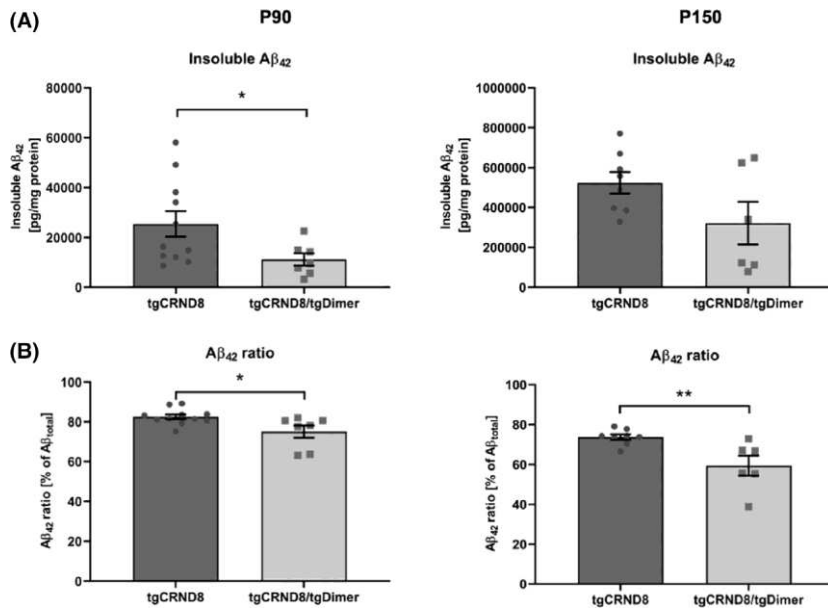


FIGURE 2 Differences in insoluble A β_{42} levels and A β ratio between tgCRND8 and tgCRND8/tgDimer mice. (A) The level of insoluble A β_{42} is higher in tgCRND8 mice ($25,392 \pm 5,149$ pg/mg protein) compared to tgCRND8/tgDimer mice ($11,138 \pm 2,501$ pg/mg protein, $p = 0.0441$) at P90. At P150, the insoluble A β_{42} is also higher in tgCRND8 mice ($523,455 \pm 53,885$ pg/mg protein) compared to tgCRND8/tgDimer mice ($321,280 \pm 106,856$ pg/mg protein), although not reaching statistical significance ($p = 0.1812$). (B) The A β_{42} /total A β ratio is significantly higher in the tgCRND8 mice (P90: $82.5 \pm 1.2\%$; P150: $73.7 \pm 1.4\%$) versus tgCRND8/tgDimer (P90: $75.1 \pm 3.1\%$; P150: $59.5 \pm 5.0\%$) mice at both ages ($p = 0.0154$ and $p = 0.0081$ respectively).

of the haPrP promoter-driven hAPP₆₉₅(Swe/Ind) gene (Figure S1A), or Thy1 promoter-driven hAPP₇₅₁(Swe/A β -S8C) gene (Figure S1B) did not differ between the tgCRND8/tgDimer and tgCRND8 mice, respectively, or between the tgCRND8/tgDimer and tgDimer mice, respectively.

The influence of the A β -S8C dimers on plaque formation was assessed by quantifying dense or core plaques. Dense plaques are fibrillar deposits of A β , that show all the classical properties of amyloid including β -sheet secondary structure and dystrophic neurites surrounding the plaques, and diffuse plaques are amorphous A β deposits – an antecedent stage of core plaques (20). At the age of 90 and 150 days, both the tgCRND8 and tgCRND8/tgDimer mice showed A β plaques (Figure 1A). We quantified both A β core and diffuse plaques by measuring the number (per mm²) and size (in μm^2) of plaques in coronal brain sections of tgCRND8 and tgCRND8/tgDimer mice at P90 and P150 (Figure 1A). In comparison to tgCRND8/tgDimer mice, tgCRND8 mice had significantly more A β core and diffuse plaques at P90 only in the earlier affected neocortex but not yet in the hippocampus (Figure 1B; $p = 0.0268$, $p = 0.0346$, $p = 0.0566$ and $p = 0.2638$, respectively). Later on, at P150, this difference also became detectable in the hippocampus (Figure 1B; $p = 0.0127$, $p = 0.0013$, $p = 0.0200$ and $p = 0.0073$ respectively). However, the average size of the plaques was not different between the groups (Figure 1C).

Insoluble A β_{40} and A β_{42} peptides from brain homogenates of tgCRND8/tgDimer and tgCRND8 mice at P90 and P150 were obtained via a four-step fractionation protocol (Figure S2) and quantified by ELISA. All concentrations were normalized using the total

protein concentration of the starting 10% brain homogenate. The level of insoluble A β_{42} was significantly higher in tgCRND8 mice at P90 ($25,392 \pm 5,149$ pg/mg protein) compared to tgCRND8/tgDimer mice ($11,138 \pm 2,501$ pg/mg protein, Figure 2A $p = 0.0441$). The level of insoluble A β_{42} at P150 in tgCRND8 mice ($523,455 \pm 53,885$ pg/mg protein) was also higher as in the tgCRND8/tgDimer mice ($321,280 \pm 106,856$ pg/mg protein) but failed statistical significance ($p = 0.1812$). The Swedish mutation of APP does not change the A β_{42} /total A β ratio compared to wild-type APP. Consistently, we observed a ratio of 20% A β_{42} /total A β in tgDimer mice, which did not significantly change throughout the lifespan and was similar to wild-type mice (14), which indicates no accumulation of A β and especially A β_{42} . The Indiana mutation of APP in tgCRND8 mice, by contrast, markedly increased the generation of A β_{42} and led to an average ratio of about 80% A β_{42} /total A β in the insoluble A β fraction derived from tgCRND8 similar to previous findings in other AD animal models (16,21). In tgCRND8/tgDimer mice, we detected a significant lower ratio of A β_{42} /total A β (P90: $75.1 \pm 3.1\%$; P150: $59.5 \pm 5.0\%$) compared to tgCRND8 mice (P90: $82.5 \pm 1.2\%$; P150: $73.7 \pm 1.4\%$; Figure 2B $p = 0.0154$ and $p = 0.0080$). We did not observe significant amounts of other A β oligomer species in the brains of these mice (Figure S3).

Next, we analysed whether we could observe a correlation between A β plaque load and the concentrations of insoluble A β_{42} . At P90, there was a trend towards a positive correlation between the levels of insoluble A β_{42} and the numbers of plaques in tgCRND8 mice (Figure S4, $p = 0.0856$) consistent with the idea that A β_{42} is the most aggregation-prone A β species initiating seeding. Interestingly,

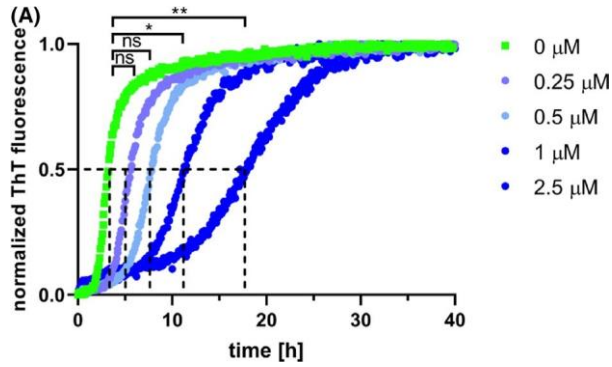


FIGURE 3 Effect of A β_{42} -S8C dimers on A β_{42} aggregation assay. A β_{42} -S8C dimers added in various concentrations to A β_{42} inhibit fibril formation. The half-time (defined as the time to reach 50% of maximum fluorescence) of 5 μ M A β_{42} without the addition of A β_{42} -S8C is 3.2 h \pm 0.1 h. At concentrations of 0.25 and 0.5 μ M of A β_{42} -S8C dimers (concentration given as monomer equivalents), a slight shift of the curve to the right is observed with an increase in aggregation half-time (5.8 h \pm 0.2 h; 7.7 h \pm 0.3 h, not significant). The addition of higher concentrations, 1 μ M and 2.5 μ M A β_{42} -S8C, results in a significant increase in the aggregation half-time (normalized data, one-way ANOVA, 11.3 h \pm 0.5 h; p = 0.0164, and 17.9 h \pm 1.2 h; p = 0.0005 respectively).

this correlation vanished later on, at P150 (Figure S4), possibly, as discussed by Burgold *et al.* (22) due to the fact that in the late “saturation phase” of plaque genesis *in vivo*, A β is mainly added to existing plaques and does not reach the critical concentration for new nucleating seeds.

In contrast, in the case of tgCRND8/tgDimer mice, while there was no correlation between the number of plaques and A β_{42} levels at P90, a significant positive correlation was present later, at P150 (Figure S5, p = 0.0382). This shift of a correlation between A β_{42} level and plaques to older age is likely to be a consequence of decreased baseline A β_{42} levels, reaching the saturation threshold later. Of note, despite the differences in the plaque burden, the level of neuroinflammation indicated by microgliosis or astrogliosis was similar in tgCRND8 versus tgCRND8/tgDimer mice (Figure S6).

The results here suggest that the presence of A β -S8C dimers slows down the formation of new A β plaques. An explanation for this observation is that the introduction of the disulfide cross-link causes steric hindrance for the dimeric A β -S8C to form fibrils. The A β -S8C dimer adopts a rather rigid conformation, which is different from the monomeric and oligomeric forms (13,23). As a result, the A β -S8C dimer in the tgDimer is not prone to seed nucleation, as has been shown by molecular modelling and the fact that they do not develop plaques during their lifetime (13,23).

In order to corroborate the effect of A β -S8C dimers on amyloid fibril formation *in vitro*, we dimerized synthetic A β_{42} -S8C by letting it incubate in 50 mM HEPES NaOH pH 7.6 at 37°C with 450 rpm shaking. After 4 h, dimerization was complete (Figure S7), and the A β -S8C dimer fraction was purified and collected via RP-HPLC and prepared for aggregation assays.

In a ThT assay, we added various concentrations of synthetic A β_{42} -S8C dimers to wild-type A β_{42} . Without A β_{42} -S8C dimers, A β_{42} fibril formation was achieved with a half-time (defined as time to reach 50% of maximum fluorescence) of 3.2 h \pm 0.1 h (Figure 3). Addition of A β_{42} -S8C dimers at a dose of 0.25 μ M and 0.5 μ M, increased the half-time of fibril formation in dose-dependent manner (5.8 h \pm 0.2 h and 7.7 h \pm 0.3 h, Figure 3, not significant). Addition of higher concentrations of A β -S8C dimers: 1 μ M and 2.5 μ M A β -S8C dimers, resulted in a more pronounced increased half-time (11.3 h \pm 0.5 h and 17.9 h \pm 1.2 h, Figure 3, normalized data, one-way ANOVA, p = 0.0164, p = 0.0005 respectively).

DISCUSSION

Our findings are remarkable in two ways: first, they show that A β dimers, the A β oligomer species best definable and likely most abundant in brains of AD patients (24), are able to inhibit A β seeding, and second, that A β plaque seeding and growth follow different dynamics. How could the discrepancy of seeding and growth be instated in molecular terms? Our previous molecular dynamics simulations demonstrated the inability of A β -S8C dimers to form nuclei (13) (explaining the absence of A β plaques in the tgDimer mouse), yet, their fundamental ability to associate with existing wild-type A β plaque nuclei (14). The formation of wild-type A β nuclei (= seeds) is fundamentally different from their growth, since the former is thermodynamically unfavourable, whereas the latter is thermodynamically favourable (25). Once the nucleus has formed, further addition of monomers becomes thermodynamically favourable because monomers contact the growing polymer at multiple sites which results in rapid growth. It is conceivable that A β -S8C dimers intercept nucleation, thereby blocking growth, more efficiently in the initial stages of seeding when the nucleus or its precursor are unstable (25). In addition, A β plaque surface area increases by an order of two relative to their radius, and thus disruptive effect of the A β dimer is more efficient when the overall A β plaque surface area is smaller in early stages rather than in late stages of plaque growth.

Our *in vivo* and *in vitro* data are also supported by findings where a single-chain dimeric variant of A β_{40} , with two A β_{40} units connected via a flexible glycine-serine-rich linker, readily formed globular oligomers and curvilinear fibrils (12). Adding this A β dimer species to A β monomers progressively slowed rigid fibril (RF) formation, which was evident in the increasing RF lag periods. It was argued that the formation of metastable oligomers therefore alters RF nucleation (12). Similarly, A β -S8C dimers may interfere with fibril formation, by inhibiting nucleation, which would be an explanation for the increased half-time of the aggregation curves in the ThT assay by addition of A β_{42} -S8C dimers.

The well-known intersubject heterogeneity of A β plaque load (1-3) likely has multiple origins. For example, it has been suggested that it may be related to different A β prion conformers that reliably replicate within one individual brain, but that are not similar between

two or more AD brains leading to a low intrasubject variability but a high intersubject variability of A β conformers (26) that may, to some degree, correspond to different numbers of plaque formation. The contribution of microglia or myeloid cells to A β plaque load has also been emphasized (27). With this study, we add evidence for the inhibiting effect of A β dimers as a cause for A β plaque load heterogeneity, if it is assumed that the equilibrium between insoluble A β seeds and the simultaneously available amount of A β dimers is highly variable between individual AD cases and subject to the influence of a multitude of factors.

We demonstrated that two neurotoxic A β species, soluble A β dimers and insoluble A β , can have opposing effects on a classical diagnostic feature of AD, the abundance of A β plaques. Our insights indicate that correlating the clinical severity of AD defined by cognitive deficits with a mere morphological phenotype, A β plaque numbers, may insufficiently reflect the underlying equilibrium of functionally active, neurotoxic A β species. Current clinical diagnostics not distinguishing different A β species like A β positron emission tomography or the detection of whole A β species levels in cerebrospinal fluids are therefore in danger of picking misleading biological variables. A more fine-grained A β species diagnostics may therefore be beneficial, including for predicting the value of A β -targeted pharmacotherapies.

In conclusion, we have demonstrated that A β oligomers – here A β -S8C dimers – are able to decrease A β plaque seeding *in vivo* and *in vitro* and are a contributing factor to the clinical heterogeneity of A β plaque load in individuals suffering from AD or even cognitively unimpaired controls.

ACKNOWLEDGEMENT

This work was supported by a grant from the DFG (KO 1679/10-1) and BMBF (01GQ1422A) to C.K. and from the Russian Science Foundation (RSF) (project no. 20-64-46027) to L.G. for A β -S8C dimer preparations and ThT aggregation assays.

CONFLICT OF INTEREST

All authors declare no conflict of interest.

AUTHOR CONTRIBUTIONS

K.K., C.K., A.H. and A.M.-S. conceived and outlined the experiments. C.K., K.K., A.M.-S., L.G., A.H. and E.v.G. planned and supervised experiments. E.v.G., A.H. and L.G. performed experiments, collected and analysed data. All authors participated in writing and correcting the manuscript.

ETHICAL APPROVAL

Animal experiments were performed in accordance with the German Animal Protection Law and were authorized by local authorities (LANUV NRW, Germany).

PEER REVIEW

The peer review history for this article is available at <https://pubon.com/publon/10.1111/nan.12685>.

DATA AVAILABILITY STATEMENT

All original data will be made available upon reasonable request.

ORCID

Lothar Gremer  <https://orcid.org/0000-0001-7065-5027>

Kathy Keyvani  <https://orcid.org/0000-0003-2558-5159>

Carsten Korth  <https://orcid.org/0000-0003-1503-1822>

REFERENCES

- Lam B, Masellis M, Freedman M, Stuss DT, Black SE. Clinical, imaging, and pathological heterogeneity of the Alzheimer's disease syndrome. *Alzheimer's research & therapy*. 2013; 5(1):
- Bird TD, Sumi SM, Nemens EJ, et al. Phenotypic heterogeneity in familial Alzheimer's disease: a study of 24 kindreds. *Ann Neurol*. 1989; 25(1): 12-25.
- Cupidi C, Capobianco R, Goffredo D, et al. Neocortical variation of Abeta load in fully expressed, pure Alzheimer's disease. *Journal of Alzheimer's disease: JAD*. 2010; 19(1): 57-68.
- Zhang S, Smailagic N, Hyde C, et al. (11)C-PIB-PET for the early diagnosis of Alzheimer's disease dementia and other dementias in people with mild cognitive impairment (MCI). *Cochrane Database Syst Rev*. 2014;7:CD010386.
- McLean CA, Cherny RA, Fraser FW, et al. Soluble pool of Abeta amyloid as a determinant of severity of neurodegeneration in Alzheimer's disease. *Ann Neurol*. 1999; 46(6): 860-866.
- Haass C, Selkoe DJ. Soluble protein oligomers in neurodegeneration: lessons from the Alzheimer's amyloid beta-peptide. *Nature Rev Mol Cell Biol*. 2007; 8(2): 101-112.
- Lee J, Culyba EK, Powers ET, Kelly JW. Amyloid-beta forms fibrils by nucleated conformational conversion of oligomers. *Nat Chem Biol*. 2011; 7(9): 602-609.
- Gaspar RC, Villarreal SA, Bowles N, Hepler RW, Joyce JG, Shughrue PJ. Oligomers of beta-amyloid are sequestered into and seed new plaques in the brains of an AD mouse model. *Exp Neurol*. 2010; 223(2): 394-400.
- Koffie RM, Meyer-Luehmann M, Hashimoto T, et al. Oligomeric amyloid beta associates with postsynaptic densities and correlates with excitatory synapse loss near senile plaques. *Proc Natl Acad Sci U S A*. 2009; 106(10): 4012-4017.
- Yamaguchi T, Yagi H, Goto Y, Matsuzaki K, Hoshino M. A disulfide-linked amyloid-beta peptide dimer forms a protofibril-like oligomer through a distinct pathway from amyloid fibril formation. *Biochemistry*. 2010; 49(33): 7100-7107.
- Sandberg A, Luheshi LM, Sollvander S, et al. Stabilization of neurotoxic Alzheimer amyloid-beta oligomers by protein engineering. *Proc Natl Acad Sci U S A*. 2010; 107(35): 15595-15600.
- Hasecke F, Miti T, Perez C, et al. Origin of metastable oligomers and their effects on amyloid fibril self-assembly. *Chemical science*. 2018; 9(27): 5937-5948.
- Muller-Schiffmann A, Andreyeva A, Horn AH, Gottmann K, Korth C, Sticht H. Molecular engineering of a secreted, highly homogeneous, and neurotoxic abeta dimer. *ACS Chem Neurosci*. 2011; 2(5): 242-248.
- Muller-Schiffmann A, Herring A, Abdel-Hafiz L, et al. Amyloid-beta dimers in the absence of plaque pathology impair learning

- and syn-aptic plasticity. *Brain*. 2016; 139(Pt 2): 509-525.
15. Abdel-Hafiz L, Muller-Schiffmann A, Korth C, et al. Abeta dimers induce behavioral and neurochemical deficits of relevance to early Alzheimer's disease. *Neurobiol Aging*. 2018; 69: 1-9.
 16. Chishti MA, Yang D-S, Janus C, et al. Early-onset amyloid deposition and cognitive deficits in transgenic mice expressing a double mutant form of amyloid precursor protein 695. *J Biol Chem*. 2001; 276(24): 21562-21570.
 17. Müller-Schiffmann A, März-Berberich J, Andreyeva A, et al. Combining independent drug classes into superior, synergistically acting hybrid molecules. *Angew Chem*. 2010; 49(46): 8743-8746.
 18. Sisodia SS, Koo EH, Hoffman PN, Perry G, Price DL. Identification and transport of full-length amyloid precursor proteins in rat peripheral nervous system. *J Neurosci*. 1993; 13(7): 3136-3142.
 19. Kawarabayashi T, Younkin LH, Saido TC, Shoji M, Ashe KH, Younkin SG. Age-dependent changes in brain, CSF, and plasma amyloid (beta) protein in the Tg2576 transgenic mouse model of Alzheimer's disease. *J Neurosci*. 2001; 21(2): 372-381.
 20. Rak M, Del Bigio MR, Mai S, Westaway D, Gough K. Dense-core and diffuse Abeta plaques in TgCRND8 mice studied with synchrotron FTIR microspectroscopy. *Biopolymers*. 2007; 87(4): 207-217.
 21. Sturchler-Pierrat C, Abramowski D, Duke M, et al. Two amyloid precursor protein transgenic mouse models with Alzheimer disease-like pathology. *Proc Natl Acad Sci U S A*. 1997; 94(24): 13287-13292.
 22. Burgold S, Filser S, Dorostkar MM, Schmidt B, Herms J. In vivo imaging reveals sigmoidal growth kinetic of beta-amyloid plaques. *Acta Neuropathol Commun*. 2014; 2: 30.
 23. Horn AH, Sticht H. Amyloid-beta42 oligomer structures from fibrils: a systematic molecular dynamics study. *J Phys Chem B*. 2010; 114(6): 2219-2226.
 24. Shankar GM, Li S, Mehta TH, et al. Amyloid-beta protein dimers isolated directly from Alzheimer's brains impair synaptic plasticity and memory. *Nat Med*. 2008; 14(8): 837-842.
 25. Jarrett JT, Lansbury PT Jr. Seeding "one-dimensional crystallization" of amyloid: a pathogenic mechanism in Alzheimer's disease and scrapie? *Cell*. 1993; 73(6): 1055-1058.
 26. Condello C, Lemmin T, Stohr J, et al. Structural heterogeneity and intersubject variability of Abeta in familial and sporadic Alzheimer's disease. *Proc Natl Acad Sci U S A*. 2018; 115(4): E782-E791.
 27. Prokop S, Miller KR, Drost N, et al. Impact of peripheral myeloid cells on amyloid-beta pathology in Alzheimer's disease-like mice. *J Exp Med*. 2015; 212(11): 1811-1818.

SUPPORTING INFORMATION

Additional supporting information may be found online in the Supporting Information

How to cite this article: Gerresheim EF, Herring A, Gremer L, Müller-Schiffmann A, Keyvani K, Korth C. The interaction of insoluble Amyloid- β with soluble Amyloid- β dimers decreases Amyloid- β plaque numbers. *Neuropathol Appl Neurobiol*.

2021;00:1-8. <https://doi.org/10.1111/nan.12685>

**The interaction of insoluble Amyloid- β with soluble Amyloid- β dimers decreases
Amyloid- β plaque numbers**

Else F. van Gerresheim¹, Arne Herring², Lothar Gremer³, Andreas Müller-Schiffmann¹, Kathy Keyvani², Carsten Korth^{1*}

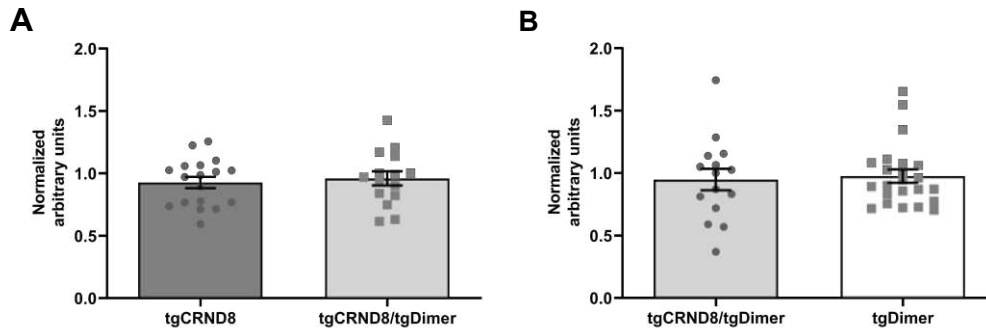
¹ Department of Neuropathology, Heinrich Heine University Düsseldorf, Düsseldorf, Germany

² Institute of Neuropathology, University of Duisburg-Essen, Essen, Germany

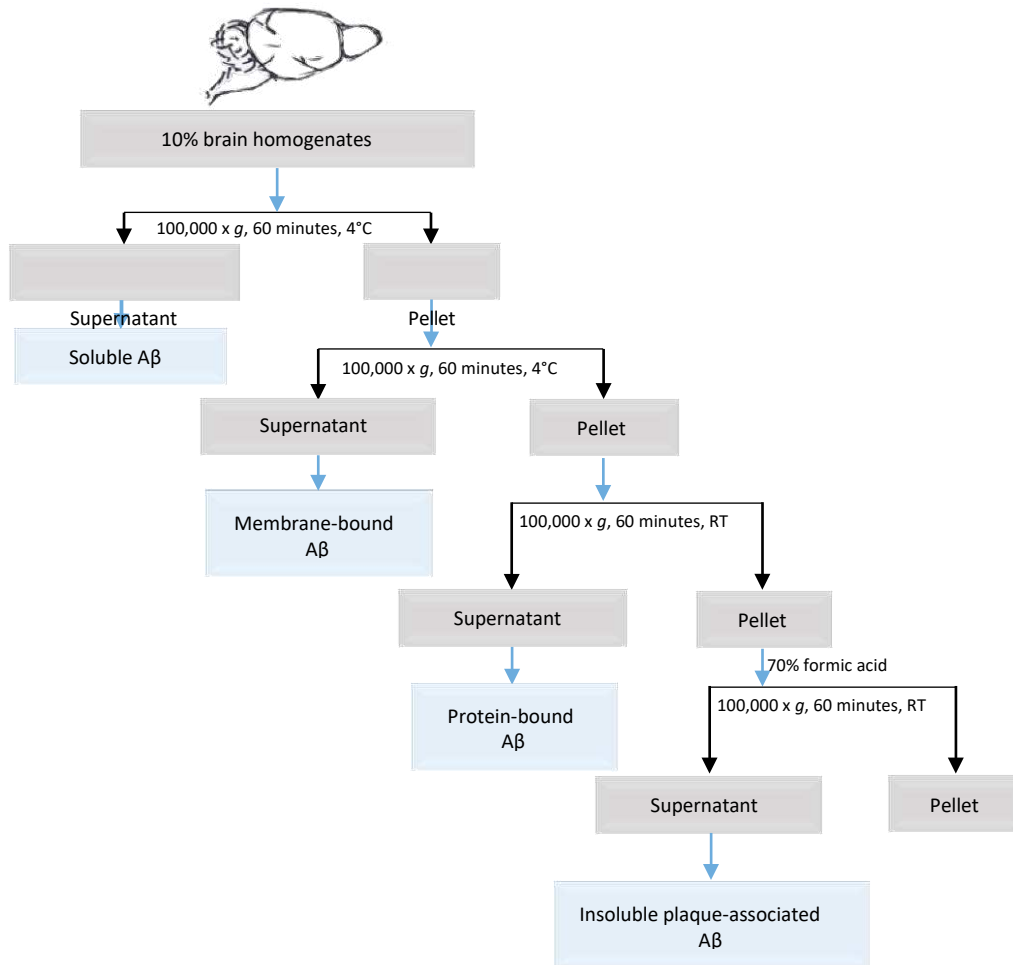
³ Institute of Physical Biology, Heinrich Heine University Düsseldorf, Düsseldorf, Germany; Institute of Biological Information Processing (IBI-7); JuStruct: Jülich Center for Structural Biology, Research Centre Jülich, Jülich, Germany; Research Center for Molecular Mechanisms of Aging and Age-Related Diseases, Moscow Institute of Physics and Technology (State University), Dolgoprudny, Russia

Supplementary Material

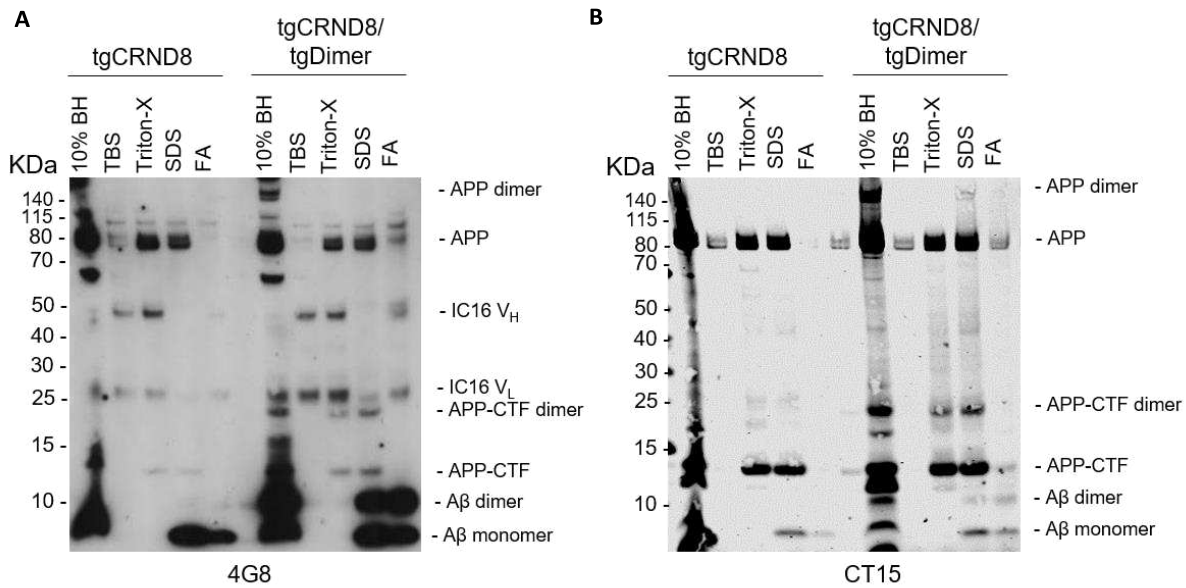
Figure S1. hAPP₆₉₅(Swe/Ind) and hAPP₇₅₁(Swe/A β -S8C) gene dose in TgCRND8, TgCRND8/tgDimer, and tgDimer mice



S1. Normalized arbitrary units of hAPP₆₉₅ (Swe/Ind) (A) and hAPP₇₅₁ (Swe/A β -S8C) (B) gene doses in TgCRND8 (n=18), TgCRND8/tgDimer (n=15), and tgDimer (n=23) mice. There was no significant difference in the gene doses among the groups (Mann Whitney U-test). Here, P90 and P150 are taken together.

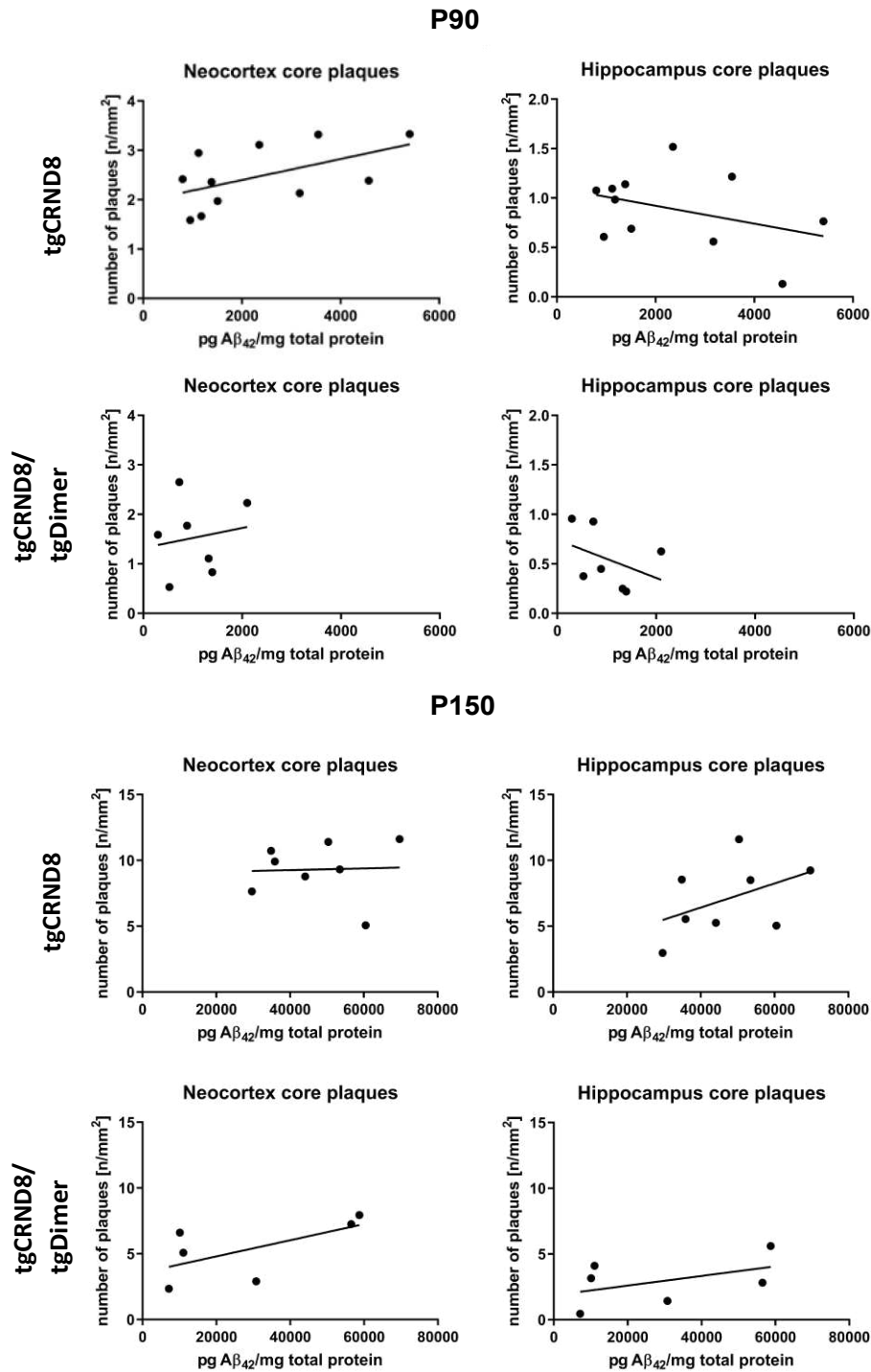
Figure S2. Schematic protocol of the 4-step fractionation

S2. Schematic representation of the four-step fractionation protocol according to Kawarabayashi et al (1). Levels of A β were measured after a four-step fractionation. In short, 100 μ L of 10% brain homogenate underwent several rounds of centrifugation in different buffers. After the last spin, the supernatant consists of the insoluble plaque-associated A β , which was then measured by ELISA. (TBS, Tris Buffered Saline, RT, room temperature) The fractions were used for immunoprecipitation of A β species.

Figure S3. A β species in the brain homogenates of tgCRND8 and tgCRND8/tgDimer mice

S3. 10% brain homogenates and fractions obtained via four-step fractionation protocol (1), similar to Lesne et al. (2), were incubated with mAB IC16 NHS agarose beads. Bound APP/A β was eluted with NuPAGE sample buffer and separated on 4-12% Bis-Tris gel and transferred onto 0.2 μ m nitrocellulose membrane. The membrane was first incubated with the 4G8 antibody (A,1:500). After 3x washing with TBST and incubation with secondary horseradish peroxidase conjugated (POD) antibody, signals were detected with SuperSignal™ West Pico PLUS Chemiluminescent Substrate (Thermofisher). The same blot was washed and incubated with CT15 (1:3,500) in TBST for APP fragment detection, and signals were visualized using the LI-COR system. Residual A β dimer and monomer species are visible in the α -CT15 blot, however, the APP- β CTF and APP- β CTF dimer signal is enhanced in the left blot.

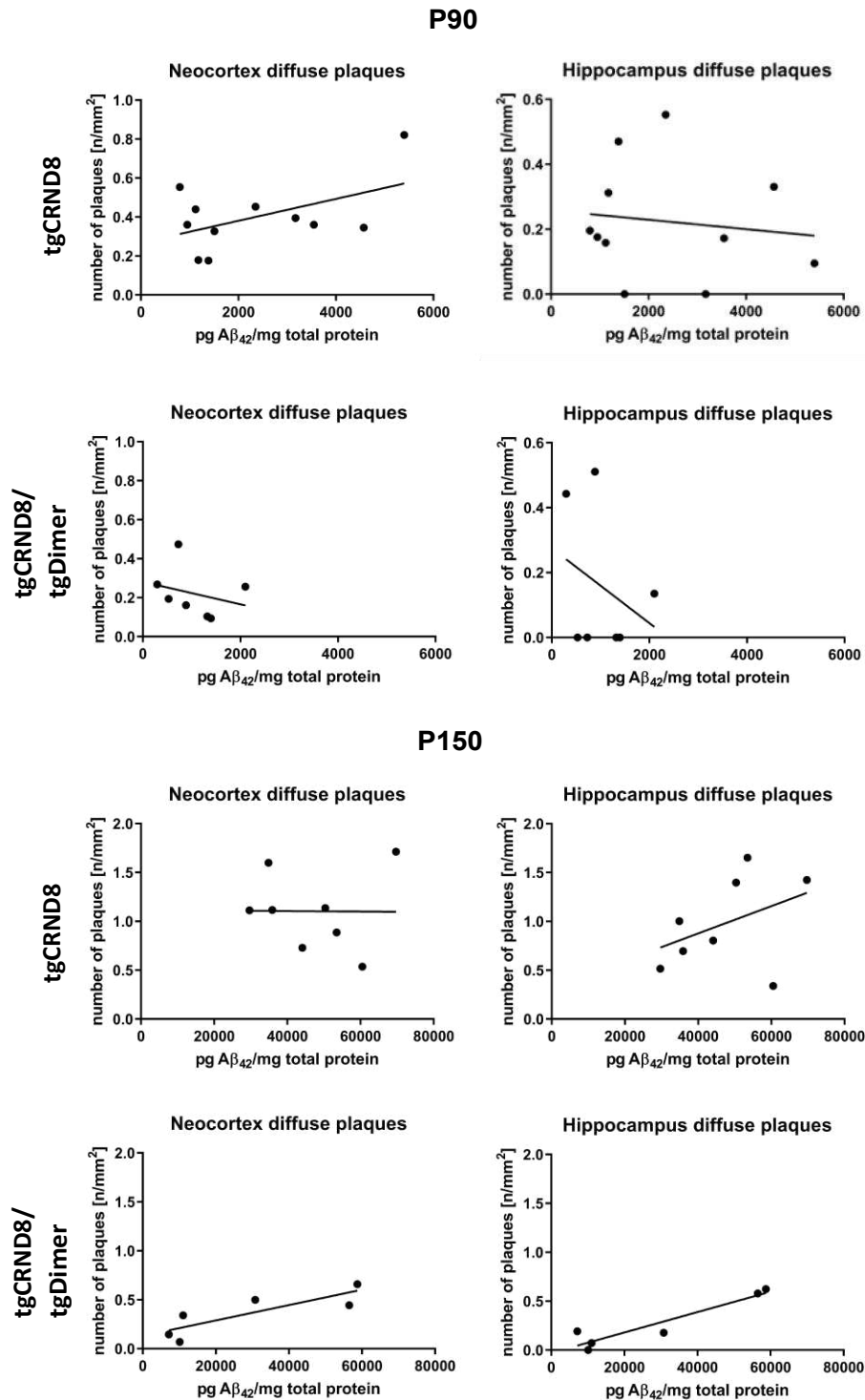
Figure S4. Correlations of insoluble A β ₄₂ with number of core plaques in neocortex or hippocampus of tgCRND8 and tgCRND8/tgDimer mice.



S4. Graphs show the correlation between the number of A β core plaques in the neocortex and hippocampus correlated with the amount of insoluble A β ₄₂. In mice aged 3 months, there was a positive correlation trend visible in the tgCRND8 mice for the number of neocortex core (p=0.0856). No correlation trend was observed in the number of neocortex core versus

A β_{42} level of tgCRND8/tgDimer mice aged 3 months ($p=0.7255$). No correlation was observed between number of neocortical core plaques versus A β_{42} levels in the adult tgCRND8 mice.

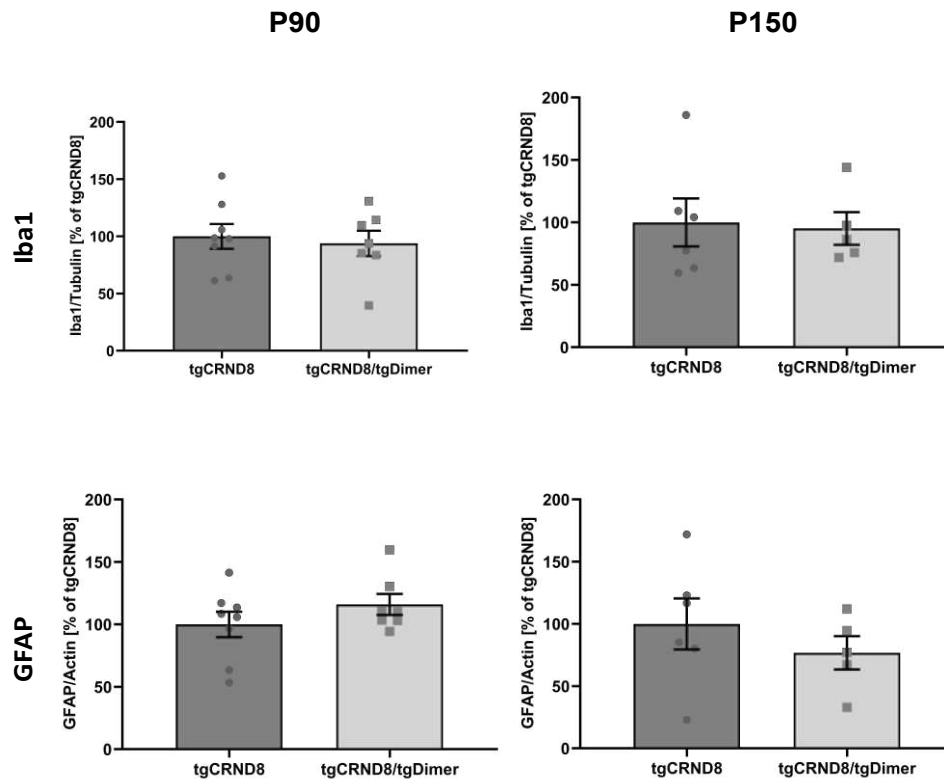
Figure S5. Correlations of insoluble $A\beta_{42}$ with number of diffuse plaques in neocortex or hippocampus of tgCRND8 and tgCRND8/tgDimer mice.



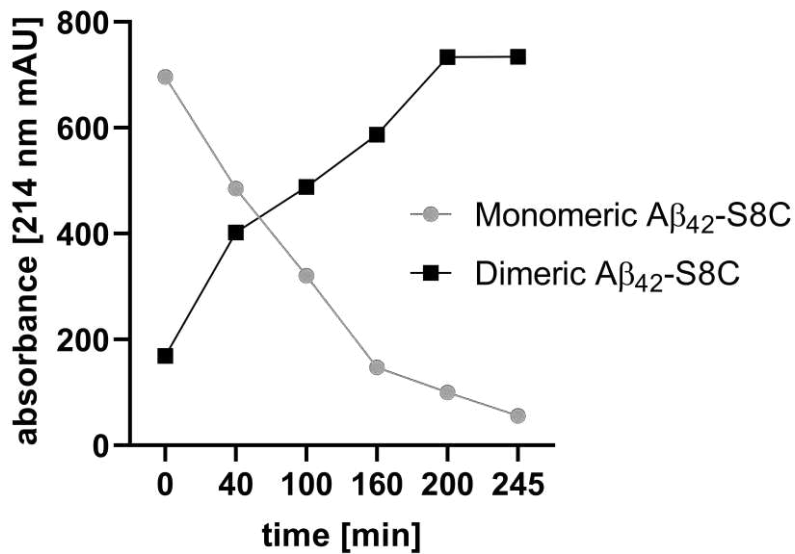
S5. Graphs show the correlation between the number of $A\beta$ diffuse plaques in the neocortex and hippocampus correlated with the amount of insoluble $A\beta_{42}$. There is a positive correlation trend for $A\beta_{42}$ levels with the number of neocortical diffuse plaques per mm² in tgCRND8 mice aged 3 months ($p=0.1154$). The graphs show no correlation for the number of diffuse

plaques in the neocortex and hippocampus versus the amount of A β ₄₂ present in the 3- months old tgCRND8/tgDimer mice (p=0.5536 and p=0.4920 respectively). In aged tgCRND8/tgDimer (P150) mice, there is a positive correlation for A β ₄₂ with number of diffuse plaques in the neocortex and hippocampus (p=0.0382 and p=0.0059 respectively). There is no correlation between the level of A β ₄₂ and the number of diffuse plaques per mm² in the aged tgCRND8 mice.

Figure S6. Iba1 and GFAP levels in 10% brain homogenate of tgCRND8 and tgCRND8/tgDimer mice



S6. Western blot quantification of Iba1 and GFAP levels in 10% brain homogenate, normalized to α -Tubulin and β -Actin respectively. Data are presented as mean \pm SEM (P90: tgCRND8 n=8, tgCRND8/tgDimer n=7; P150: tgCRND8 n=6, tgCRND8/tgDimer n=5). At both ages, Iba1 and GFAP levels were not significantly different among the genotypes. (Mann Whitney U-test)

Figure S7. Dimerization of A β ₄₂-S8C

S7. Monomeric A β ₄₂-S8C was incubated at 37°C at 450 rpm shaking in 50 mM HEPES pH 7.6 buffer. Every ~40 minutes, 20 μ L were analysed by RP-HPLC system (detection at absorbance of 214 nm). Dimerization of A β ₄₂-S8C was completed after ~4h. Subsequent concentrations in the text relate to the dimerized A β ₄₂-S8C as one molecular entity.

References

1. Kawarabayashi T, Younkin LH, Saido TC, Shoji M, Ashe KH, Younkin SG. Age-dependent changes in brain, CSF, and plasma amyloid (beta) protein in the Tg2576 transgenic mouse model of Alzheimer's disease. *J Neurosci.* 2001;21(2):372-81.
2. Lesne S, Koh MT, Kotilinek L, Kaye R, Glabe CG, Yang A, et al. A specific amyloid-beta protein assembly in the brain impairs memory. *Nature.* 2006;440(7082):352-7.

Study II

Soluble amyloid- β dimers are resistant to amyloid- β prions suggesting anti-prion properties

van Gerresheim EF, Müller-Schiffmann A, Schäble S, Koopmans B, Loos M, Korth C.

Neuropathology and Applied Neurobiology (submitted)

Soluble amyloid- β dimers are resistant to amyloid- β prions suggesting antiprion properties

Else F. van Gerresheim¹, Andreas Müller-Schiffmann¹, Sandra Schäble², Bastijn Koopmans³, Maarten Loos³, Carsten Korth^{1*}

¹Department of Neuropathology, Heinrich Heine University Düsseldorf, Düsseldorf, Germany

²Comparative Psychology, Institute of Experimental Psychology, Heinrich Heine University Düsseldorf, Düsseldorf, Germany

³Sylics (Synaptologics BV), Antonie van Leeuwenhoeklaan 9, Bilthoven, The Netherlands

Neuropathology and Applied Neurobiology

Scientific Correspondence

*corresponding author

Carsten Korth. MD PhD

Department of Neuropathology

Heinrich Heine University Düsseldorf

Moorenstrasse 5

40225 Düsseldorf, Germany

Tel +49 211 811 6153

Email: ckorth@hhu.de

Keywords: Alzheimer's disease, amyloid-beta, dimer, antiprion, plaque formation

Word count (main text): 1270

Number of Figures: 1 in main text, 3 in supplementary (S1-3)

For Alzheimer's disease (AD), one neuropathological hallmark is the accumulation of insoluble amyloid-beta ($A\beta$) peptide, a protease-processed fragment of amyloid precursor protein (APP), into extracellular amyloid plaques in the brain. Pathological conformations and multimerization of $A\beta$ are assumed a critical initial step in $A\beta$ fibrilization culminating in massive deposition of extracellular $A\beta$ plaques. Such plaques may arise *de novo* from spontaneous seeds or may spread by disintegration of existing fibrils into smaller ones providing seeds and thus accelerating $A\beta$ -related neuropathology, termed $A\beta$ prions [1] in analogy to protein-based replication of macromolecular fibrils as seen classical prion replication, for example in Creutzfeldt Jakob disease [2]. Animal experiments established that intracerebral injection of transgenic APP23 mice, a mouse model reflecting $A\beta$ pathology of AD, with brain extracts from AD patients containing $A\beta$ seeds accelerated the formation of $A\beta$ plaques leading to astrogliosis [1]. In the last 20 years, extensive studies have established the existence of different $A\beta$ prion strains [3] with a potential relevance of their propagation for human AD cases [4].

Since $A\beta$ plaques are the consequence of decade-long aggregation of $A\beta$ oligomer precursors, a common assumption is that $A\beta$ oligomers accelerate $A\beta$ plaque pathology by providing abundant, "ready-made" precursors. The tgDimer mouse is a transgenic mouse that expresses human APP with the Swedish mutation and an artificial mutation (S679C), replacing a serine at position 8 of $A\beta$ with a cysteine, resulting in the generation of exclusive, stable, and neurotoxic $A\beta$ -S8C dimers [5]. Even though $A\beta$ -S8C dimers maintain the ability to associate to $A\beta$ plaques [5, 6], tgDimer mice do not develop spontaneous $A\beta$ plaques during their lifetime but display early cognitive deficits resembling early AD symptoms [5].

We have previously demonstrated that $A\beta$ dimers from the tgDimer mouse inhibit seeded nucleation but not $A\beta$ plaque growth in a genetic experiment when crossed to the

tgCRND8 mouse, a model for AD developing Abeta plaques at as early as three months of age [6, 7]. Furthermore, in the cell-free *in vitro* thioflavin T assay, A β S8C dimers inhibited seeded nucleation of wild type A β in a dose-dependent manner [6].

In order to investigate whether, on top of the above findings, A β dimers also modulated seeded nucleation, i.e. prion replication of A β fibrils, we inoculated tgDimer mice with insoluble A β , backed by various control conditions.

We crossed the tgDimer mice with GFAP-luc mice, which express luciferase when GFAP-dependent astrogliosis is turned on after A β plaques emerge, to enable *in vivo* longitudinal monitoring of A β -plaque-associated astrogliosis [8]. These double transgenic tgDimer/GFPAP-luc mice were inoculated with brain homogenates from the plaque-bearing tgCRND8 mouse [7] crossed to tgDimer mice in order to account for any potential prion strain resistance (Figure S1) [5].

Inoculated tgDimer/GFAP-luc mice did not develop astrogliosis or cognitive deficits during their lifetime compared to the negative control (Figure 1a, b, S3). A parallel-inoculated positive control, tgAPP23/GFAP-luc mice, expectedly, developed astrogliosis from around 9 months on, accelerated by the inoculum (Figure 1a) and clearly four months before the emergence of spontaneous A β plaques (Figure 1a), similarly to what has been reported several times before [5, 9]. Cognitive deficits in these mice, measured in automated reward-related learning [10] started from month 18 on (Figure 1b). No differences in general activity, measured as total distance moved and total number of entries, in the reward-related learning task were observed in the mice (Figure S2). Histological analysis for A β confirmed that A β fibril-inoculated tgDimer mice do not form A β plaques even if the right template is provided, compared to tgAPP23/GFAP-luc mice, which displayed A β plaques throughout the brain (Figure 1c). Similarly, no astrogliosis was observed in the brains of A β inoculated tgDimer mice, whereas the brains of

tgAPP23 mice showed strong astrogliosis (Figure S3). The lack of an induction of the GFAP promoter and the absence of astrogliosis (Figure S3) indicates that the presence of insoluble A β is necessary for astrogliosis.

These results are in accordance with our previous findings that even though A β -S8C dimers fundamentally are able to associate to insoluble, wild type A β both *in vivo* and *in vitro* [5, 6], they slow wild type A β aggregation and decrease seeded nucleation *in vivo* in a genetic cross with tgCRND8 mice [6]. Our findings presented here indicate that A β -S8C dimers are resistant to A β prion propagation by seeded nucleation *in vivo*.

The discovery that A β would propagate in a prion-like manner *in vivo* was, at the time, a surprise but it is now clear that protein-templated conformational replication is far more common than initially perceived. The yeast prion systems have been exemplary in investigating molecular mechanisms of prion biology and showed that an intricate system of both homologous and heterologous factors regulate prion spreading, the inhibiting ones termed antiprions [11]. Along this line, our findings indicate that A β prion propagation is regulated by homologous antiprions, and is a process that is actively regulated by homologous and possible heterologous factors, rather than being a passive process spreading through the brain once initiated.

The A β -S8C dimer was designed to mimic wild type A β dimers by covalently crosslinking A β monomers for investigating A β dimer effects independent of other A β species [12]. In fact, long-lived and stable A β dimers have also been demonstrated to build from wild type monomers and to be abundant *in vivo* [13].

From our work, we suggests that certain A β oligomers could have a so far underappreciated role as antiprions for slowing or preventing A β propagation and downstream astrogliosis. The end stage of AD where abundant A β plaques populate the

brain may therefore also be conceived as a complete breakdown of antiprion systems
unable to contain the inherent prion propensity of A β .

Acknowledgements

This research was funded by a grant from DFG (KO 1679/10-1) to C.K.

Conflict of Interest

None

Authors' contributions

E.v.G. performed experiments and data analysis, and wrote the original draft. A.M.S. was a major contributor to the experimental set up and revised the paper. S.S. provided support on behavioural experiments and analysis. B.K. and M.L. assisted with behavioural set up and data analysis. C.K. designed the project, supervised and revised the paper. All authors contributed to and approved the final manuscript.

Ethical Approval

Animal experiments were performed in accordance with the German Animal Protection Law and were authorized by local authorities (LANUV NRW, Germany).

Data availability statement

All original data will be made available upon reasonable request.

References

- 1 Meyer-Luehmann M, Coomaraswamy J, Bolmont T, Kaeser S, Schaefer C, Kilger E, Neuenschwander A, Abramowski D, Frey P, Jaton AL, Vigouret JM, Paganetti P, Walsh DM, Mathews PM, Ghiso J, Staufenbiel M, Walker LC, Jucker M. Exogenous induction of cerebral beta-amyloidogenesis is governed by agent and host. *Science* 2006; 313: 1781-4
- 2 Prusiner SB. Novel proteinaceous infectious particles cause scrapie. *Science* 1982; 216: 136-44
- 3 Watts JC, Condello C, Stohr J, Oehler A, Lee J, DeArmond SJ, Lannfelt L, Ingelsson M, Giles K, Prusiner SB. Serial propagation of distinct strains of Abeta prions from Alzheimer's disease patients. *Proc Natl Acad Sci U S A* 2014; 111: 10323-8
- 4 Jaunmuktane Z, Mead S, Ellis M, Wadsworth JD, Nicoll AJ, Kenny J, Launchbury F, Linehan J, Richard-Loendt A, Walker AS, Rudge P, Collinge J, Brandner S. Evidence for human transmission of amyloid-beta pathology and cerebral amyloid angiopathy. *Nature* 2015; 525: 247-50
- 5 Muller-Schiffmann A, Herring A, Abdel-Hafiz L, Chepkova AN, Schable S, Wedel D, Horn AH, Sticht H, de Souza Silva MA, Gottmann K, Sergeeva OA, Huston JP, Keyvani K, Korth C. Amyloid-beta dimers in the absence of plaque pathology impair learning and synaptic plasticity. *Brain* 2016; 139: 509-25
- 6 van Gerresheim EF, Herring A, Gremer L, Muller-Schiffmann A, Keyvani K, Korth C. The interaction of insoluble Amyloid-beta with soluble Amyloid-beta dimers decreases Amyloid-beta plaque numbers. *Neuropathol Appl Neurobiol* 2021; 47: 603-10
- 7 Chishti MA, Yang DS, Janus C, Phinney AL, Horne P, Pearson J, Strome R, Zuker N, Loukides J, French J, Turner S, Lozza G, Grilli M, Kunicki S, Morissette C, Paquette J, Gervais F, Bergeron C, Fraser PE, Carlson GA, George-Hyslop PS, Westaway D. Early-onset amyloid deposition and cognitive deficits in transgenic mice expressing a double mutant form of amyloid precursor protein 695. *J Biol Chem* 2001; 276: 21562-70
- 8 Watts JC, Giles K, Grillo SK, Lemus A, DeArmond SJ, Prusiner SB. Bioluminescence imaging of Abeta deposition in bigenic mouse models of Alzheimer's disease. *Proc Natl Acad Sci U S A* 2011; 108: 2528-33
- 9 Stohr J, Watts JC, Mensinger ZL, Oehler A, Grillo SK, DeArmond SJ, Prusiner SB, Giles K. Purified and synthetic Alzheimer's amyloid beta (Abeta) prions. *Proc Natl Acad Sci U S A* 2012; 109: 11025-30
- 10 Rummelink E, Smit AB, Verhage M, Loos M. Measuring discrimination- and reversal learning in mouse models within 4 days and without prior food deprivation. *Learn Mem* 2016; 23: 660-7
- 11 Wickner RB, Edskes H, Son M, Wu S, Niznikiewicz M. Innate immunity to prions: anti-prion systems turn a tsunami of prions into a slow drip. *Current Genetics* 2021:
- 12 Muller-Schiffmann A, Andreyeva A, Horn AH, Gottmann K, Korth C, Sticht H. Molecular engineering of a secreted, highly homogeneous, and neurotoxic abeta dimer. *ACS Chem Neurosci* 2011; 2: 242-8
- 13 Nick M, Wu Y, Schmidt NW, Prusiner SB, Stöhr J, WF. D. A long-lived A β oligomer resistant to fibrillization. *Biopolymers* 2018; 109: e23096

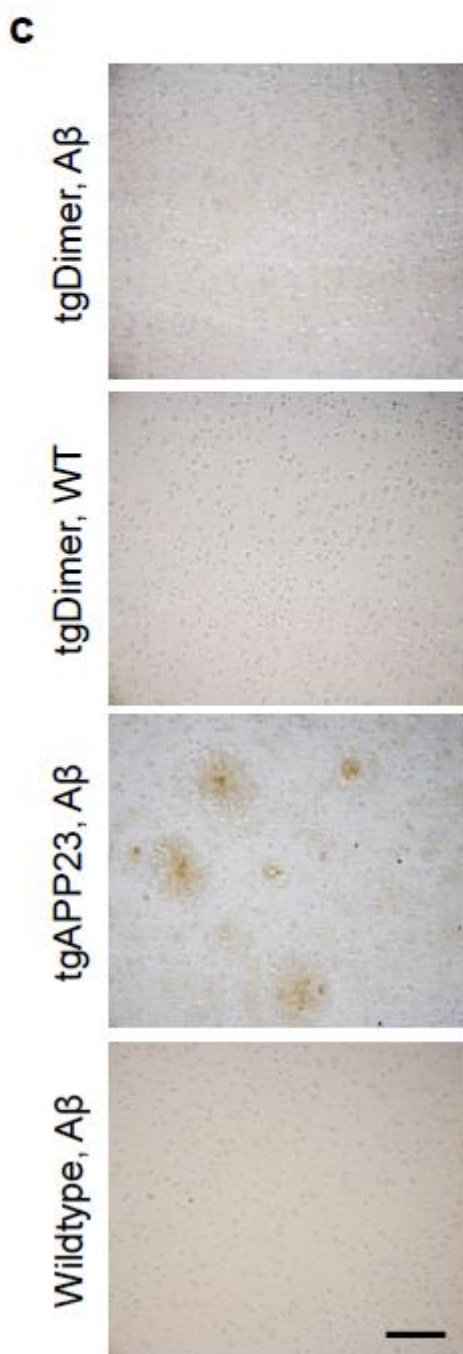
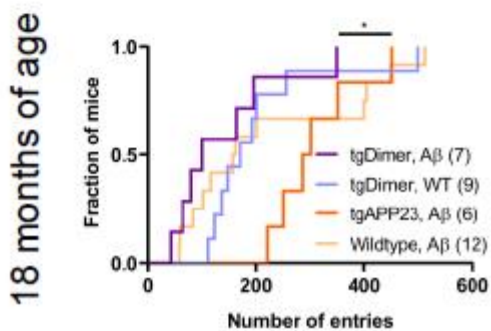
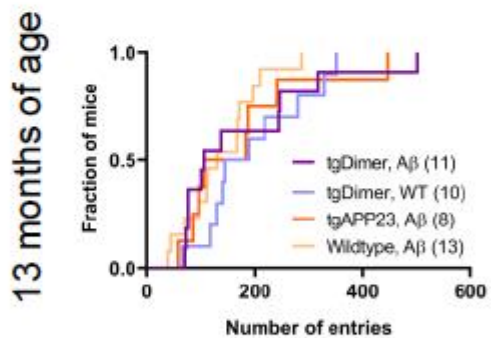
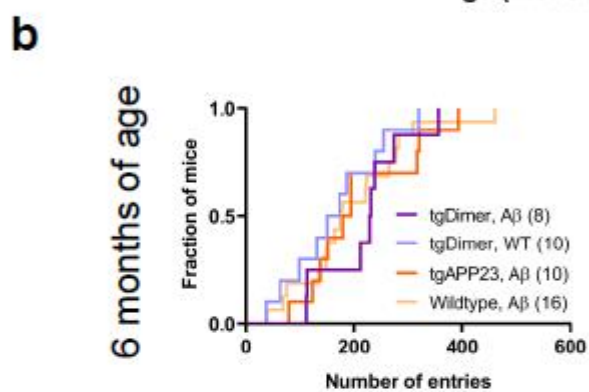
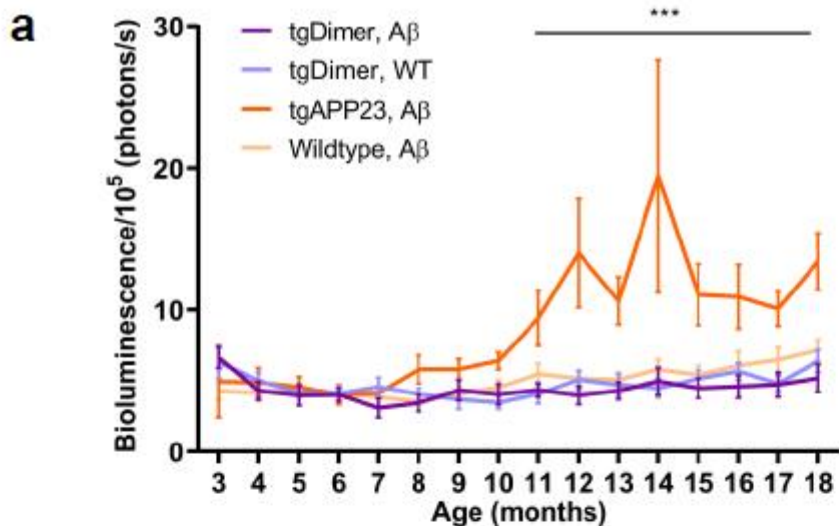
Figure legend

Figure 1.

a. The bioluminescence signal for tgAPP23/GFAP-luc mice inoculated with A β , started to increase at 9 months, and was significant higher at 11 months of age compared to other genotypes. (Mixed-effects analysis, tgAPP23/GFAP-luc, A β , males (m)=7, females (f)=4; tgDimer/GFAP-luc, A β , m=6, f=5; tgDimer/GFAP-luc, WT/GFAP-luc, m=6, f=5; WT, A β , m=6, f=8; *** $p < 0.05$, no sex differences observed)

b. Kaplan–Meier plots of reward-related performance at ages 6 (tgAPP23/GFAP-luc, A β , m=7, f=3; tgDimer/GFAP-luc, A β , m=4, f=4; tgDimer/GFAP-luc, WT, m=5, f=5; WT/GFAP-luc, A β , m=7, f=9) 13 (tgAPP23/GFAP-luc, A β , m=6, f=2; tgDimer/GFAP-luc, A β , m=6, f=5; tgDimer/GFAP-luc, WT, m=6, f=4; WT/GFAP-luc, A β , m=6, f=7) and 18 months (tgAPP23/GFAP-luc, A β , m=4, f=2; tgDimer/GFAP-luc, A β , m=5, f=2; tgDimer/GFAP-luc, WT, m=5, f=4; WT/GFAP-luc, A β , m=5, f=7). The y-axis shows the fraction of mice that reached the criterion at a given number of entries (x-axis). At age 6 and 13 months, mice needed comparable numbers of entries to reach the 80% criterion. 18-month old tgAPP23/GFAP-luc mice needed significant more entries to reach the 80% criterion compared to tgDimer/GFAP-luc, A β inoculated mice (Log-rank test, $p = 0.0215$, no sex differences observed), but not compared to Wildtype/GFAP-luc mice.

c. Representative immunohistochemical images of the cortex. A β plaques were only observed throughout the sections in tgAPP23/GFAP-luc mice, and not in the other genotypes. Scale bar = 100 μm .



Soluble amyloid- β dimers are resistant to amyloid- β prions suggesting antiprion properties

Else F. van Gerresheim¹, Andreas Müller-Schiffmann¹, Sandra Schäble², Bastijn Koopmans³, Maarten Loos³, Carsten Korth^{1*}

¹Department of Neuropathology, Heinrich Heine University Düsseldorf, Düsseldorf, Germany

²Comparative Psychology, Institute of Experimental Psychology, Heinrich Heine University Düsseldorf, Düsseldorf, Germany

³Sylics (Synaptologics BV), Antonie van Leeuwenhoeklaan 9, Bilthoven, The Netherlands

Supplementary Material

A. Supplementary Figures

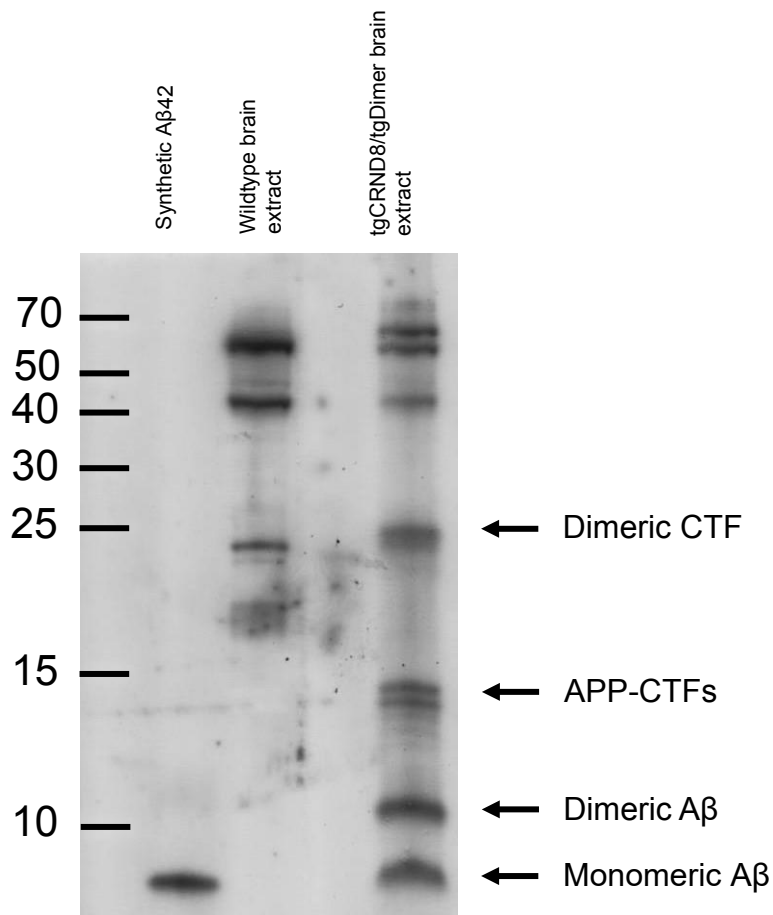


Figure S1. 10% brain extracts from 5 months old tgCRND8/tgDimer mice in sterile phosphate-buffered saline (PBS) were centrifuged at 3000 x g. 5 μ L of the supernatant and 2.5 ng of synthetic A β ₄₂ was separated on a 16.5% Tris-Tricine gel and transferred to a nitrocellulose membrane. Immunoblotting for A β (antibody 4G8, 1:500) revealed the presence of A β monomers and dimers in tgCRND8/tgDimer brain extracts. Bands visualized around 15 kDa and 25 kDa are APP-CTF signals [1].

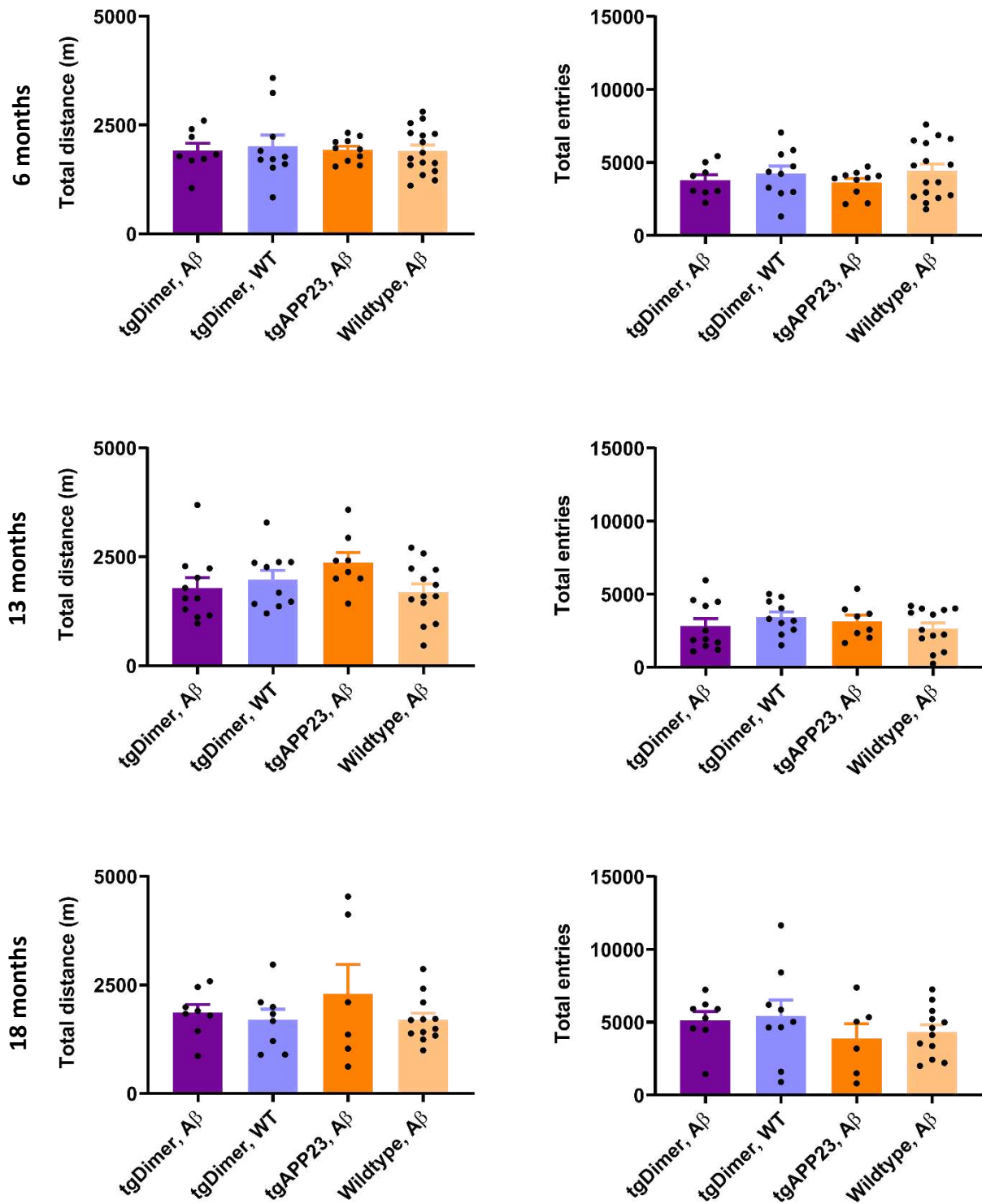


Figure S2. Total distance moved and total number of entries to assess the general activity of the mice during reward-related learning task. No significant differences were observed in the total distance moved and total entries made during the task performed at 6, 13 and 18 months of age.

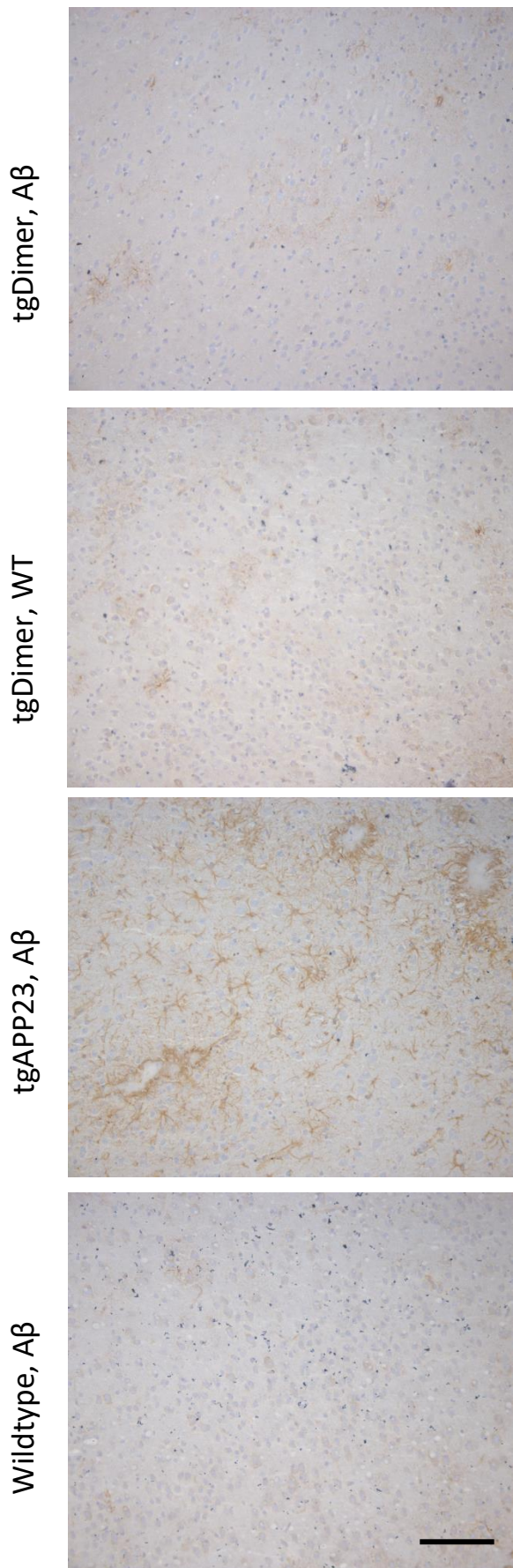


Figure S3. Representative immunohistochemical images of the cortex of 18 months old mice stained with GFAP antibody (DAKO). Cortices of inoculated tgDimer and Wildtype mice showed little astrogliosis, compared to A β inoculated tgAPP23/GFAP-luc mice, which showed strong astrogliosis in the cortex. Scale bar = 100 μ m.

Supplementary Methods

Animals

TgDimer and tgAPP23 mice were generated on a C57BL/6N background and express human APP (751-aa isoform) under the control of the Thy-1.2 promoter with the Swedish mutation (K670M/N671L). In addition, the APP₇₅₁ of the tgDimer includes the dimer mutation within the A β domain (S679C) that generates exclusively A β -S8C dimers, cross linked-through an intramolecular disulfide bridge [2, 3]. To create bigenic mice, tgDimer and tgAPP23 mice were crossed with GFAP-luc mice (FVB/N background;Taconic), expressing firefly luciferase under the control of the murine GFAP promoter [4], and screened for the presence of both transgenes using qPCR [2, 5]. Male and female bigenic mice that were heterozygous for APP23 (K670M/N671L) or APP (K670M/N671L/S679C) and homozygous for GFAP-luc were used. As a negative control, mice without the human APP751 transgene, and expressing GFAP-luc were used, here named Wildtype. Animal experiments were performed in accordance with the German Animal Protection Law and were authorized by local authorities (LANUV NRW, Germany). Mice were housed under standard laboratory conditions with lights on from 7 a.m. to 7 p.m. and with water and food provided *ad libitum*. Mice were sacrificed at the end of the experiments, or when humane endpoints were reached, under deep sodium pentobarbital anaesthesia (Narcoren, 150 mg/kg) by transcardial perfusion with PBS, pH 7.4. The brains were frozen in iso-pentane on a cork plate using glue and sectioned at the coronal plane at 10 μ m thickness.

Brain homogenates

Brains from five 5-month-old tgCRND8/tgDimer mice and Wildtype mice were homogenized at 10% (w/v) in sterile PBS using a Potter-Elvehjem tissue grinder attached to an overhead stirrer (IKA Eurostar 20) and were vortexed, sonicated 3 x 5 seconds and centrifuged at 3000 \times g for 5 minutes. The cleared supernatant was aliquoted and immediately frozen (10% extract) [6]. TgCRND8/tgDimer produce both amyloid-beta monomers, dimers and higher order oligomers [2, 7].

Western Blot

Brain homogenates from Wildtype and tgCRND8/tgDimer mice, used for inoculations, were investigated for the presence of A β species. Samples were sonicated first and then prepared in 1 \times Tricine loading buffer (Bio-Rad) without β -mercaptoethanol and

boiled for 5 min before loading on a 16.5% Tris-Tricine gel. After SDS/PAGE using the Tricine buffer system, the proteins were transferred to a 0.2 µm nitrocellulose membrane (Amersham). The membrane was boiled for 10 min in PBS after separation and before blocking with PBS containing 0.05% Tween-20 (PBST)/5% skimmed milk for 1h at room temperature. The membrane was incubated with 4G8 against A β (1:500, BioLegend) in PBST at 4 °C overnight. After washing three times with PBST and incubation with a secondary goat anti mouse horseradish peroxidase conjugated antibody, signals were detected with SuperSignal™ West Pico PLUS Chemiluminescent Substrate (1:25.000, Thermofisher) on film (Amersham Hyperfilm ECL).

Stereotaxic inoculation

Mice were anaesthetised with 3% isoflurane and placed in a stereotaxic frame (Model 900 Small Animal Stereotaxic Instrument, David Kopf Instruments) with a gas anaesthesia head holder and ear bars for mice. Body temperature was maintained at 37°C with a heating pad during surgery. After making a midline incision of the scalp, burr holes were drilled with 0.6 mm drill bits in the appropriate location (AP – 2.5 mm, DV – 1.8 mm, L +/- 2 mm). Bilateral intra-hippocampal injections of 5 µL of 10% cleared brain extracts into 8-12 weeks old tgDimer/GFAP-luc, tgAPP23/GFAP-luc and Wildtype/GFAP-luc mice were performed using an internal-cannula connected with tubing to a 26-gauge Hamilton syringe. Injection speed was 1.25 µL/min, regulated by an infuse pump (Harvard Apparatus) and the needle was kept in place for an additional 2 min. before it was slowly withdrawn. The surgical area was cleaned with sterile saline, the incision was sutured, and the mice were monitored until recovered from anaesthesia. A small amount of ophthalmic ointment was applied on the corneas during the surgery.

Discrimination Learning

Mice were individually placed in a PhenoTyper cage (model 4500, Noldus Information Technology), an automated home-cage, in which behaviour was tracked by video [8]. Cages (length, width and height; 45 cm) were made of matted Perspex walls with an opaque or black Perspex floor covered with either light or dark bedding (ALPHA dri, Paperchip). Cages were washed with Incidin wipes in between experiments. For the discrimination learning (DL), an opaque Perspex wall (CognitionWall™, Sylics) with three holes was placed in a corner, in front of the pellet dispenser. Mice were placed

in the Phenotyper in the morning, and fifteen minutes before the start of the DL protocol at 16:30, the CognitionWall was placed in front of the reward dispenser spout. The standard chow was then removed from the feeding station. Water was provided *ad libitum* during the protocol. Mice had to learn to get a sucrose pellet reward (Dustless Precision Pellets, 20 mg, Bio-Serve, USA) by going through the left hole in the wall. Passing through the incorrect holes, here the right and middle hole did not have any consequences. The number of entries needed to reach a criterion of 80% correct, computed as a moving window with window size 30 (i.e. 24 correct entries out of the 30 last entries), was used as a measure of learning during DL. Mice were not required to make five consecutive correct entries, i.e. no chaining requirement [9]. After the mice reached this criterion, randomization was started, where the reward hole was changed to random, to test the same mice multiple times throughout the study. Due to technical errors, some mice had to be excluded from the data analysis.

Bioluminescence Imaging (BLI)

Mice were imaged every month using an IVIS Spectrum In Vivo Imaging System (PerkinElmer). BLI was initiated at 3-4 months of age, one month after inoculation, and continued until 18 months of age. Before each scan, the heads of the mice were shaved bald. Mice were anaesthetised with 2.5% isoflurane and given an intraperitoneal injection of D-luciferin potassium salt solution (Gold Biotechnology) prepared in PBS, pH 7.4 (Invitrogen). Each mouse received a dose of ~30 mg/kg and was imaged 10 min later for 60 s under constant anaesthesia. Black construction paper cutouts were placed over the ears and body to minimize extraneous signals. Bioluminescence values were quantified from images displaying surface radiance using circular regions of interest and then converted to total flux of photons (photons per second) using Living Image 3.0 software (Caliper Life Sciences).

Immunohistochemistry

A β (biotinylated IC16), and astrocytes (GFAP) staining was performed on coronal hippocampal brain sections of 10 μ m thickness. Sections were first dried at 37 °C overnight and fixated using 4% ice cold paraformaldehyde in PBS for 5 minutes. After rinsing with PBS, slides were first incubated with Avidin (Thermoscientific) for 10 min at room temperature (RT) and D-biotin (Thermoscientific) for 10 min at RT to block endogenous avidin, biotin and biotin-binding proteins. Slides were washed with TBST. For A β staining, the slides were incubated with the primary antibody, biotinylated IC16

recognizing residues 2-8 of human A β diluted 1:1000 [2] in Antibody Diluent (DAKO) at 4 °C overnight. Slides were washed with TBST and next, slides were incubated with Streptavidin-POD conjugate (1:10.000 Thermoscientific) for 30 min at RT. Before adding DAB Quanto Chromogen and Substrate (Thermoscientific) for 3 min, slides were washed in TBST. To stain astrocytes, slides were first incubated with Hydrogen Peroxide Block (Thermoscientific) for 10 min at RT, and washed in TBST 2 times. Next, slides were incubated in Protein Block (Thermoscientific) for 10 min. at RT, followed by incubation with rabbit α -GFAP (1:1000) in Antibody Diluent (DAKO) at 4°C overnight. Next day, slides were washed in TBST, and the secondary antibody α -rabbit diluted 1:500 in Antibody Diluent (DAKO) applied for 1h at RT. In the meantime, the tertiary antibody solution was prepared 30 min beforehand to let complexes form. Slides were incubated in tertiary antibody solution for 30 min at RT, after washing with TBST. Before visualization by incubation with DAB Quanto Chromogen and Substrate (Thermoscientific) for 3 min, slides were washed in TBST. Slides were shortly rinsed in TBST before they were stained with haematoxylin 1:10 in PBS for 3 min. After another TBST wash followed by a water wash step, slides were dehydrated in three different concentrations of ethanol and fixed with xylol. Sections were mounted with Eukitt®. Images were captured using a Leica DM5000 B microscope through a 20 \times objective.

Statistical Analysis

All statistical analysis was performed using GraphPad Prism software (GraphPad Software). All data sets were tested for normality using the Shapiro-Wilk test. Statistical differences between groups were assessed using ANOVA One-way or Two-way for normal distributed data sets and Mann-Whitney test or Kruskal Wallis for data sets that were not normal distributed. Differences in reward-related performance between genotypes were assessed using the G^P weighted log-rank test for differences between two or more Kaplan–Meier survival curves.

References

- 1 van Gerresheim EF, Herring A, Gremer L, Muller-Schiffmann A, Keyvani K, Korth C: The interaction of insoluble Amyloid-beta with soluble Amyloid-beta dimers decreases Amyloid-beta plaque numbers. *Neuropathology and applied neurobiology* 2021, 47(5):603-610.
- 2 Muller-Schiffmann A, Herring A, Abdel-Hafiz L, Chepkova AN, Schable S, Wedel D, Horn AH, Sticht H, de Souza Silva MA, Gottmann K *et al*: Amyloid-beta dimers in the absence of plaque pathology impair learning and synaptic plasticity. *Brain* 2016, 139(Pt 2):509-525.
- 3 Sturchler-Pierrat C, Abramowski D, Duke M, Wiederhold KH, Mistl C, Rothacher S, Ledermann B, Burki K, Frey P, Paganetti PA *et al*: Two amyloid precursor protein transgenic mouse models with Alzheimer disease-like pathology. *Proc Natl Acad Sci U S A* 1997, 94(24):13287-13292.
- 4 Zhu L, Ramboz S, Hewitt D, Boring L, Grass DS, Purchio AF: Non-invasive imaging of GFAP expression after neuronal damage in mice. *Neurosci Lett* 2004, 367(2):210-212.
- 5 Tamguney G, Francis KP, Giles K, Lemus A, DeArmond SJ, Prusiner SB: Measuring prions by bioluminescence imaging. *Proc Natl Acad Sci U S A* 2009, 106(35):15002-15006.
- 6 Meyer-Luehmann M, Coomaraswamy J, Bolmont T, Kaeser S, Schaefer C, Kilger E, Neuenschwander A, Abramowski D, Frey P, Jaton AL *et al*: Exogenous induction of cerebral beta-amyloidogenesis is governed by agent and host. *Science* 2006, 313(5794):1781-1784.
- 7 Chishti MA, Yang DS, Janus C, Phinney AL, Horne P, Pearson J, Strome R, Zuker N, Loukides J, French J *et al*: Early-onset amyloid deposition and cognitive deficits in transgenic mice expressing a double mutant form of amyloid precursor protein 695. *J Biol Chem* 2001, 276(24):21562-21570.
- 8 Maroteaux G, Loos M, van der Sluis S, Koopmans B, Aarts E, van Gassen K, Geurts A, Neuro BMPC, Largaespada DA, Spruijt BM *et al*: High-throughput phenotyping of avoidance learning in mice discriminates different genotypes and identifies a novel gene. *Genes Brain Behav* 2012, 11(7):772-784.
- 9 Remmelink E, Aartsma-Rus A, Smit AB, Verhage M, Loos M, van Putten M: Cognitive flexibility deficits in a mouse model for the absence of full-length dystrophin. *Genes Brain Behav* 2016, 15(6):558-567.